AD-A093 492 TEXAS INSTRUMENTS INC DALLAS SEMICONDUCTOR GROUP F/G 9/1
ELECTROMIGRATION TESTING OF AL-ALLOY FILMS.(U)
OCT 80 P B GHATE F30602-78-C-0186
UNCLASSIFIED TI-03-80-29 RADC-TR-80-328 NL

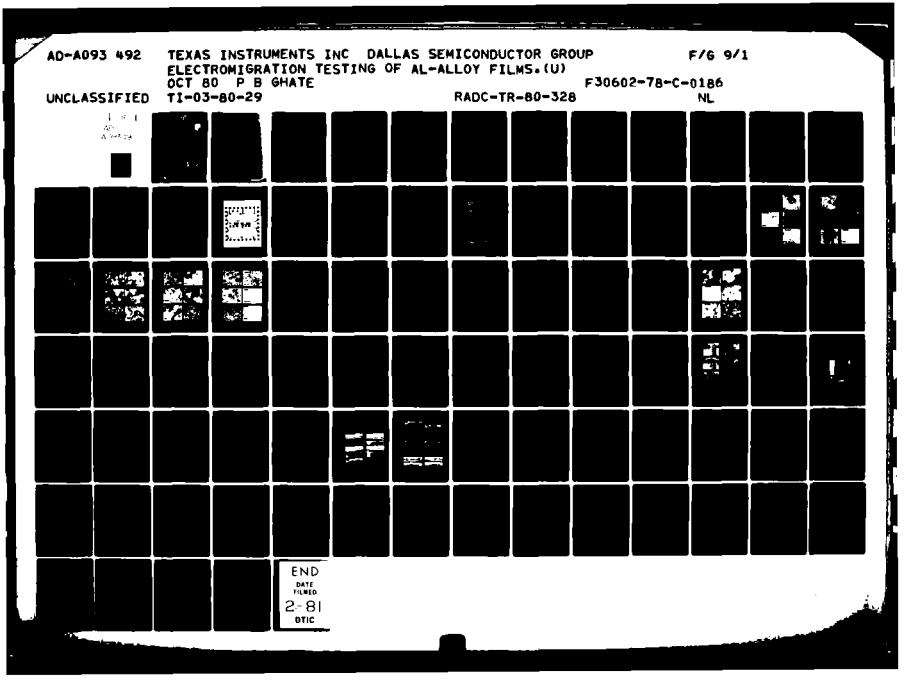

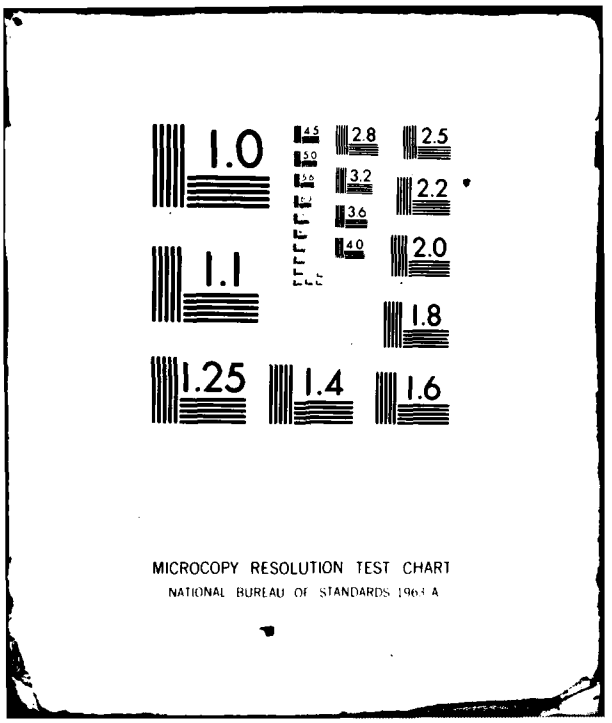
1.0
1.1
1.25
1.4
1.6
1.8
2.0
2.2
2.5
2.8
3.2
3.6
4.0
4.5
5.0
5.6
MICROCOPY RESOLUTION TEST CHART
NATIONAL BUREAU OF STANDARDS 1963 A

RADC-TR-80-328
Final Technical Report
October 1980

ELECTROMIGRATION TESTING OF Al ALLOY FILMS

Texas Instruments Incorporated

P. B. Ghate

ROME AIR DEVELOPMENT CENTER
Air Force Systems Command
Griffiss Air Force Base, New York 13441

This report has been reviewed by the RADC Public [illegible]
is releasable to the National Technical Information [illegible]
it will be releasable to the general public, including [illegible]

RADC-TR-80-328 has been reviewed and is approved for [illegible]

APPROVED: John J. Bart

JOHN J. BART
Project Engineer

APPROVED: David C. Luke

DAVID C. LUKE, Colonel, USAF
Chief, Reliability & Compatibility Division

FOR THE COMMANDER:

JOHN P. HUSS
Acting Chief, [illegible]

If your address has changed or if you wish to be removed from the mailing list, or if the addressee is no longer employed by your organization, please notify RADC (RBRP) Griffiss AFB NY 13441. This will assist us in maintaining a current mailing list.

Do not return this copy. Retain or destroy.

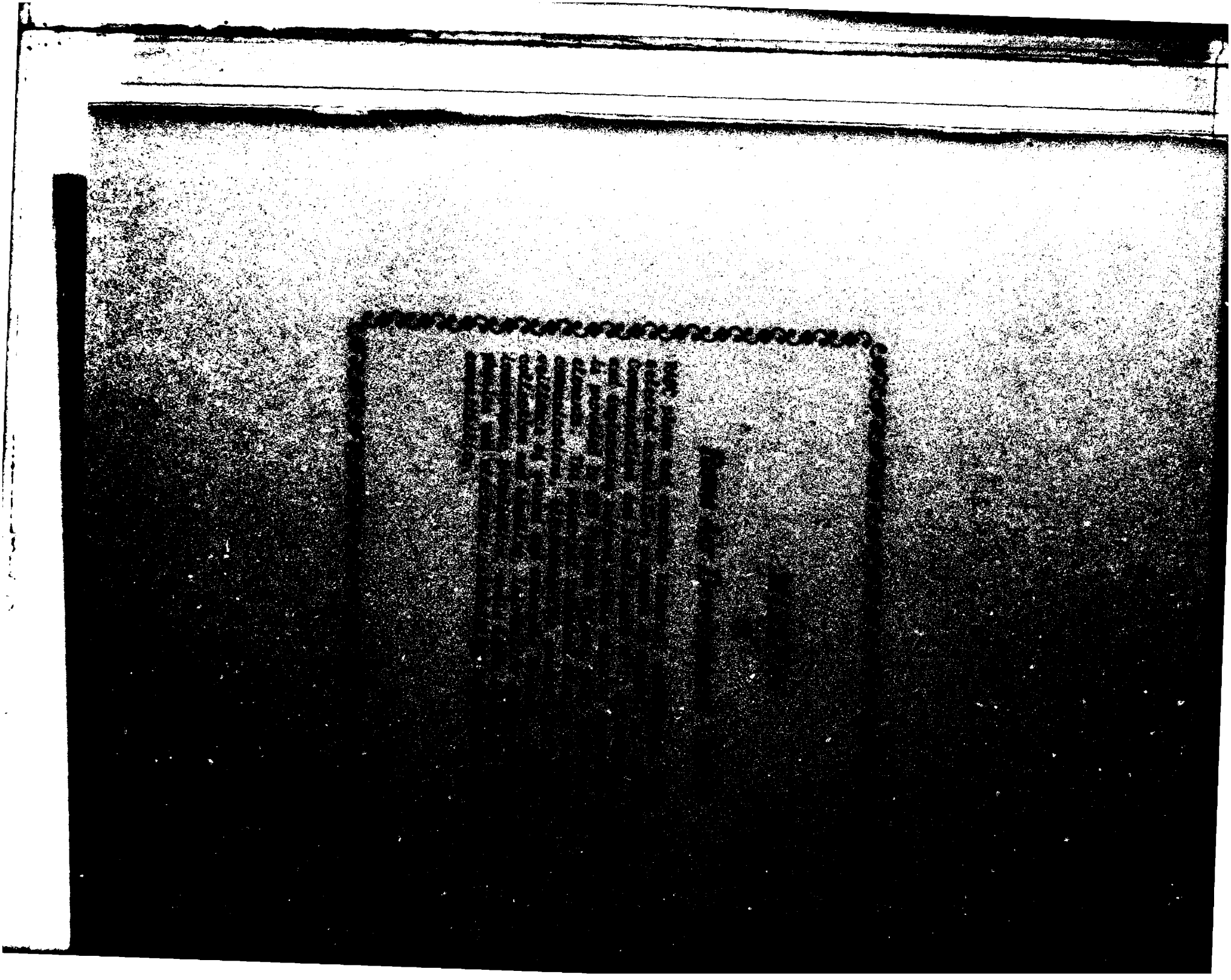

UNCLASSIFIED

SECURITY CLASSIFICATION OF THIS PAGE (When Data Entered)

REPORT DOCUMENTATION PAGE

READ INSTRUCTIONS BEFORE COMPLETING FORM

1. REPORT NUMBER: RADC-TR-80-328	2. GOVT ACCESSION NO.: AD A093492
3. RECIPIENT'S CATALOG NUMBER:	
4. TITLE (and Subtitle): ELECTROMIGRATION TESTING OF Al-ALLOY FILMS	5. TYPE OF REPORT & PERIOD COVERED: Final Technical Report, 25 Sep 78 - 30 Jun 80
	6. PERFORMING ORG. REPORT NUMBER: TI-03-80-29
7. AUTHOR(s): P. B. Ghate	8. CONTRACT OR GRANT NUMBER(s): F30602-78-C-0186
9. PERFORMING ORGANIZATION NAME AND ADDRESS: Texas Instruments Incorporated, Semiconductor Group, P. O. Box 225012, Dallas TX 75265	10. PROGRAM ELEMENT, PROJECT, TASK AREA & WORK UNIT NUMBERS: 62702F, 23380155
11. CONTROLLING OFFICE NAME AND ADDRESS: Rome Air Development Center (RBRP), Griffiss AFB NY 13441	12. REPORT DATE: Oct 80
	13. NUMBER OF PAGES: 85
14. MONITORING AGENCY NAME & ADDRESS(if different from Controlling Office): Same	15. SECURITY CLASS. (of this report): UNCLASSIFIED
	15a. DECLASSIFICATION DOWNGRADING SCHEDULE: N/A

16. DISTRIBUTION STATEMENT (of this Report)

Approved for public release; distribution unlimited.

17. DISTRIBUTION STATEMENT (of the abstract entered in Block 20, if different from Report)

Same

18. SUPPLEMENTARY NOTES

RADC Project Engineer: John J. Bart (RBRP)

19. KEY WORDS (Continue on reverse side if necessary and identify by block number)

Electromigration testing
Al-Alloy film
Microstructure of Al-Alloy films

20. ABSTRACT (Continue on reverse side if necessary and identify by block number)

A search for reliability improvement of Al film interconnections has led to the introduction of Al-Alloy films such as Al+Cu, Al+Cu+Si and so on. This report describes the results of an in-depth study of Al, Al+Cu (2 wt % Cu) and Al+Cu+Si (2 wt % Cu + 1% Si) film interconnections and Silicon/Al-Alloy film contacts as they impact reliability of integrated circuits. Resistivity, microstructure and composition of Al-Alloy films vacuum deposited from an induction heated source (IN-Source) and dc magnetron sputter deposition techniques have been investigated and it is concluded that IN-Source and dc magnetron sputter deposition techniques are equally capable of

DD FORM 1 JAN 73 1473

UNCLASSIFIED (Cont'd)

SECURITY CLASSIFICATION OF THIS PAGE (When Data Entered)

Item 20 (Cont'd)

producing Al, Al+Cu (2 wt %) and Al+Cu+Si (2 wt % Cu + 1% Si) films of comparable compositions, resistivity and microstructure. Chemical Analysis X-Ray Fluorescence Electron Microprobe, Scanning and Transmission Electron Microscopy and Ion Microprobe have been employed for Al-Alloy film characterization. Availability of automated dc magnetron sputter (M-S) deposition equipment was a primary factor in the selection of magnetron sputter deposited Al-Alloy films for electromigration testing.

Electromigration life tests on Al, Al+Cu and Al+Cu+Si film conductors (0.8 μm thick 6 μm wide and 380 μm long) at 1×10^6 A/cm^2 in the 150°C to 215°C show that:

(1) Electromigration induced failures are distributed at random along the length of the stripe

(2) $(MTF)_{Al+Cu+Si} > (MTF)_{Al+Cu} > (MTF)_{Al}$

(3) $Q_{Al+Cu+Si} = 0.5$ eV, $Q_{Al+Cu} = 0.7$ eV and $Q_{Al} = 0.46$ eV

(4) Activation energy of 0.7 eV determined for M-S Al+Cu (2 wt % Cu) is equal to that of IN-Source Al+Cu (1.6 wt % Cu)

Present data on Al film conductors indicate that MTF degrades approximately a factor of four with the decrease in width from 9.6 μm to 6 μm.

Shallow junction devices with junction depths on the order of 0.35 μm have been employed for electromigration life tests on Si/Al, Si/Al+Cu and Si/Al+Cu+Si contacts in series with respective film conductors. Test results indicate that open failures at the contacts are primarily due to Si diffusion in Al, and

1) $(MTF)_{Al+Cu+Si} > (MTF)_{Al+Cu} > (MTF)_{Al}$

2) $Q_{Al+Cu+Si} = 0.76$ eV, $Q_{Al+Cu} = 0.64$ eV, $Q_{Al} = 0.58$ eV

Specific contact resistance of Si/Al-Alloy contacts is on the order 0.36 to 1.45×10^{-6} Ω-cm^2. SEM examination shows nonuniform Si/Al interaction and growth of Si precipitates in the contacts.

Bond strength of ultrasonically bonded 25 μm (1 mil) diameter Al (1% Si) wire to Al, Al+Cu and Al+Cu+Si films are equal to each other ($\approx$ 2.7 gm).

Test samples have been subjected to a temperature storage at 150°C for a cumulative period of 1000 hours to collect reliability data on Si/Al-Alloy contacts, stability of Al-Alloy films, bond strengths and so on.

Results of this study indicate that Al+Cu+Si (2 wt % Cu and 1 wt % Si) films are superior to Al+Cu (2 wt % Cu) in terms of their electromigration resistance and that Al+Cu+Si films are compatible with forming Si/metal contacts for shallow junction devices with 0.35 μm junction depths. Though Si precipitates are observed in contact areas, present data are not sufficient to estimate the adverse effects, if any, on the contact resistance of these contacts.

A test procedure for electromigration testing of Al-Alloy film interconnections has been suggested.

PREFACE

This report is prepared by Texas Instruments Incorporated, Dallas, Texas, under contract number F30602-78-C-0186. The work was administered under the direction of Mr. John Bart Rome Air Development Center, Griffiss AFB, New York, 13440.

At Texas Instruments, the present study was carried out in the Semiconductor Research and Development Laboratories with Dr. P. B. Ghate as the principal investigator. Professionals from Semiconductor R&D Laboratories, Military Products department, Environmental Testing Laboratories of Quality and Reliability Assurance department, and Materials Characterization Laboratories of Corporate Research and Engineering Laboratories provided technical support during the course of this study.

This final report covers the period 25 September 1978 through 30 June 1980 and bears the contractor's report number 03-80-29.

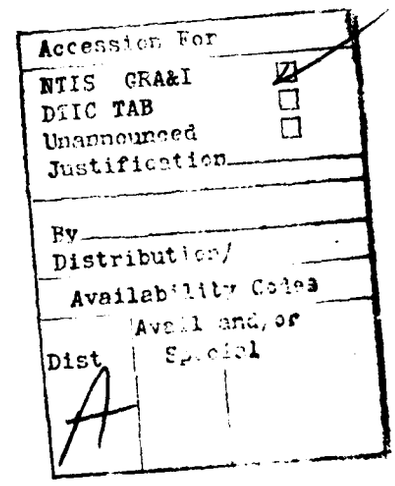

TABLE OF CONTENTS

TABLE OF CONTENTS (Continued)

LIST OF ILLUSTRATIONS

LIST OF ILLUSTRATIONS (Continued)

LIST OF TABLES

EVALUATION

The study of electromigration failure of aluminum alloy films was conducted under the solid state device reliability portion of the RADC Technology Planning Objective. This technology base contract was aimed at developing a quantitative description of the phenomenon of failure of thin film metallization stripes under the operating conditions of high current density and elevated temperature. This mechanism is of special significance to the design and operation of Very Large Scale Integrated Circuits which employ fine geometry feature sizes.

Special emphasis was given to the development of models for conductor film electromigration behavior which would be valid for operational devices. The use of reasonably low test temperatures and the detailed characterization of the chemical and structural microproperties of the aluminum alloy films assures that this information can be used as a valid basis for assessing the reliability of a range of device technologies evaluated under other portions of our exploratory development project entitled "Assurance Procedures for Electronics." The goal of all of these programs is the assurance of the availability of highly reliable solid state components for use in Air Force electronic systems.

JOHN J. BART
Project Engineer

SECTION I
INTRODUCTION

Reliability studies on microelectronic circuits sponsored by Rome Air Development Center in the mid-sixties led to the identification of "electromigration in thin films" as one of the primary failure mechanisms limiting the reliability of film interconnections used in microelectronics.[1] This significant discovery ushered in a period of intense activity in the study of electromigration phenomena in thin films which has led to a better understanding of the several factors affecting reliability of film interconnections of integrated circuits (ICs). Most of the electromigration testing has been carried out with Al film conductors as they happen to be most widely used on ICs.[2-7]

A review of the life tests on Al film conductors points out the universal agreement on the phenomena; however the activation energies derived from the life test data vary between 0.4 eV to 1.0 eV and the mean time to failures (MTFs) for use conditions vary over several orders of magnitude.[8] This is to be anticipated because of the wide differences in the film deposition procedures and test conditions. However, it is encouraging to note that in the last 5 or 6 years a consensus on the activation energy and current dependence of MTF has been emerging as a result of carefully controlled experiments on characterized films.

A search for reliability improvement has led to the introduction of Al-Alloy films such Al-Cu, Al-Si, and Al-Cu-Si. Several workers have demonstrated that addition of Cu to Al films increases MTF under high current stress.[9-10] The activation energies have varied from 0.4 eV to 1.0 eV, depending on the test conditions. The Al-Si films were introduced to minimize erosion of Si in contact windows due to the Si dissolution in Al films during contact annealing.[11] With recent advances in film deposition technology, Al-Cu-Si ternary alloy films have been explored to utilize the beneficial effects of (1) Cu for electromigration resistance and (2) Si for minimizing the erosion in contact windows.[12] However, microstructure of these alloy films strongly depends on deposition techniques and affects the electromigration life test data.

The present investigation is concerned with the study of electromigration behavior of Al-Alloy films (Al+Cu and Al+Cu+Si) and the influence of this mechanism on the reliability of microelectronic devices which use these films for interconnections. Control samples of pure Al films have also been investigated.

Microstructure, the grain size distribution, is one of the most important parameters of vacuum deposited films and significantly affects the reliability of IC interconnections.[13,14]

For alloy films, deposition techniques are important in controlling not only the solute (Cu and/or Si) content but also the microstructure of these films. In this study, resistivity and microstructure (grain size) of Al and Al-Alloy films deposited from an IN-Source (RF induction heated source supplied by Applied Materials Inc.)[15] and from a planar magnetron have been characterized.

Scanning Transmission Electron Microscopy (STEM) has been employed for grain size determination. X-ray fluorescence, electron microprobe and wet chemical methods have been used to determine the Cu and/or Si content in these films.

A test vehicle consisting of several test structures has been designed. Test structures fabricated with magnetron sputtered Al, Al+Cu and Al+Cu+Si films have been employed for electromigration testing at 1×10^6 A/cm^2 and also to determine the respective activation energies for electromigration-induced failures for these films. A suitable test structure has also been employed to study the interaction of Al, and Al-Alloy films on silicon/metal contacts on shallow junction devices (junction depth is ≈ 0.35 μm) stored at 150°C for 1000 hours. Bond strengths of 25 μm (1 mil) Al + 1% Si wire ultrasonically bonded to Al and Al-Alloy pads have been determined before and after 50 temperature cycles from −65°C to +150°C. Finally, the present experimental data have been analyzed to determine the reliability of Al-Alloy film interconnections. A procedure for electromigration testing of Al-Alloy film conductors has also been proposed.

SECTION II
TEST VEHICLE

A test vehicle consisting of several test structures has been designed to carry out the electromigration testing of Aluminum-Alloy film conductors and also to determine the contact resistance of metal-silicon contacts. Fabrication of the test vehicle is accomplished with a mask set consisting of four levels;

Level 1: Oxide Removal (OR) for n^+ Diffusion/Ion Implant
Level 2: Contact OR
Level 3: Lead Pattern
Level 4: Bond Pad Via Openings

Figure 1 displays the test vehicle and also the placement of individual test structures on the test bar (95 X 95 mil^2). Test structures HCSO1, HCSO3, and HCSO4 have been designed for electromigration testing; test structures CRLT4 and CRLT7 have been designed for contact resistance determination of silicon/metal contacts; and test structure HCSO5 has been designed for sheet resistance measurement of n^+ diffused resistors. The remaining two test structures, CBSR6 and SR6MM, were designed for sheet resistance measurements of the diffused regions and metal films respectively. These latter two test structures are referred to as "Cross Bridge Sheet Resistor Test Structures."

Five of these test structures are illustrated in Figures 2 through 5. The test structure HCSO1 shown in Figure 2 consists of a 15-mil long by 0.25-mil wide conductor lead on an oxidized substrate and the current to the lead is provided through a silicon/metal contact (0.15 X 0.25 mil^2) located in an n^+ diffused resistor (0.75 X 1.1 mil^2). The test structure HCSO3, shown in Figure 3, is also a 15-mil long by 0.25-mil wide conductor located on the oxidized substrate and current to the lead is provided from metal pads also located on the oxidized substrate. Test structure HCSO4 is another variation of HCSO1.

A schematic of the contact resistance test structure CRLT4 and CRLT7 is shown in Figure 4. This test structure is a stitch-through pattern consisting of 200 silicon/metal contacts (0.15 X 0.25 mil^2 each) in series with 100 n^+ diffused resistors of 1 square each for CRLT4 and 1.15 squares each for CRLT7 respectively. The diffused resistors are arranged in four rows each consisting of 25 diffused resistors. The test structure HCSO5, shown in Figure 5, is a conventional four-point probe used for sheet resistance measurement. In this illustration, five squares of n^+ diffused region have been chosen for the resistance measurement. The experimental work to be described in the following pages has been carried out primarily with five test structures: HCSO1, HSCO3, CRLT4, CRLT7, and HCSO5.

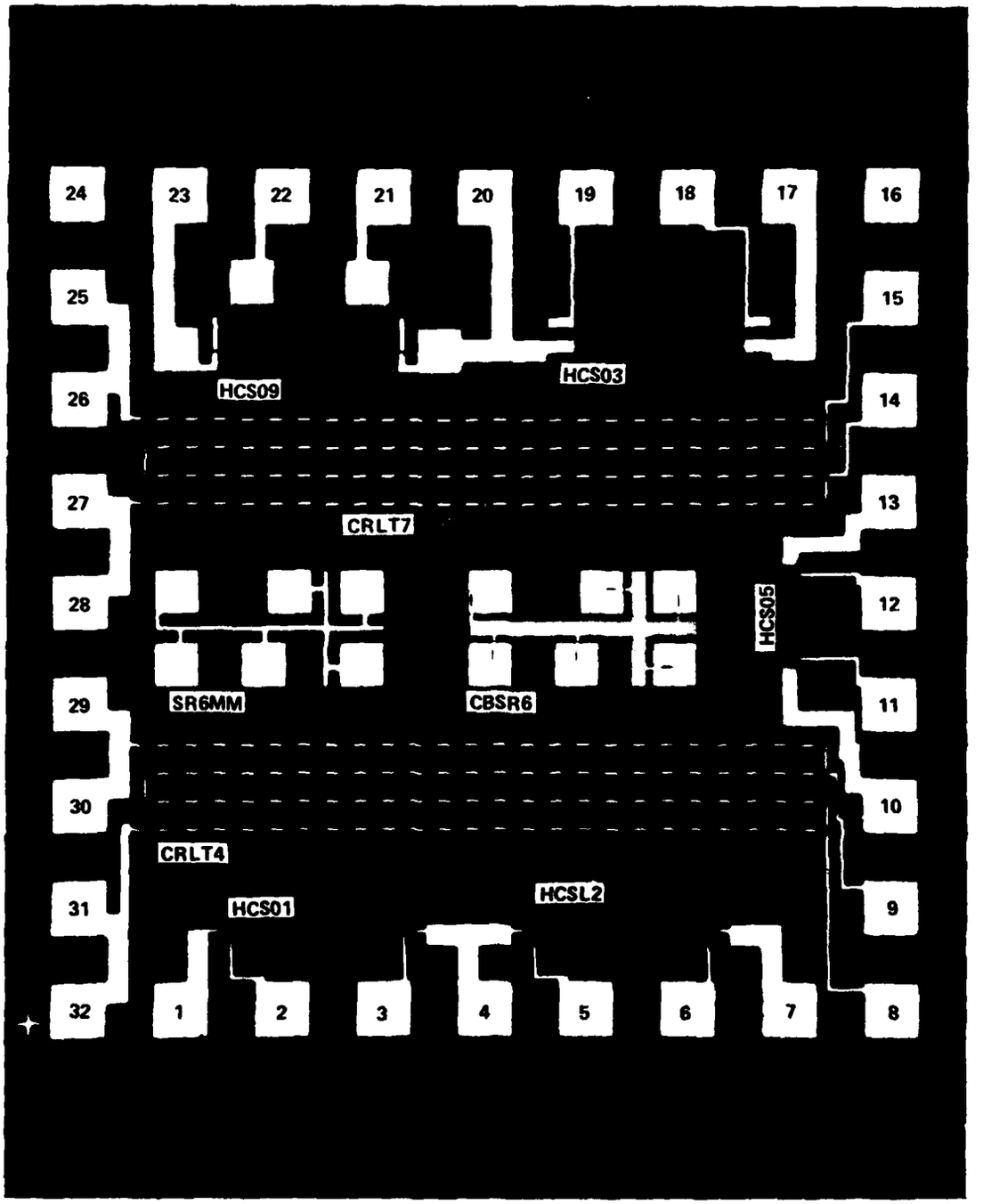

Figure 1. Test Vehicle

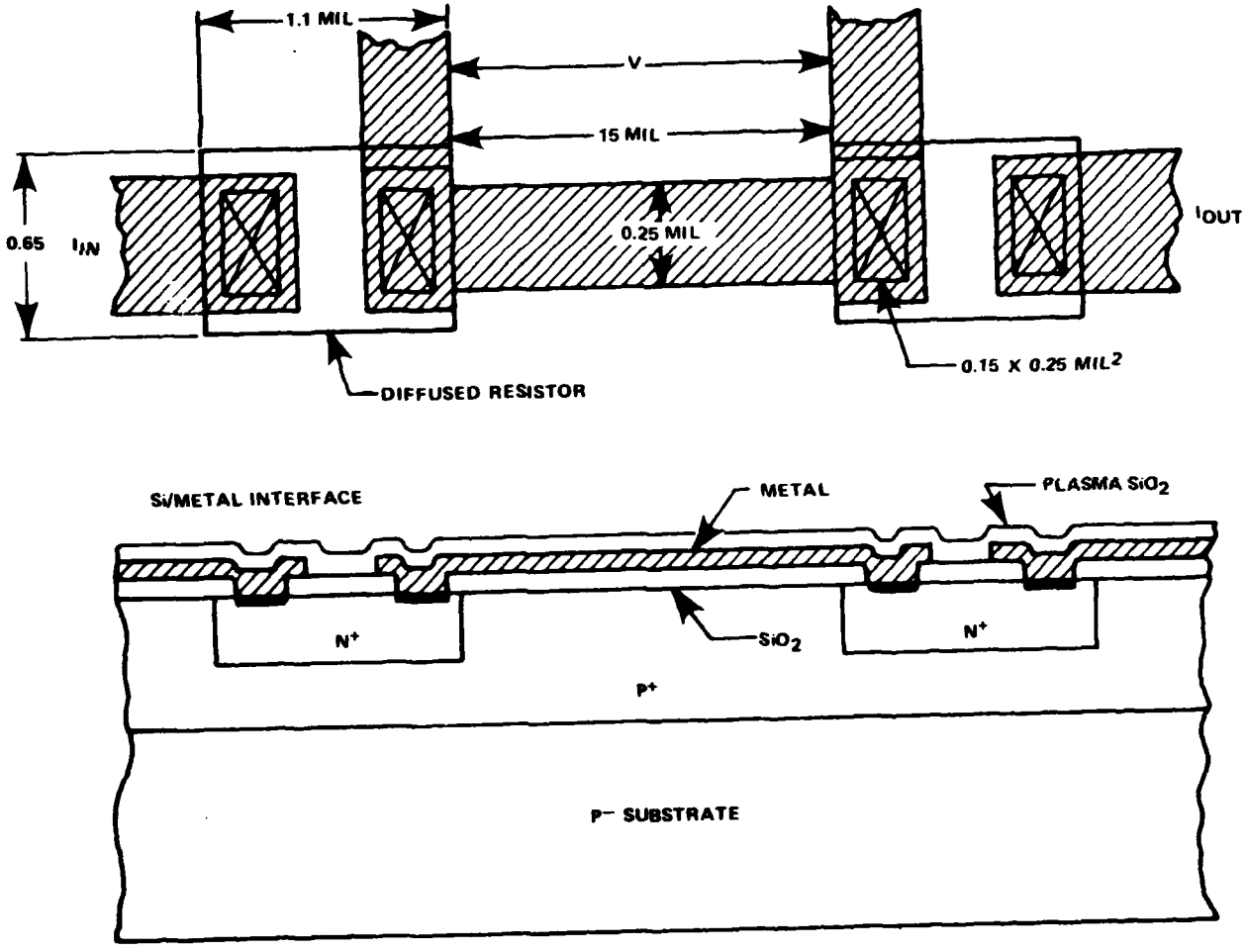

Figure 2. Test Structure HCSO1 – High Current Stress Si/Metal Interface

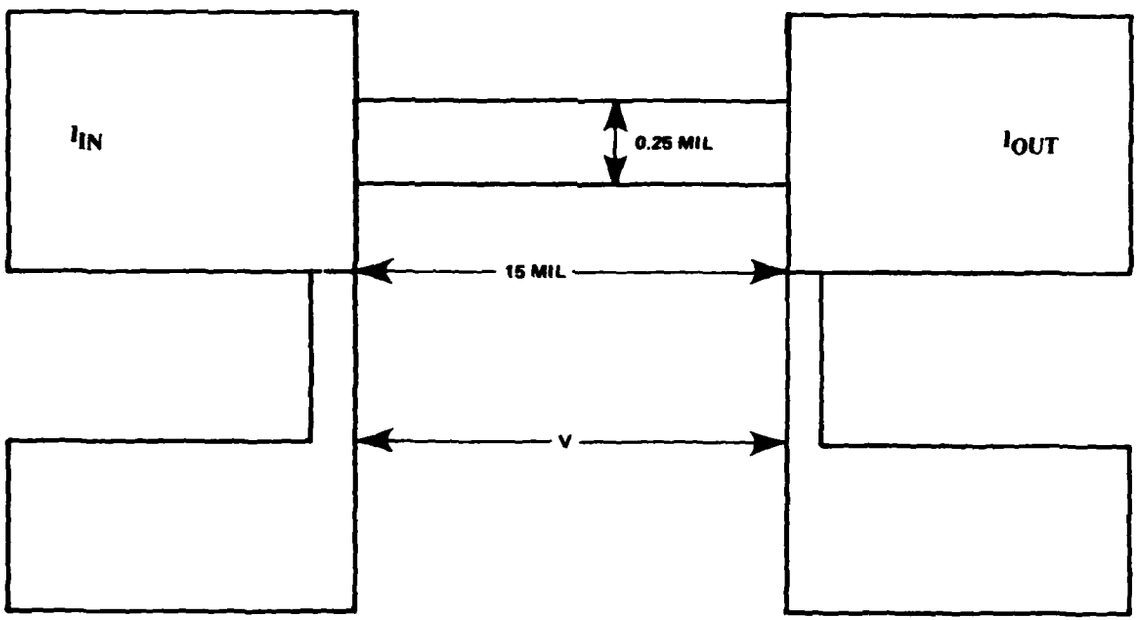

Figure 3. Test Structure HCSO3 – High Current Stress

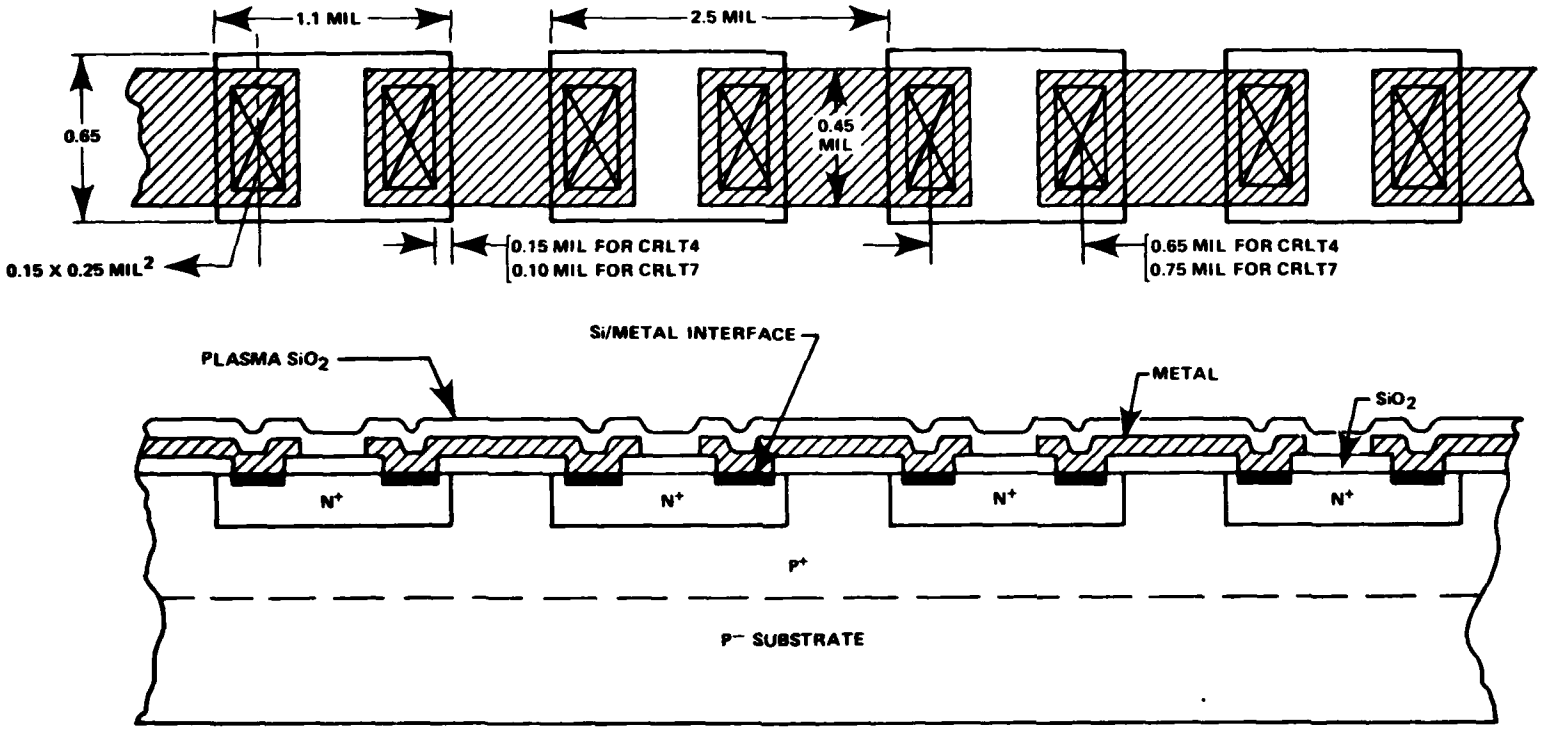

Figure 4. Test Structures CRLT4 and CRLT7 – Contact Resistance and Leakage Test

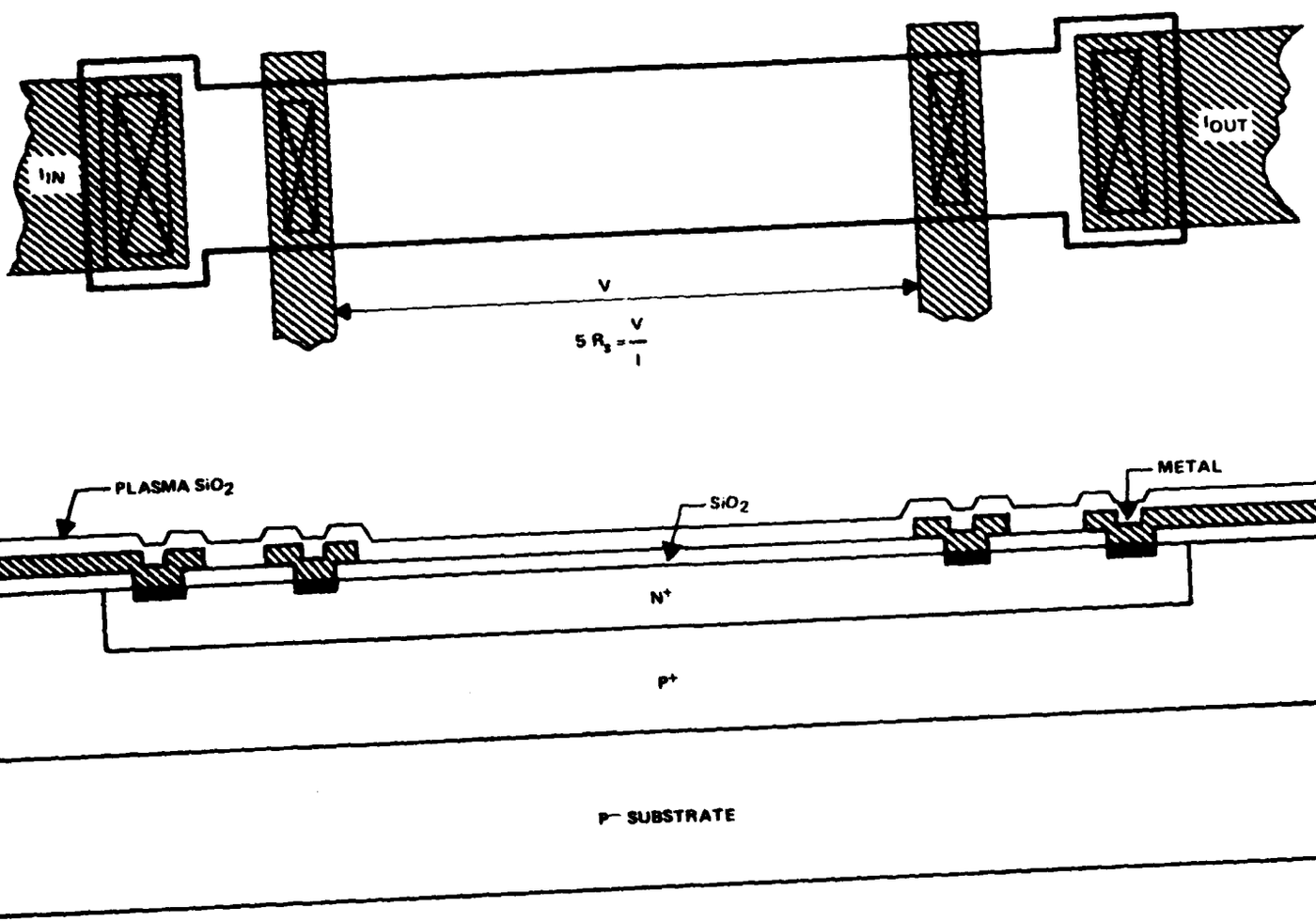

Figure 5. Test Structure HCSO5 – Sheet Resistance Measurements

SECTION III
ALUMINUM-ALLOY FILMS

A. FILM DEPOSITIONS

Aluminum films for IC contacts and interconnections are vacuum deposited by several techniques including (1) filament evaporation, (2) flash evaporation, (3) induction heating, (4) electron-beam heating, (5) sputtering (RF diode, RF magnetron and dc magnetron), etc. Electron beam and induction heating tend to dominate the film deposition technology because of their ability to deposit high purity Al films to within 5-10% of bulk resistivity (ρ = 2.7 $\mu\Omega$-cm) at reasonable rates with minimum device damage (MOS devices are sensitive to deposition techniques). With a continued trend toward shallower junctions and the common observation of erosion of silicon from contact windows, there has been a growing interest in the deposition of Al+Si films with reproducible physical properties.[11,12] Since d'Heurle and co-workers at IBM reported an improvement in MTF of film conductors against electromigration by a factor of 70 by copper doping aluminum films, there has been considerable interest in the usage of Al+Cu films for IC interconnections.[8] Ternary alloy Al+Cu+Si films have also been considered for IC contacts and interconnections to achieve MTF improvement against electromigration-induced failures and also to minimize erosion of silicon contacts.[12] Electron-beam deposition, while meeting the demanding SC requirements of pure Al films, has proved to be marginal for Al-Alloy films. Over the years, flash evaporation techniques have been attempted, however these techniques have not been pervasive in the semiconductor industry because of inherent problems in achieving reproducible films in manufacturing. With recent advances in equipment manufacturing, there seems to be at least two attractive solutions for Al-Alloy film depositions, namely, an induction heated source (IN-Source) and dc magnetron sputtering. These techniques are capable of meeting SC device requirements and also are compatible with slice production rates demanded in manufacturing. For this study, Al, Al+Cu and Al+Cu+Si films have been deposited by IN-Source and dc magnetron sputtering techniques and an attempt has been made at fully characterizing the properties of these Al-Alloy films.

1. In-Source Film Depositions

The deposition system used in this investigation consisted of an NRC 3117 pumping station with an Applied Materials RF-induction heated source. The system attains a base pressure of 1×10^{-7} torr, and chamber pressure is monitored with an ion gauge (NRC 836). Detailed description of an IN-Source is readily available.[15] This deposition system is also equipped with quartz crystal thickness monitor, canted domed planetary system to handle[18] 3-inch diameter silicon substrates and quartz lamps for substrate heating.

Aluminum charge used for film depositions has a nominal purity of 99.999%. For Al+Cu and Al+Cu+Si film depositions, it is necessary to comprehend the vastly different vapor pressures of Al, Cu, and Si in preparing the Al+Cu and Al+Cu+Si charges to be used in the crucibles (referred to

as sources) and also the power setting for the IN-Source for desired film deposition rates. Three sources (crucibles filled with charge) of Al, Al+Cu and Al+Cu+Si, all of the same weight were prepared from high purity Al and Al+Cu slugs purchased from Materials Research Corporation and very high-resistivity Si. Weights of sources used in these experiments were as follows: 50 grams of Al for Al Source; 44.0 grams of Al and 6.9 grams of Cu for Al+Cu Source; and 22 grams of Al plus 25.0 grams of Si and 3.3 grams of Cu for Al+Cu+Si Source. Once the sources of desired weights were prepared and several deposition runs were carried out, the sources were fed with Al-Alloy pellets of compositions equivalent to those desired for Al-Alloy films; e.g., Al+Cu pellets of 98% Al and 2% Cu by weight percent were added to the source that was prepared for deposition of Al films doped with 2% Cu. A similar procedure was followed for Al+Cu+Si film depositions. In order to achieve reproducible film compositions and film deposition rates, it is almost mandatory to hold the weight of the crucible constant by feeding the crucible with Al-Alloy pellets after every deposition run.

Al, Al+Cu and Al+Cu+Si films were deposited on oxidized silicon substrates using the respective sources with film deposition chamber pressures in the range of 5×10^{-7} to 1×10^{-6} torr. For each source material, two film depositions were carried out: (1) the first set of films were deposited on unheated substrates and (2) for the second set of films, the substrates were heated to 200°C. Data on Al-Alloy films deposited from the IN-Source, and referred to as IN-S, are summarized in Table 1. Film compositions planned to be achieved are also shown in the first column.

The room-temperature resistivities (ρ_{RT}) of Al, Al+Cu and Al+Cu+Si films were determined from four-point probe sheet resistance measurements and film thickness measurements with a Taylor Hobson Talystep. Also, the sheet resistances of these films were subsequently measured after a 450°C, 15-minute anneal in N_2. The room temperature resistivities of these Al-Alloy films in the as-deposited and post-annealed conditions are also shown in Table 1.

2. DC Magnetron Film Depositions

The Al, Al+Cu and Al+Cu+Si films were deposited in a commercially acquired sputtering system which was designed for RF sputtering but subsequently modified for dc magnetron sputtering. The film deposition chamber was a nonload locked stainless cylinder which was side-pumped assisted by a cryo-cooled titanium sublimation pump. The Perkin-Elmer circular planar magnetron cathode assembly (8 inches in diameter) was mounted in each of three symmetrically located positions in the bottom plate (i.e., sputter-up configuration). Literature on the Perkin Elmer dc magnetron sputtering system is readily available.[16] All three targets of Al, Al+Cu and Al+Cu+Si have a quoted Al purity of 99.999% and high-purity Cu and Si (99.999%) have been used in cathode fabrication. The Al and 98 Al/2 Cu targets were procured from Materials Research Corporation[17] and the 97 Al/2 Cu/1 Si target was procured from Specialty Metals Division of Varian.[18] Details of the cathode and substrate holder assembly have been described in an earlier publication.[19] The 3-inch oxidized silicon substrates used in this study were placed on the shouldered holes of the substrate plate through a door in the chamber lid. Prior to film deposition, the chamber was pumped to 5×10^{-7} torr [ultimate pressure of 8×10^{-8} torr] and back filled with argon 99.999% pure to a pressure of 2.5×10^{-3} torr). The substrate plate was rotated at 0.33/min. Desired film

Table 1. Film Deposition, Resistivity and Grain Size Data for Al-Alloy Films

No.	Film		Planned Compositions Cu %	Si %	Substrate Temp.	Rate (nm/sec)	Thickness (nm)	Specific Resistivity As-Deposited	Grain Size After 450°C 15 min Anneal in N_2 ($\mu\Omega$-cm)	As-Deposited Average Size (μm)	As-Deposited Range (μm)	After 450°C 15 min Anneal in N_2 Average Size (μm)	After 450°C 15 min Anneal in N_2 Range (μm)
1	Al	IN-S	–	–	RT	3.3	838	2.77	2.43*	0.53	0.2-0.7	0.9	0.2-1.2
2	Al	IN-S	–	–	200 C	3.6	828	2.65	2.40*	0.96	0.2-1.5	1.4	0.2-1.8
3	Al	M-S	–	–	RT	2.1	813	2.93	2.68	0.30	0.1-1.0	0.7	0.1-1.8
4	Al+Cu	IN-S	2	–	RT	2.9	762	4.19	3.28	0.23	0.1-0.5	1.0	0.1-1.8
5	Al+Cu	IN-S	2	–	200 C	2.9	762	3.12	3.35	0.67	0.2-1.0	2.3	0.2-2.6
6	Al+Cu	M-S	2	–	RT	1.6	836	4.10	3.51	0.22	0.1-0.5	1.2	0.2-2.0
7	Al+Cu+Si	IN-S	3.85	1.0	RT	3.0	850	7.99	4.42	0.55	–	0.2	–
8	Al+Cu+Si	IN-S	3.85	1.0	200 C	2.4	813	6.02	4.07	0.07	–	0.2	–
9	Al+Cu+Si	M-S	2.0	1.0	RT	1.3	938	4.50	3.47†	0.07	–	0.1	–

*Room temperature resistivity of annealed Al film (IN S) is low (2.43), this is possibly due to an error in thickness measurements. All our previous data show a specific resistivity of 2.71 $\mu\Omega$ cm.

†DC magnetron sputter deposited, Al+Cu+Si films show a lower resistivity as compared to the resistivity of films prepared from an IN Source. This difference is attributed to the difference in copper concentration.

deposition rates are realized by selecting the appropriate system power. The film thickness uniformity is within ±5% for a 3-inch diameter substrate whose center sweeps over the target center. In these Al and Al-Alloy film depositions, no substrate heating was employed. Data on dc magnetron sputtered Al, Al+Cu and Al+Cu+Si films and referred to as M-S films are summarized in Table 1.

The room-temperature resistivities of these Al and Al-Alloy films before and after a 450°C, 15-minute anneal in N_2 have been determined from sheet resistance and thickness measurements and these data are also presented in Table 1.

B. *Al-ALLOY FILM CHARACTERIZATION*

1. Microstructure

Microstructure, the grain size distribution, is one of the most important properties of deposited films. Scanning and transmission electron microscopy have been used to examine the microstructure of films (see Table 1) in as-deposited condition and also of equivalent films subsequent to annealing at 450°C for 15 minutes in N_2. The scanning electron micrographs (SEM) of Al, Al+Cu and Al+Cu+Si films before and after a 450°C anneal are presented in Figures 6, 7 and 8 respectively. These films were thinned for transmission electron microscopy (TEM). The transmission electron micrographs of Al, Al+Cu and Al+Cu+Si films before and after a 450°C anneal for 15 minutes in N_2 are presented in Figures 9, 10 and 11 respectively. These micrographs have been used to determine the average grain size by a linear intercept method.[20] Grain size distribution has been examined by constructing the histograms. Al and Al+Cu films tend to display the anticipated log-normal distribution.[21,22] Data on the grain sizes and also the observed minimum and maximum sizes are summarized in Table 1.

Examination of the micrographs of Al+Cu films shows that the Cu Al_2 (or Cu?) precipitates are finely distributed in annealed films as compared to those observed in as-deposited films. The Al+Cu+Si films have a very fine grain on the order of $\approx 0.2\ \mu m$ and no large ($< 0.1\ \mu m$) precipitates are visible in the micrographs. Selected area diffraction patterns, not presented here, show that as-deposited Al+Cu and Al+Cu+Si films share randomly oriented grains with some degree of ⟨111⟩ texture, whereas Al films display a strong ⟨111⟩ texture. After 450°C anneal, the degree of ⟨111⟩ texture increases for all the films.

2. Al-Alloy Film Characterization

a. Chemical Analysis

The copper and silicon content of Al+Cu and Al+Cu+Si films have been analyzed using standard wet chemical methods and these results are summarized in Table 2; however for silicon analysis, Al+Cu+Si films deposited on sapphire substrates are used.

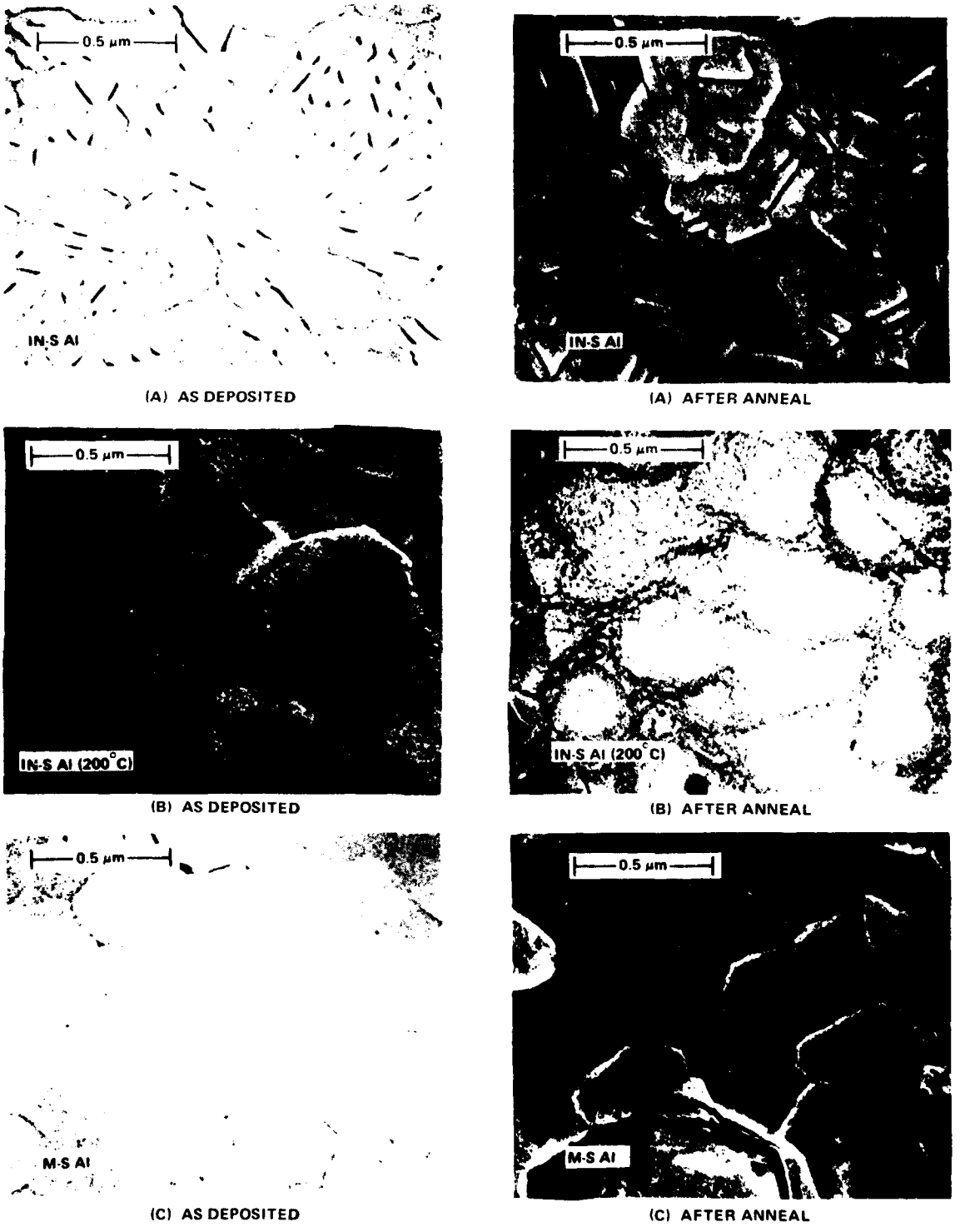

Figure 6. Scanning Electron Micrographs of Three Al Films: (A) IN-S Al (RT), (B) IN-S Al (200°C), (C) M-S Al

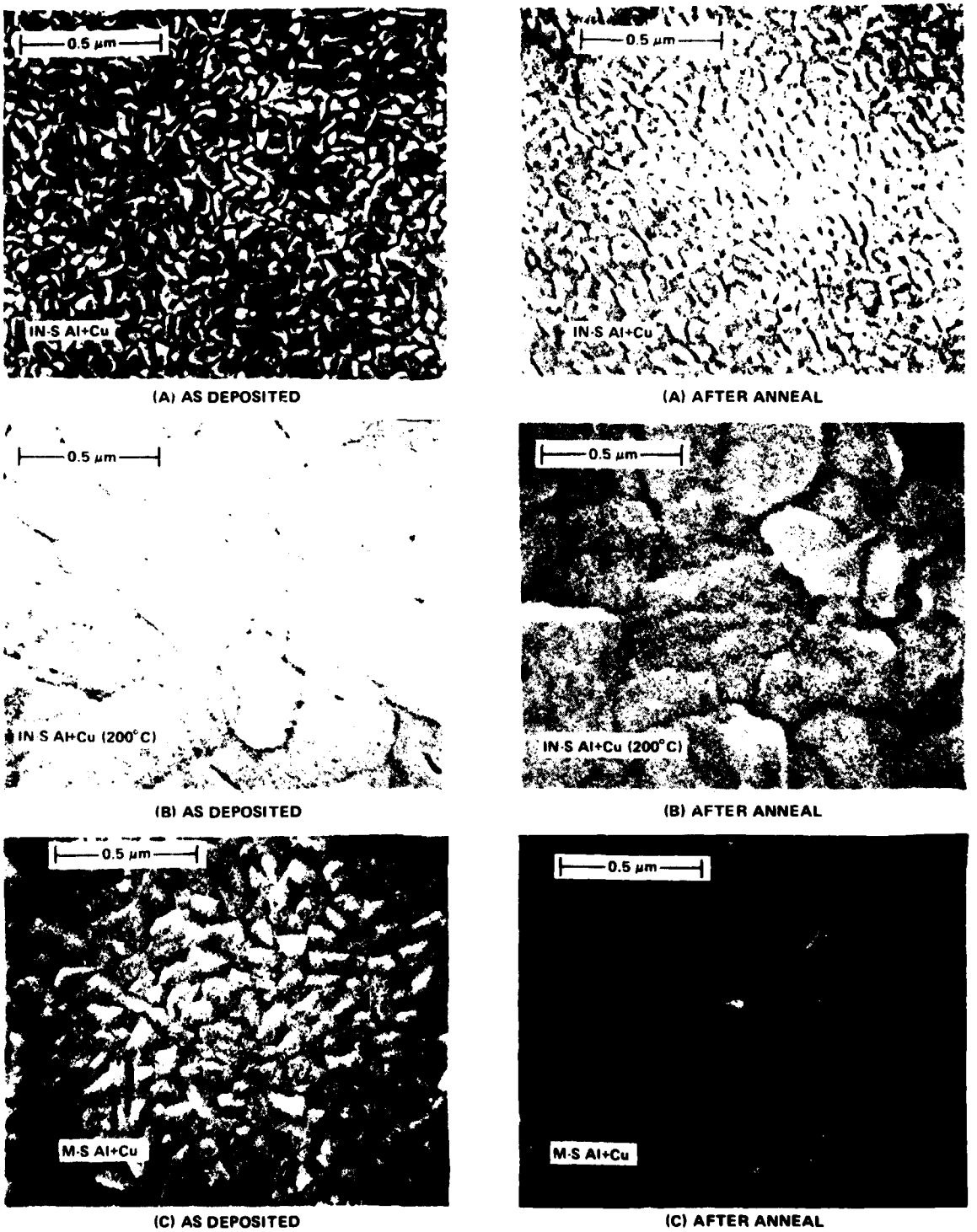

Figure 7. Scanning Electron Micrographs of Three Al+Cu Films: (A) IN-S Al+Cu (RT), (B) IN-S Al+Cu (200°C), (C) M-S Al+Cu. Before and After Anneal at 450°C for 15 minutes in N_2.

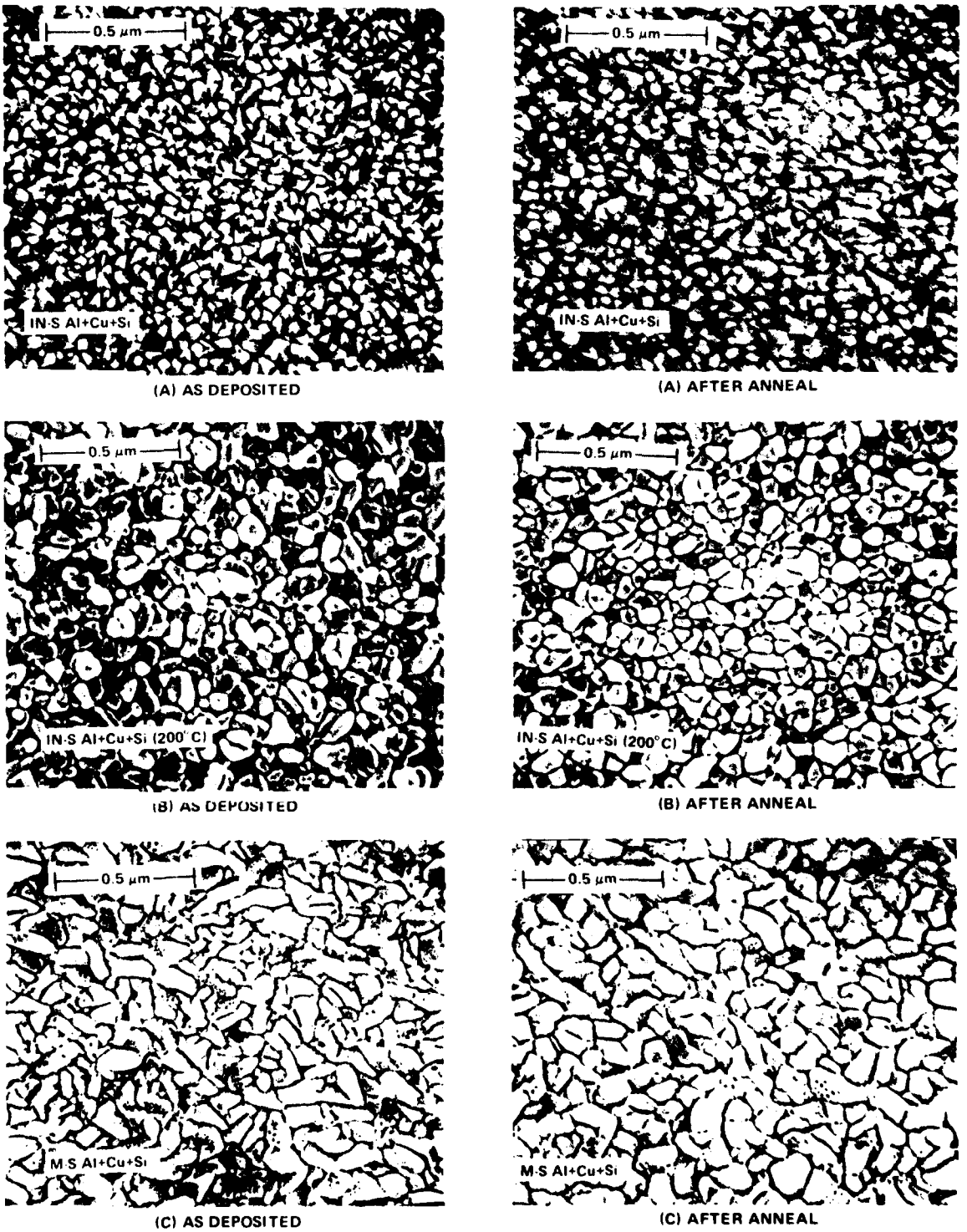

Figure 8. Scanning Electron Micrographs of Three Al+Cu+Si Films: (A) IN-S Al+Cu+Si (B) IN-S Al+Cu+Si (200°C), (C) M-S Al+Cu+Si

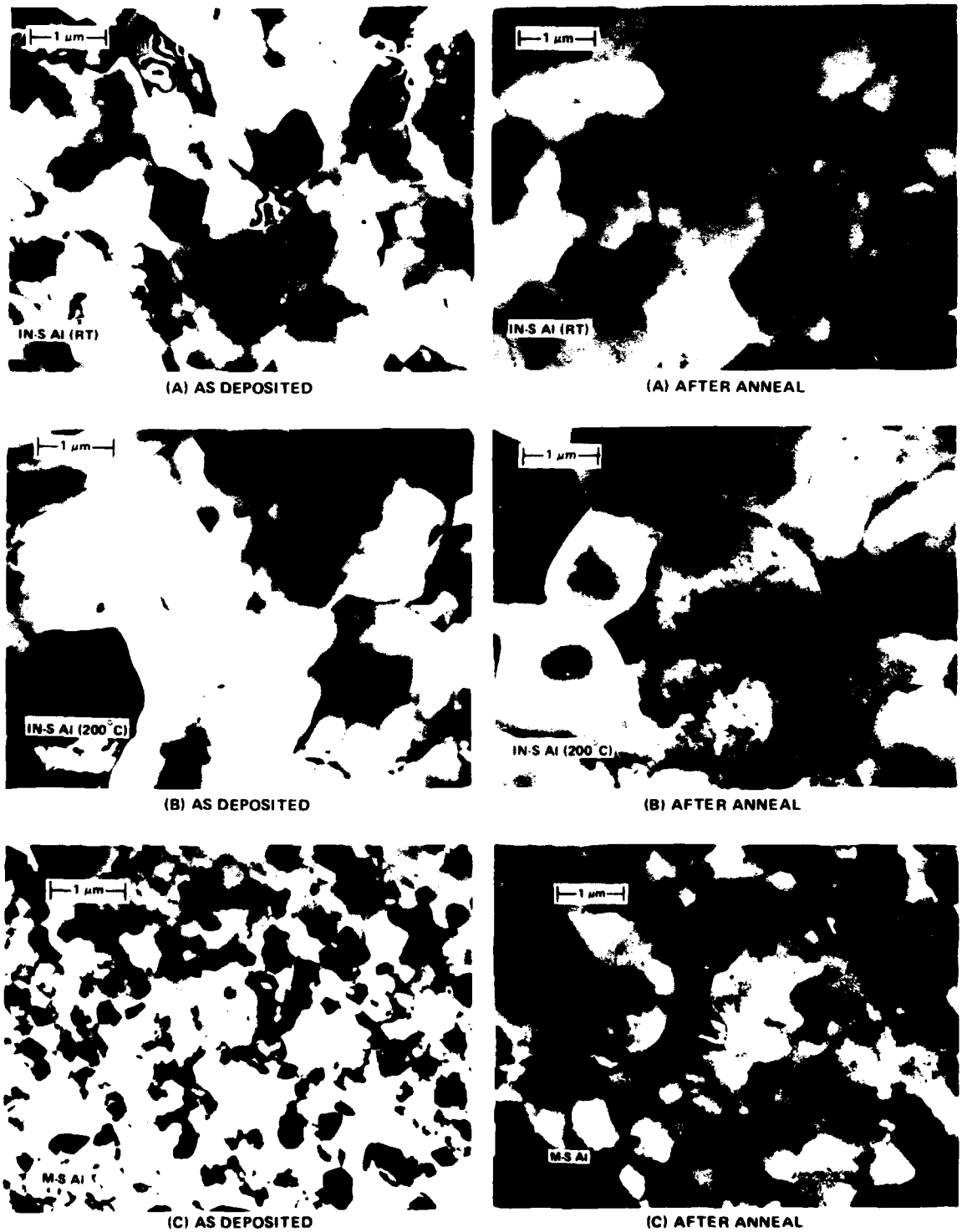

Figure 9. Transmission Electron Micrographs of Three Al Films: (A) IN-S Al (RT) (B) IN-S Al (200°C), (C) M-S Al. Before and After a 450°C Anneal for 15 minutes in N_2.

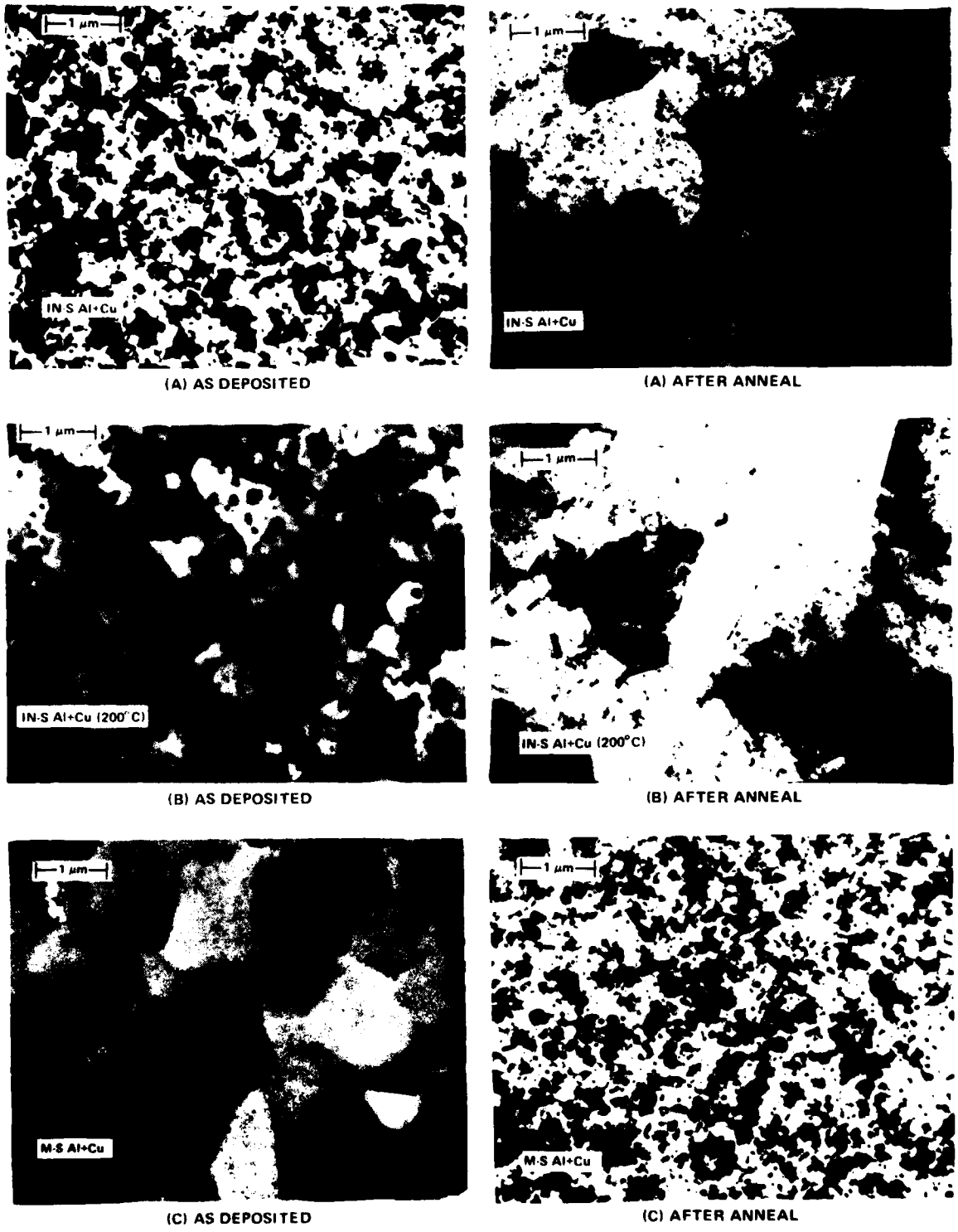

Figure 10. Transmission Electron Micrographs of Three Al+Cu Films: (A) IN-S Al+Cu (RT), (B) IN-S Al+Cu (200°C), (C) M-S Al+Cu. Before and After a 450°C Anneal for 15 minutes in N_2.

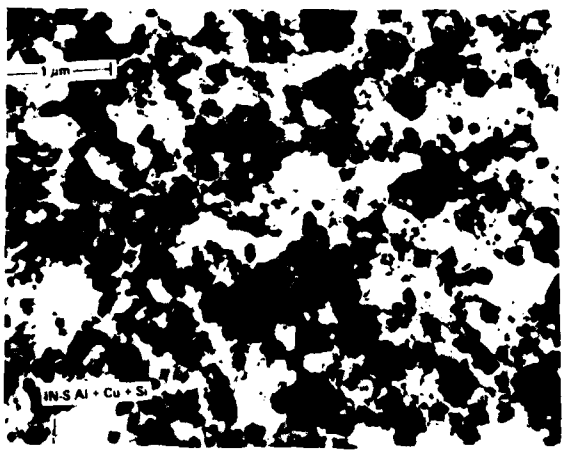

(A) AS DEPOSITED

(A) AFTER ANNEAL

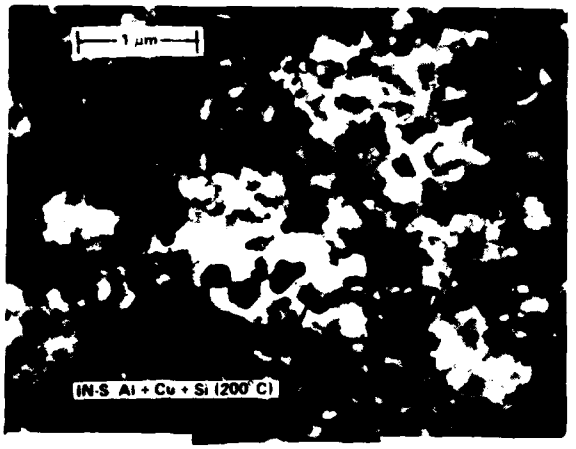

(B) AS DEPOSITED

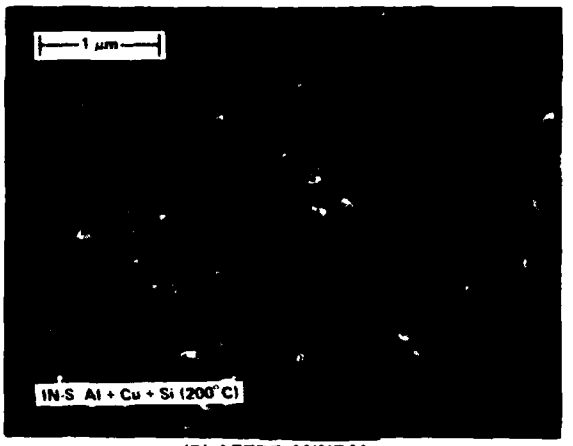

(B) AFTER ANNEAL

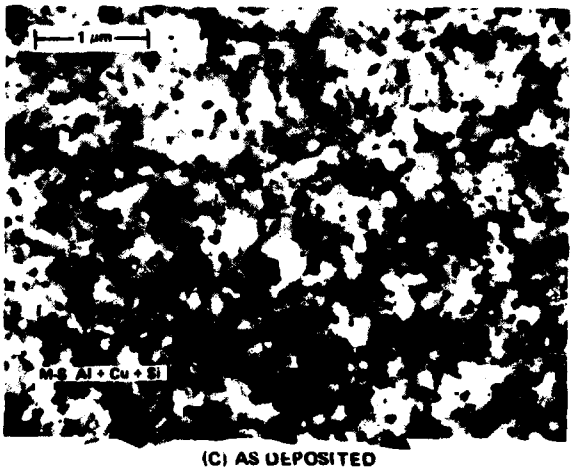

(C) AS DEPOSITED

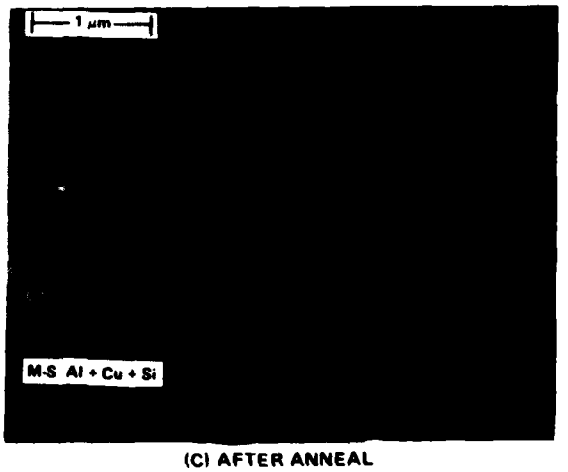

(C) AFTER ANNEAL

Figure 11. Transmission Electron Micrographs of Three Al+Cu+Si Films: (A) IN-S Al+Cu+Si (RT), (B) IN-S Al+Cu+Si (200°C), (C) M-S Al+Cu+Si. Before and After a 450°C Anneal for 15 minutes in N_2.

Table 2. Copper and Silicon Concentration in Al+Cu and Al+Cu+Si Films

No.	Film		Planned Composition Cu %	Planned Composition Si %	Substrate Temp	Film Thickness	Chemical Analysis† Cu %	Chemical Analysis† Si %	X-Ray Fluorescence Cu μgm/cm²	X-Ray Fluorescence Cu %	Electron Microprobe As-Deposited Film Al %	Electron Microprobe As-Deposited Film Cu %	Electron Microprobe As-Deposited Film Si %	Electron Microprobe Annealed Film Al %	Electron Microprobe Annealed Film Cu %	Electron Microprobe Annealed Film Si %
4	Al+Cu	IN-S	2.0	–	RT	762	1.94	–	3.3	1.6	98.78	1.22	–	98.17	1.74	0.09
4*	Al+Cu	IN-S	2.0	–	RT	762	–	–	–	–	98.57	1.43	–	97.96	1.95	0.09
5	Al+Cu	IN-S	2.0	–	200°C	762	2.20	–	3.6	1.8	99.46	0.54	–	97.84	2.04	0.12
5*	Al+Cu	IN-S	2.0	–	200°C	762	–	–	–	–	98.83	1.17	–	97.30	2.58	0.12
6	Al+Cu	M-S	2.0	–	RT	836	1.94	–	3.7	1.6	98.57	1.43	–	98.35	1.53	0.12
6*	Al+Cu	M-S	2.0	–	RT	836	–	–	–	–	98.42	1.58	–	98.28	1.60	0.12
7	Al+Cu+Si	IN-S	3.85	1.0	RT	850	3.94	0.71	7.4	3.2	96.18	3.03	0.79	98.13	1.29	0.58
8	Al+Cu+Si	IN-S	3.85	1.0	200°C	813	5.29	0.84	10.3	4.7	95.71	3.35	0.94	98.29	1.01	0.70
9	Al+Cu+Si	M-S	2.0	1.0	RT	938	1.86	1.1	4.2	1.7	98.0	1.45	0.55	98.13	1.27	0.60

*Copper concentration determined by sweeping the electron beam over a 40 X 40 μm^2 area of the film

†Films deposited on sapphire substrates were employed for silicon analysis

b. X-Ray Fluorescence

Copper concentration in Al+Cu and Al+Cu+Si films prepared by IN-Source and dc magnetron have been determined by using X-Ray Fluorescence techniques,[23] and the results are summarized in Table 2. The values of copper content are good to within ±10%.

c. Electron Microprobe Analysis

Copper concentration in Al+Cu films and Cu and Si concentrations in Al+Cu +Si films were determined by electron microprobe analysis[24] using an accelerating voltage of 5 kV to limit electron penetration to about 500 nm. Beam diameter was on the order of 1 to 1.5 μm. Results are tabulated in wt % in Table 2.

A comparison of these results with those obtained by the X-Ray Fluorescence technique points out a discrepancy in the copper concentration of Al+Cu films. This is possibly due to inhomogeneous distribution of Cu in the film. Since the electron-beam size (1 to 1.5 μm in diameter) is on the same order of magnitude as that of the grain size of the film (1 to 1.5 μm), a statistical variation of Cu and Si distribution in the film may have contributed to this discrepancy.

Experiments were repeated to resolve the discrepancy in the Cu concentration by using a beam swept over an approximate area of 40 X 40 μm^2. These results are shown in Table 2 with an asterisk.

d. Ion Microprobe

An attempt has been made to determine the Cu distribution within the films by depth profiling and ion microprobe.[25,26] Depth profiles for three samples: (1) film number 5: Al+Cu IN-S (200°C), (2) film number 6: Al+Cu M-S (RT,) and (3) film number 9 Al+Cu+Si M-S (RT) are shown in Figure 12. There appears to be some accumulation of copper near the substrate as reported earlier by other workers.[16]

e. Summary

Several characterization techniques, such as Scanning Transmission Electron Microscopy, X-ray Fluorescence, Electron Microprobe, and standard wet chemical methods have been employed to examine the Al, Al+Cu and Al+Cu+Si films deposited by IN-Source and dc magnetron sputtering. An attempt has been made to depth profile three films of Al+Cu and Al+Cu+Si films with Ion Microprobe. Table 3 summarizes the Al-Alloy films used for characterization by various techniques.

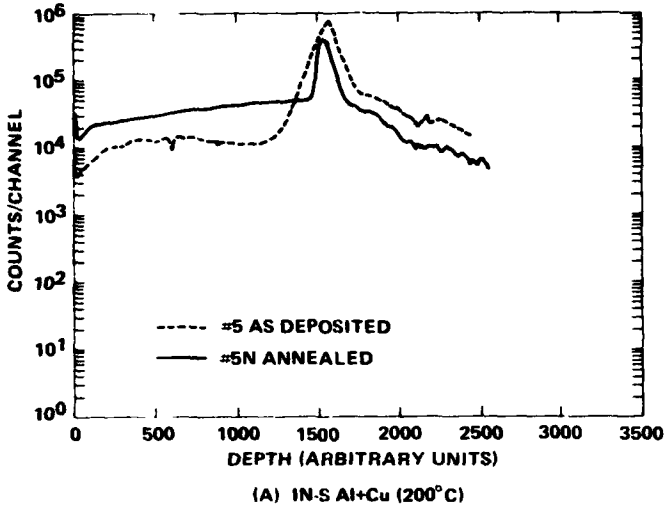

(A) IN-S Al+Cu (200°C)

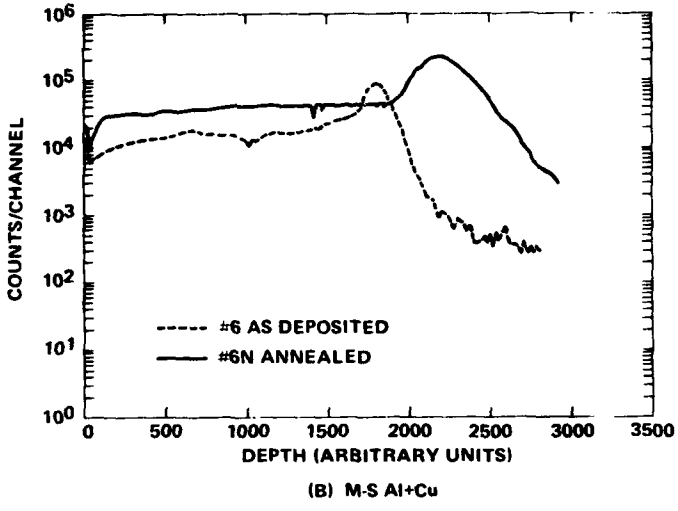

(B) M-S Al+Cu

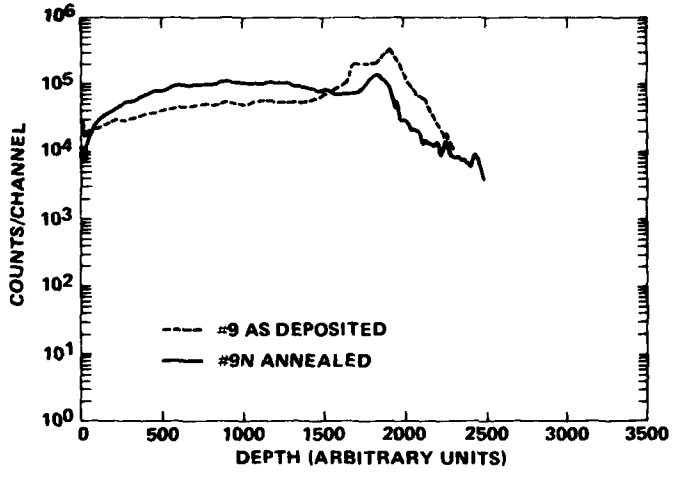

(C) M-S Al+Cu+Si

Figure 12. Copper Profiles of Three Films by Ion Microprobe: (A) IN-S Al+Cu (200°C), (B) M-S Al+Cu and (C) M-S Al+Cu+Si

Table 3. Summary of Characterized Al, Al+Cu and Al+Cu+Si Film Samples

Characterization	Film Deposition Technique	Al-Alloy Films						Films Used For Testing					
		Al		Al+Cu		Al+Cu+Si		Al		Al+Cu		Al+Cu+Si	
		I	F	I	F	I	F	I	F	I	F	I	F
Scanning Transmission	IN-S	1	1	4	4	7	7	–	–	–	–	–	–
Electron Microscopy	IN-S	2	2	5	5	8	8	–	–	–	–	–	–
	M-S	3	3	6	6	9	9	10	10	11	11	12	12
X-Ray Fluorescence	IN-S	–	–	4	–	7	–	–	–	–	–	–	–
	IN-S	–	–	5	–	8	–	–	–	–	–	–	–
	M-S	–	–	6	–	9	–	–	–	11	–	12	–
Electron Microprobe	IN-S	–	–	4	4	7	7	–		–		–	–
	IN-S	–	–	5	5	8	8	–		–		–	–
	M-S	–	–	6	6	9	9	–		11		12	–
Chemical Analysis	IN-S	–	–	4	–	7	–	–	–	–		–	
	IN-S	–	–	5	–	8	–	–	–	–		–	
	M-S	–	–	6	–	9	–	–	–	11		12	
Ion Microprobe	IN-S	–	–	–	–	–	–	–		–		–	
	IN-S	–	–	–	5	–	–	–		–		–	
	M-S	–	–	–	6	–	9	–		–		–	

I As Deposited film

F After anneal at 450°C for 15 minutes in N_2

Numbers in the table correspond to sample numbers referred to in Tables 1 and 2 and text.

SECTION IV
TEST STRUCTURE FABRICATION

A. SELECTION OF FILM DEPOSITION METHOD AND JUNCTION DEPTHS FOR CONTACTS

The present investigation has been undertaken to study the electromigration behavior of Al, Al+Cu and Al+Cu+Si films used for IC interconnections. Addition of Cu to Al has been considered to realize the beneficial effects of Cu in improving electromigration resistance; also the addition of Si is considered to minimize the erosion of Si from contact windows of shallow junction devices by providing adequate amounts of Si to meet solid solubility requirements of Al at the maximum device processing temperature subsequent to Al film deposition. Device annealing and packaging temperatures range from 400°C to 530°C and solid solubility of Si in Al at 530°C is 1 wt %. It is worth noting that electromigration behavior of Al+Cu films depends not only on the Cu content but also on the microstructure of films. Several authors have shown that MTFs of Al film conductors (usually 10 to 20 μm wide) under high current stress increase with average grain size and also with homogeneity of the film.

In the present study, an attempt has been made to characterize the composition and microstructure of Al, Al+Cu and Al+Cu+Si films vacuum-deposited by two methods: (1) an IN-Source, i.e., evaporation from a molten Al-Alloy source held at predetermined temperature (power setting) and source composition is tailored to yield a desired composition in the deposited films, and (2) dc magnetron sputtering from a target whose composition is chosen to be that of the desired film. In case of IN-Source deposition, process controls are necessary at the source level. It does not induce radiation damage in MOS devices. In the dc magnetron case, once the target material is fabricated to specification, control of film composition appears to be a minor problem and MOS device damage, if any, is considered annealable. However, if one examines the possibility of depositing ternary Al-Alloy films and also refractory metal films such as Ti:W, Mo, W, $MoSi_2$, etc., in a single deposition system with multiple sources, sputter deposition has a distinct advantage over evaporation by IN-Source. If one considers the availability of high throughput automated metal deposition equipment, dc magnetron sputter deposition has a certain advantage over IN-Source deposition because deposition systems equipped with dc magnetrons are commercially available and automated deposition systems equipped with IN-Sources are being introduced.

Since our film characterization experiments have shown that both IN-Source and dc magnetron deposition methods are capable of producing desired film compositions with almost equivalent microstructure, and that no data are available on the electromigration behavior of sputter-deposited Al-Alloy films, a basic decision was made to proceed with dc magnetron-deposited Al-Alloy films for electromigration testing.

With recent advances in device designs and process technologies, it is somewhat difficult to state precisely the depth of a shallow junction device. It is true that Al films doped with Si are considered to minimize the erosion of silicon from contact windows. About 3 to 5 years ago, devices with 0.8 to 1.0 μm junction depths, fabricated by conventional diffusion processes, would have been considered shallow junction devices; however, with recent improvements in Ion Implantation technology, 0.3 to 0.5 μm junction depths are routinely achievable and at this time it seems reasonable to categorize devices with 0.3 to 0.5 μm junction depths as shallow junction devices.[27,28] Hence Ion Implantation technology was chosen to form n^+ resistor tanks in the p^+ regions with a shallow junction depth ($\approx$ 350 nm) for studying Silicon/Al-Alloy film contacts.

B. PROCESS FLOW

A process flow as shown in Figure 13 was used to fabricate the test structures starting with 3-inch diameter, 20-mil thick, p^- 0.5 to 5.0 Ω-cm (100) orientation silicon substrates. These substrates were carried through appropriate implants, anneals and/or steps to fabricate the n^+/p^+ structures shown in Figure 13.

After the ion implants and anneals, the substrates were subdivided into three groups and each group was metallized with dc magnetron sputter-deposited Al, Al+Cu and Al+Cu+Si films approximately 8KÅ in thickness. Film thickness and resistivity data collected on pilots from the same deposition runs for all three films are summarized in Table 4. Specific resistivity data shown in parentheses are those for corresponding films mentioned in Table 1. Agreement is well within 3%. The Al, Al+Cu and Al+Cu+Si films on pilot slices were used for characterization experiments as outlined in Table 3. Transmission electron micrographs of these film samples in as-deposited condition and after a 450°C, 15-minute anneal in N_2 are presented in Figure 14. Film composition data collected from wet chemical analysis, Electron Microprobe and X-Ray Fluorescence are summarized in Table 4. Histograms of grain size distribution of Al, Al+Cu and Al+Cu+Si films before and after a 450°C anneal for 15 minutes in N_2 are shown in Figure 15. These data, when compared with those presented earlier, show that film properties are reproducible.

The metallized substrates were regrouped and carried through lead definition and a contact anneal at 450°C for 15 minutes in N_2. Subsequently, a protective coating of silicon dioxide of nominal thickness, 8KÅ, was deposited on these substrates in a TI-built plasma reactor. Actual thickness of the oxide as measured on a pilot slice was closer to 9KÅ. Finally, the slices were processed through bond-pad oxide removal step and made ready for multiprobe.

A special probe card was fabricated to facilitate probing of the various test structures on the bar. Three slices from each group of metallization were chosen for multiprobe. Individual test structures, except CBSR6 and SR6MM (see Figure 1), were tested to determine their respective resistance values. Since resistance values of the film conductors (test structures HCSO1 and HCSO3) designed for electromigration testing are in the 2 to 5 Ω range, efforts were concentrated on probing these low value resistors. Also, as an internal check, two pilots with patterned leads of Al and Al+Cu films on oxidized slices were probed to determine the resistance values of HCSO3 test patterns with nominal dimensions of 60 squares (15-mil long by 0.25-mil wide). Probe data on HCSO3 test structures on Al and Al+Cu pilot slices are summarized in Table 5. The measured

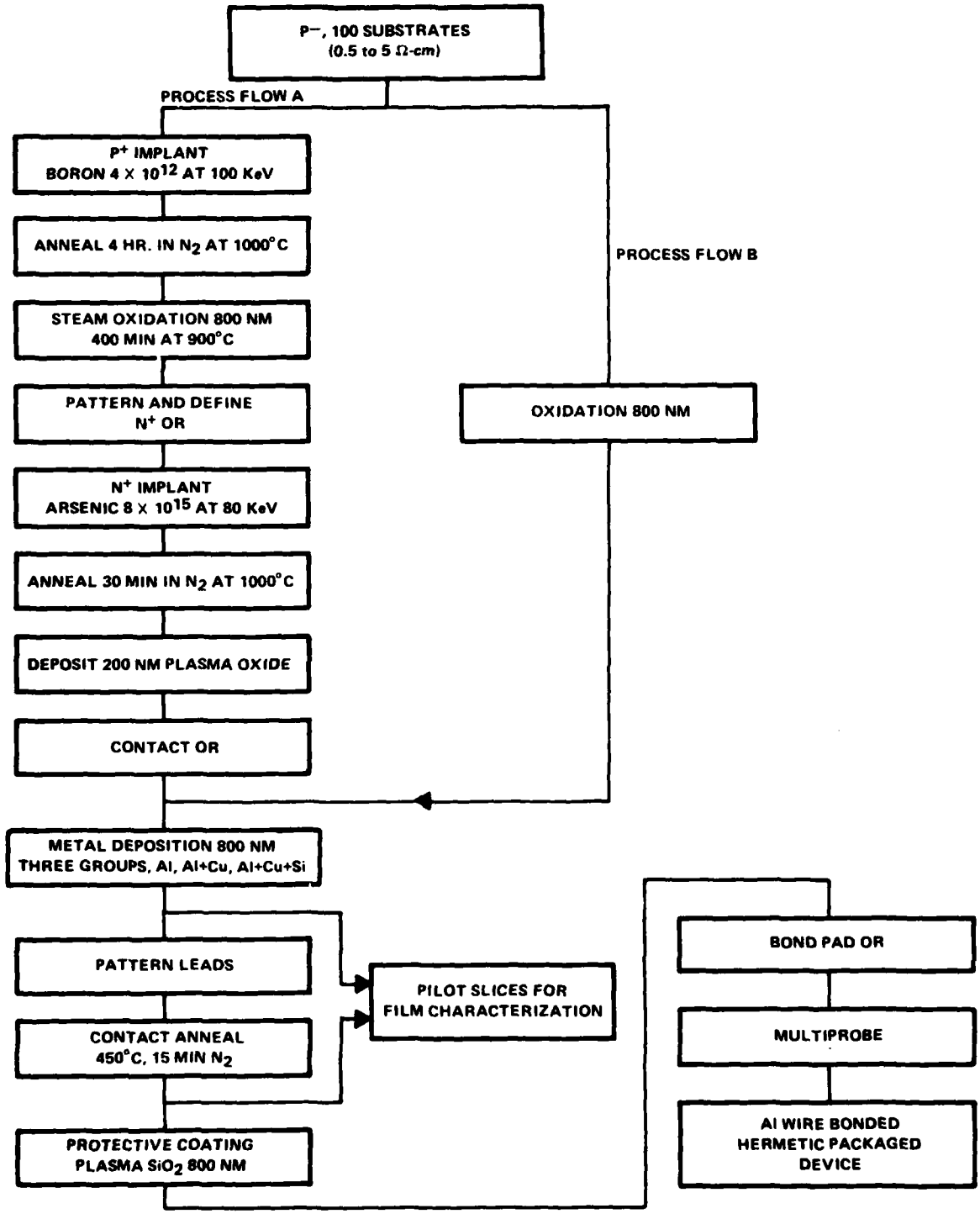

Figure 13. Process Flow

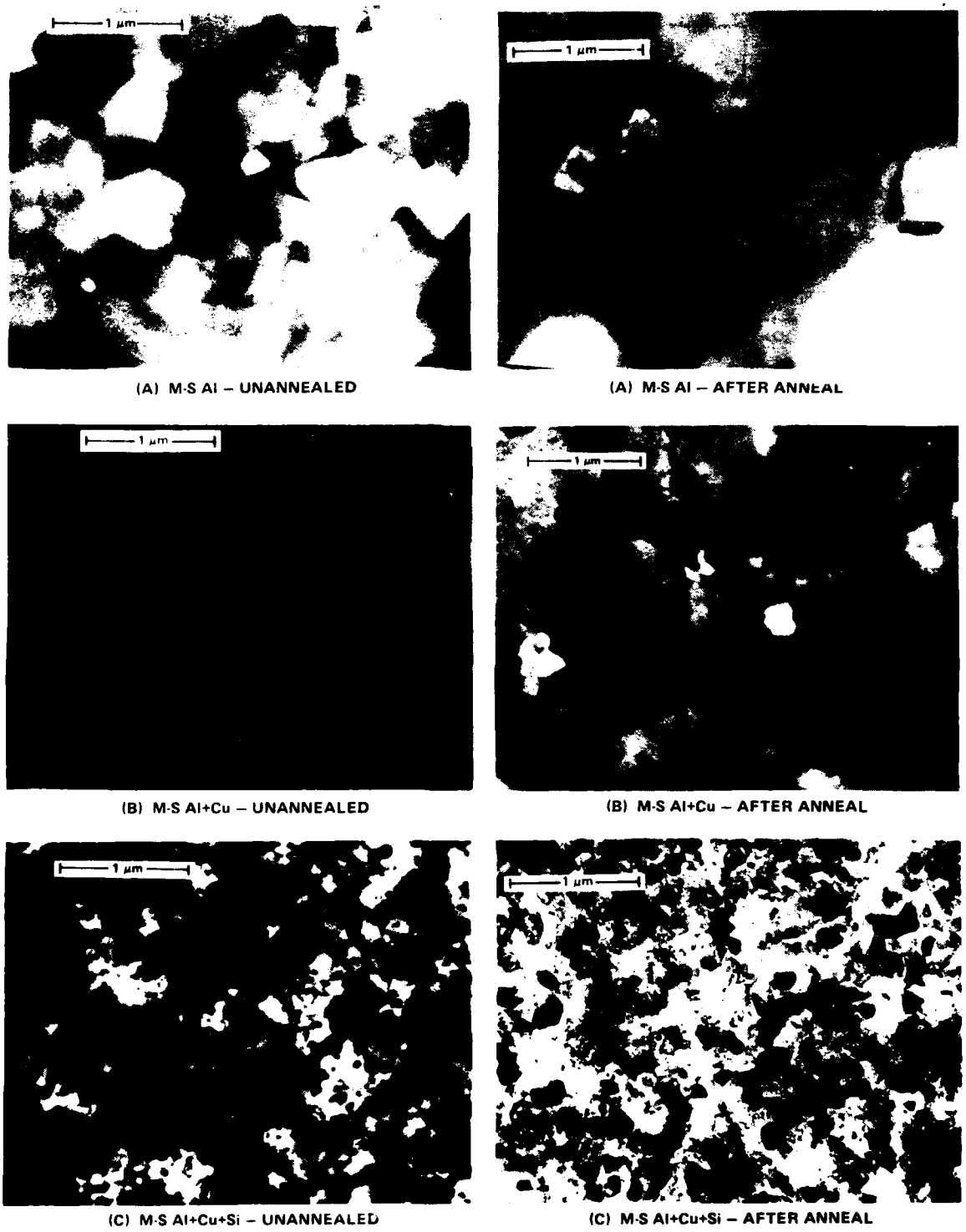

Figure 14. Transmission Electron Micrograph of DC Magnetron Sputtered (A) Al, (B) Al+Cu and (C) Al+Cu+Si. Before and After 450°C 15 minutes Anneal in N_2.

Table 4. Magnetron Sputter Deposited Al, Al+Cu, and Al+Cu+Si Films used for Fabricating Test Structures

Sample	Film		Planned Composition		Thickness (nm)	Specific Resistivity (μΩ-cm)*	Grain Size (μm)		Chemical Analysis		X-Ray Fluorescence		Electron Microprobe	
			% Cu	% Si			As Deposited	Annealed	Cu %	Si %	Cu %	Si %	Cu %	Si %
10	Al	M-S	–	–	787	2.83 (2.90)	0.75	1.25	–	–	–	–	–	–
11	Al+Cu	M-S	2.0	–	798	3.99 (4.10)	0.30	0.75	2.0	–	2.0	–	2.18	–
12	Al+Cu+Si	M-S	2.0	1.0	781	4.53 (4.50)	0.12	0.32	2.8	0.8	1.8	–	1.93	0.82

*Numbers in parentheses are for corresponding films described in Table 1.

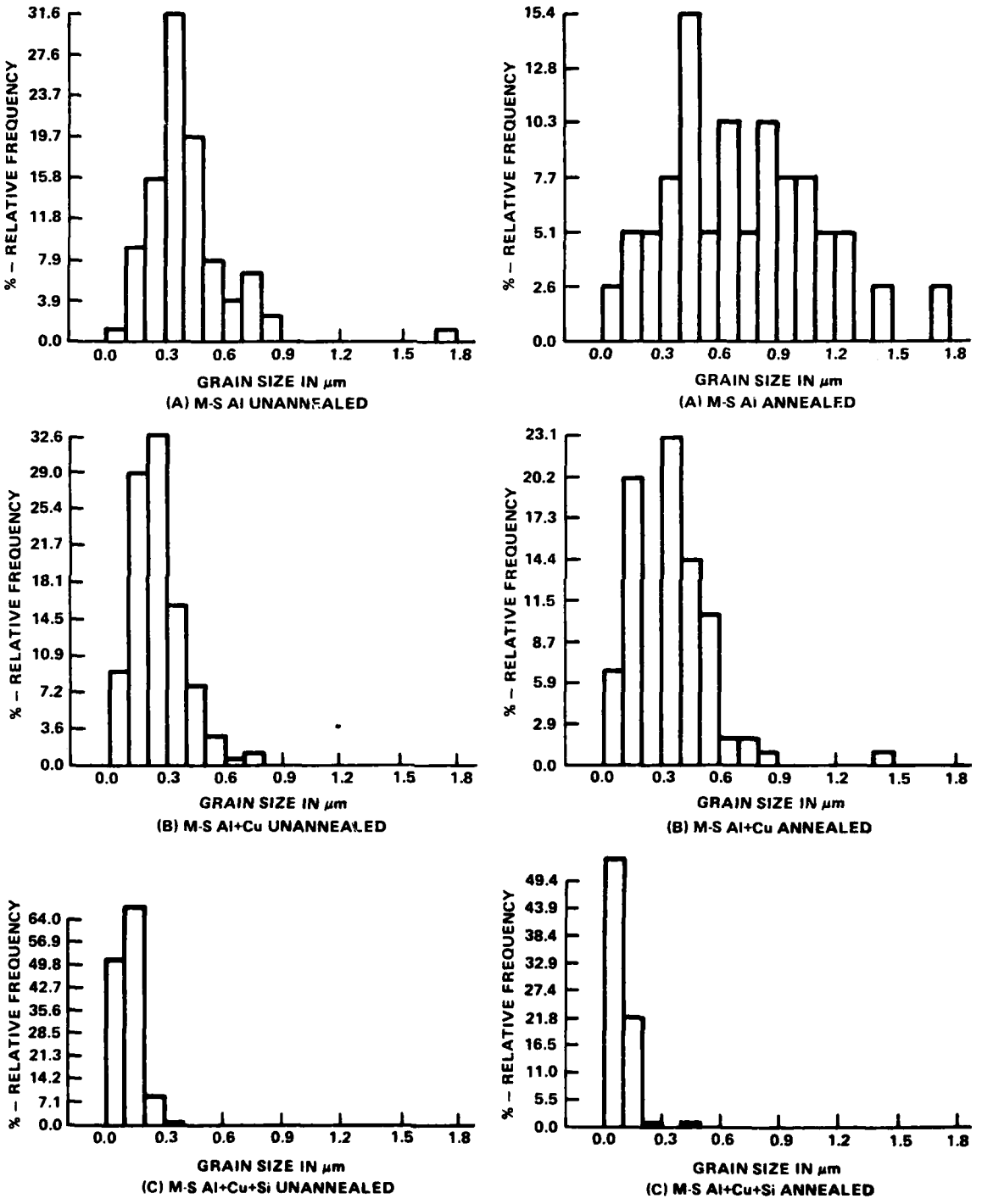

Figure 15. Histograms of the Grain Sizes of (A) M-S Al, (B) M-S Al+Cu and (C) M-S Al+Cu+Si Films

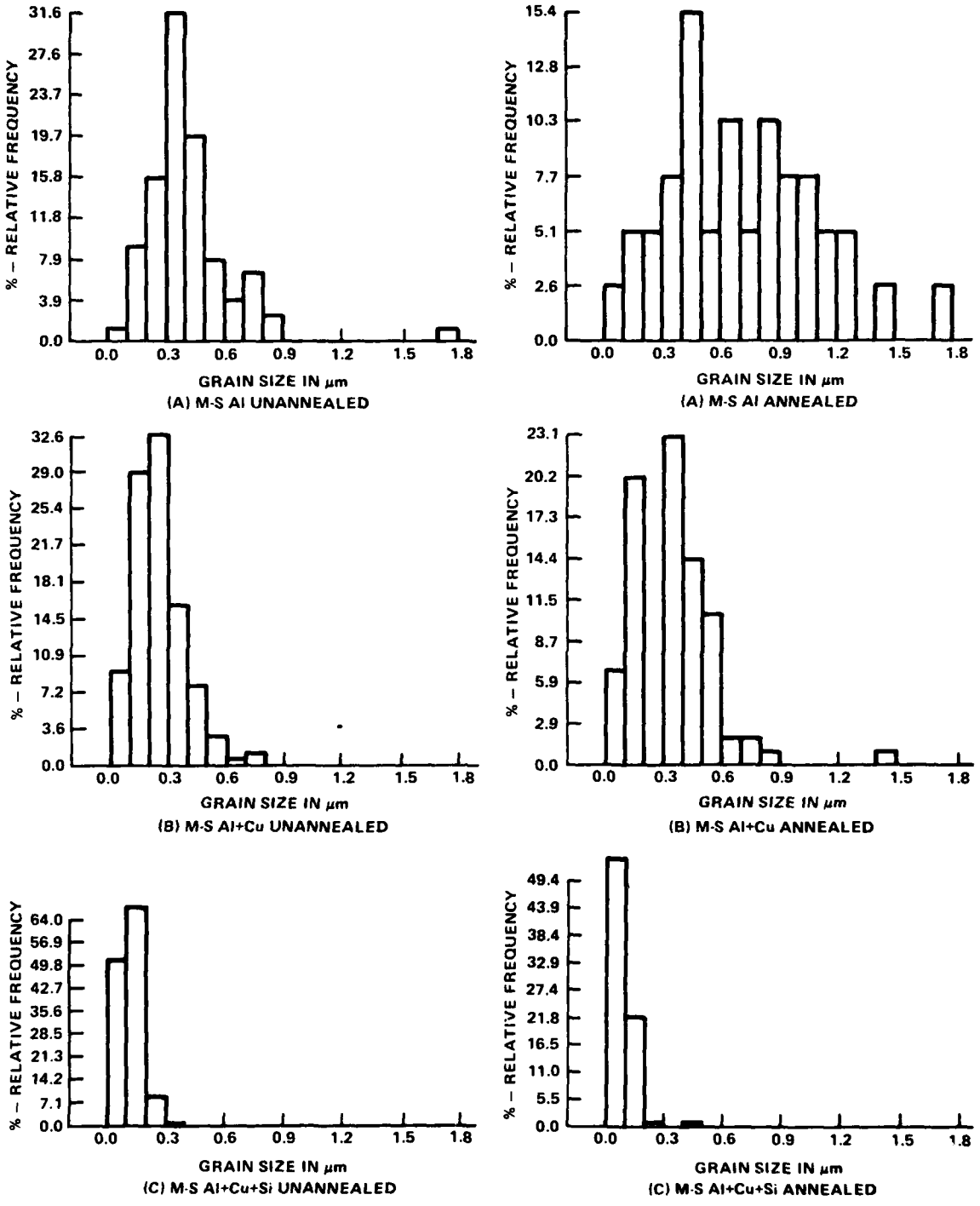

Figure 15. Histograms of the Grain Sizes of (A) M-S Al, (B) M-S Al+Cu and (C) M-S Al+Cu+Si Films

Table 5. Sample Data on Resistance of HCSO3 Lead Patterns on Pilot Slices

Film	Resistance Sheet Ω/□	Anticipated Value Ω	Measured Value Ω	Total No. of Units Tested
Al	0.036	2.2	3.066 · 0.08	751
Al+Cu	0.050	3.0	3.491 · 0.09	748

values are somewhat higher than the anticipated values. This discrepancy is possibly due to contact problems of probe tips at bond pads and associated measuring equipment and not due to dimensional variations of the leads. The data are presented here to highlight one of the multiprobe problems in measuring low resistance values. Multiprobe data for test structures HCSO1 and HCSO3 on three groups of slices with Al, Al+Cu and Al+Cu+Si metallizations are presented in Table 6. Analysis of multiprobe data shows that HCSO3 values track those of HCSO1.

Table 6. Summary of Probe Data

Metal	Slice No.	No. of Units Tested	Test Structures			
			HCSO1		HCSO3	
			Range (Ω)	No. of Units	Range (Ω)	No. of Units
Al	10-1	755	2.713 4.469	415	2.879 4.367	209
	10-2	756	2.685 4.161	525	3.077 4.644	523
	10-3	651	3.038 4.170	619	2.876 4.394	641
Al+Cu	11-1	300	3.150 4.264	276	2.972 4.238	144
	11-2	675	3.132 4.430	304	2.776 4.385	637
	11-3*					
Al+Cu+Si	12-1	435	2.778 3.879	360	2.786 3.884	391
	12-2	616	2.740 4.252	516	2.655 3.880	528
	12-3	596	2.662 4.090	370	2.670 3.836	500

*Slice No. 11-3 has contact problems on bond pads.

The electrically probed slices were carried through back-lap (thinning the slice), scribe, and assembly operations. Electrically good bars were alloy (Au+Ge) mounted on standard 16-pin dual in-line packages. One-mil Al (with 1 wt % Si) wire was ultrasonically bonded to the bond pads. Appropriate bonding schemes were used to facilitate testing of test structures HCSO1, HCSO3, HCSL2, CRLT4, and CRLT7. The packages were hermetically sealed the glass sealing temperature of the package was in the 450°C to 500°C range. The 16-pin CERDIP packages were symbolized and ready for testing.

Resistance values of some of the test structures were measured at 5 mA current) using a sample size of 20 packaged units. Data are summarized in Table 7. The resistance values of CRLT4 and CRLT7 consist of: (1) resistance of Al-Alloy leads, (2) contact resistance of 50, 150 or 200 contacts, depending on the 1, 3 and 4 strings included for measurement, and (3) resistance of a number of diffused resistors depending on the 1, 3 and 4 strings included in the measurements. Further analysis of this data will be discussed in a later section.

Table 7. Sample Data on Resistance Values of HSCO3, CRLT4 and CRLT7 Test Structures

Test Structure	Al	Al+Cu	Al+Cu+Si
HCSO3	2.96 ± 0.24	3.04 ± 0.26	2.84 ± 0.19
CRLT4			
1 String*	791 ± 78	1037 ± 120	852 ± 82
3 Strings	2012 ± 241	2684 ± 313	2555 ± 242
4 Strings	2658 ± 284	3510 ± 407	3405 ± 316
CRLT7			
1 String	832 ± 67	1136 ± 126	953 ± 88
3 Strings	2112 ± 209	2692 ± 389	2870 ± 259
4 Strings	2777 ± 251	3860 ± 516	3817 ± 345

* Resistance of CRLT4 = $R_{\text{metal leads}} + 50\,R_c + 25\,R_s$
R_c = contact resistance of Si/Al-Alloy interface.
R_s = sheet resistance of diffused resistor

SECTION V
TESTING

A. ELECTROMIGRATION TESTING

Electromigration testing of Al, Al+Cu and Al+Cu+Si films has been carried out with two test structures HCSO1 and HCSO3. These two test structures have identical dimensions for the conductor stripes to be used for electromigration testing except for the fact that current to the test stripe of HCSO1 is fed through a silicon/metal interface, whereas current to the test stripe of HCSO3 is fed through an Al/Al interface at the bond pad (see Figure 3). Nominal dimensions of the test stripe are: length = 380 μm (15 mils); width = 6.35 μm (0.25 mil). Film thickness of all three films is close to 0.8 μm. The average cross section of these three film conductor stripes, as determined from thickness and width measurements on actual stripes, is equal to 4.8×10^{-8} cm^2 within ±5%; hence a 48-mA current through any one of the test stripes corresponds to a current density of 1×10^6 A/cm^2.

Electromigration testing of these three films was carried out at a current density of 1×10^6 A/cm^2 at four different ambient temperatures 150°C, 175°C, 195°C and 215°C. For each test temperature, a sample size of 20 has been chosen to determine the MTF for each film. Hence at a given test temperature, 20 samples each of test structures HCSO1 and HCSO3 with Al, Al+Cu and Al+Cu+Si films, with a cumulative total of 120 samples are to be tested at a current density of 1×10^6 A/cm^2 and hence each test sample carries 48 mA.

In order to accomplish this task, test boards with sockets for 16-pin CERDIP and associated control panels have been fabricated. All test samples, appropriately identified, can be loaded on the test boards and placed in temperature-controlled air circulating ovens. Each test sample is connected in series with a standard 100-Ω resistor and a variable (0 to 100 Ω) resistor pot. All the test samples, each one with its two resistors, are connected in parallel across a 9-volt power supply. Current in each test sample can be set at 48 mA by adjusting the variable resistor to read 4.8 V across the standard 100-Ω resistor. Test boards are filled with 20 samples each of test structure HCSO1 and HCSO3 for each film and these six boards are placed in an oven set at a predetermined temperature. Current in the samples is turned on. The oven temperatures stabilize in less than 30 minutes. Then voltage drop across the conductor stripe [e.g., bond pads 18 and 19 for HCSO1 (see Figure 1)] is measured at regular intervals to determine the time to failure (t_f) of each sample. Criterion for t_f is adopted as follows: time to develop an electrical open or a 50% increase in lead resistance, whichever occurs first. For HCSO1, junction shorting to the substrates reduces the voltage drop.

Following this procedure, time to failure data for Al, Al+Cu and Al+Cu+Si films tested at 150°C, 175°C, 195°C, and 215°C have been collected. Since t_f data have been collected by reading the voltage drops across the test stripes at predetermined intervals, t_f for any failed sample is in error by the time interval between two successive readings. As a result, relative magnitude of the

errors is somewhat larger for samples tested at 215°C and 195°C temperatures, as compared to those tested at 150°C and 175°C. Since the MTFs of Al, Al+Cu and Al+Cu+Si film conductors at a fixed current density are so different from each other for any test temperature, some discretion has been exercised to interrupt the tests even though all the samples from each group did not fail. The 150°C and 175°C tests on Al+Cu and Al+Cu+Si films with the HCSO3 test structures have been interrupted after 1840 hours.

Time to failure (t_f) data are assumed to obey log-normal distribution and have been plotted on log-normal probability paper to verify the accuracy of this assumption. The 150°C t_f data for test structure HCSO1 and the 175°C t_f data for test structure HCSO3, plotted on log-normal probability graphs are presented in Figures 16 and 17 respectively. Early failures with HCSO1 test structure for Al+Cu and Al+Cu+Si films show some deviation from the anticipated log-normal distribution, however most of the observations tend to follow the anticipated log-normal distribution. If the early failures (freak failures?) are ignored, the log-normal probability plot is an excellent aid for determining MTF and σ for a given set of t_f data. The t_f data collected with HCSO1 and HCSO3 test structures for Al, Al+Cu and Al+Cu+Si films have been analyzed using the log-normal probability plots and the MTF data for all these tests are summarized in Table 8. Average values of σ are also shown in Table 8.

In the 150°C test with HCSO3 test structures, only one sample from each group of Al+Cu and Al+Cu+Si films had failed when the test was interrupted after 1840 hours; hence no MTF values for Al+Cu and Al+Cu+Si films at 150°C are shown in Table 8. Furthermore, in the 175°C test with HCSO3 test structures, only three samples of Al+Cu+Si films, as compared to 10 samples of Al+Cu films, had failed when the testing was suspended after 1840 hours. The MTFs of Al+Cu+Si films, shown in Table 8, are extrapolated values of t_{50} from the log-normal probability plots developed from a limited number of failed samples, hence these values should be considered with a certain amount of caution. In this series of experiments, Al+Cu+Si film samples showed longer times to failure than those observed for Al+Cu samples under equivalent test conditions.

An Arrhenius plot of MTF versus (1000/absolute temperature) is shown in Figure 18 for Al, Al+Cu and Al+Cu+Si films tested with HCSO1 test structures and a similar plot for these films tested with HCSO3 test structures is shown in Figure 19. The activation energies derived from these plots are shown in Table 8.

In Figure 20, the early data on Ti:W/Al and Ti:W/Al+Cu film conductors, 0.8-μm thick, 9-μm wide, and 1140-μm long are included.

B. FAILURE MODE

1. Test Structure HCSO1

At the conclusion of electrical tests, all hermetically glass sealed units were opened and examined with an optical microscope at magnifications ranging from 200 to 2000X. Typical examples of the failure modes observed with Al, Al+Cu and Al+Cu+Si films are presented in Figure 21. In all cases, the failure mode was shorted (burned) contacts and only in a few isolated cases were open leads and

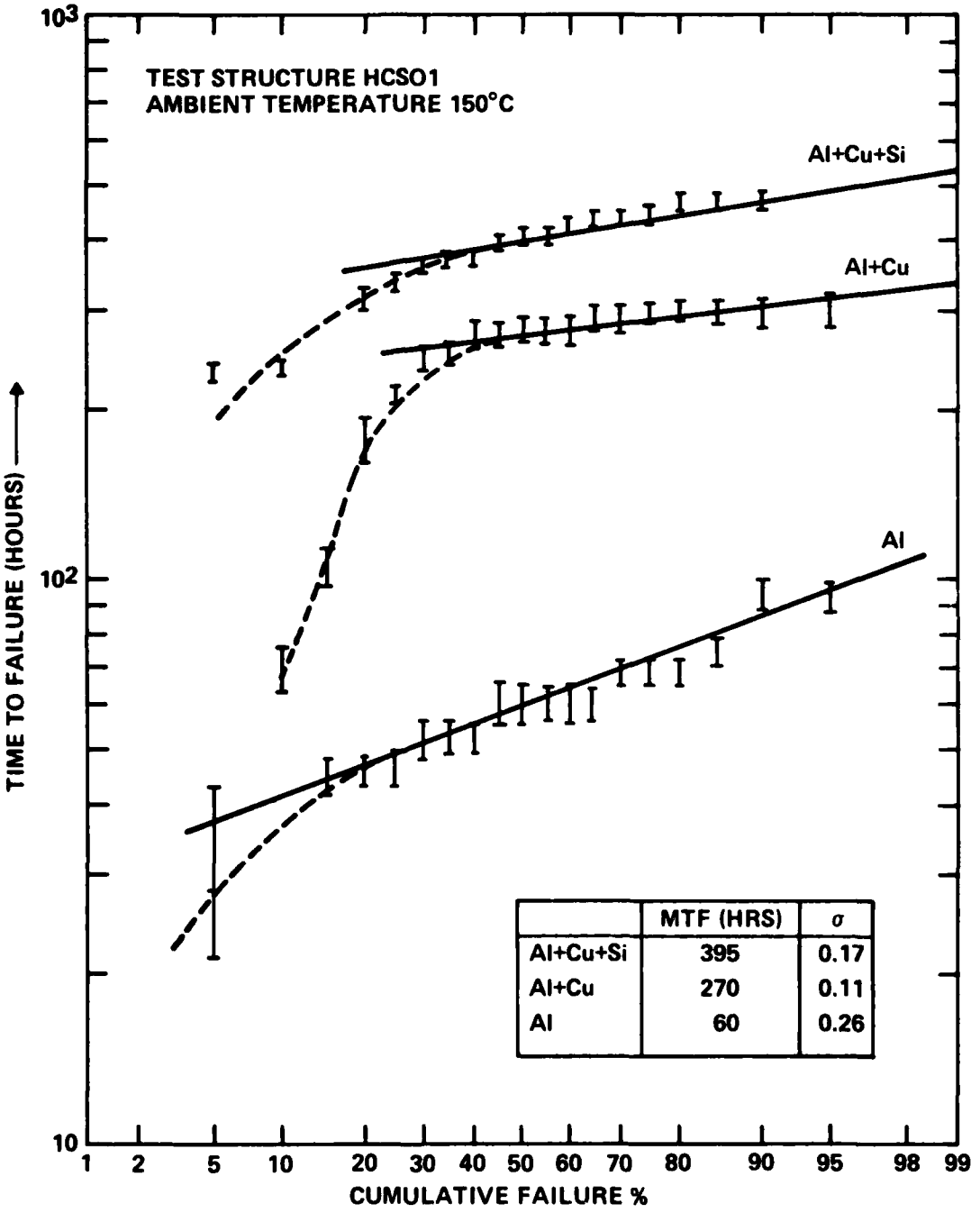

Figure 16. Log-Normal Probability Plots of the Times to Failures of HCSO1 Test Structure Subjected to 1×10^6 A/cm^2 at 150°C

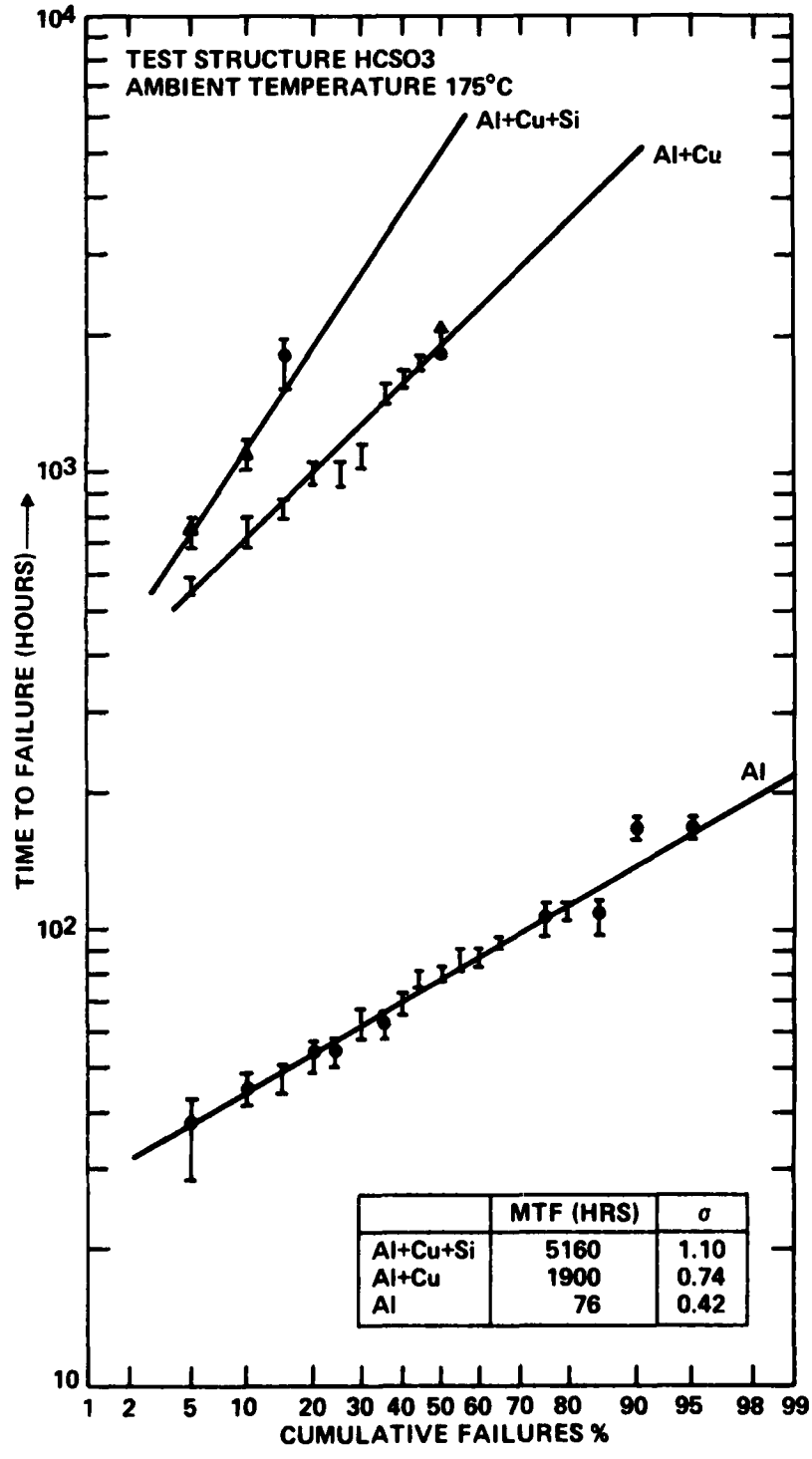

Figure 17. Failures for HCSO3 Test Structures Metallized with Al, Al+Cu and Al+Cu+Si Films Subjected to Current Density of 1×10^6 A/cm^2 at 175°C

Table 8. Mean Time to Failure Data for Al-Alloy Film Conductors Tested at 1×10^6 A/cm^2

Ambient Temperature °C	Test Structure HCSO1 – Si/Al Contacts MTF (hr)			Test Structure HCSO3: Lead Pattern MTF (hr)		
	Al	Al+Cu	Al+Cu+Si	Al	Al+Cu	Al+Cu+Si
215	8	31	27	26	420	(1750)*
195	16	53	49	34	720	(2700)*
175	42	230	165	76	1900	(5100)*
150	60	270	395	115	–	–
$<\sigma>$	0.15	0.13	0.15	0.45	0.80	1.24
Q eV	0.58	0.64 (0.60)†	0.76 (0.74)†	0.43	0.70	0.50
MTF at 80°C in Hours	1582	11,555 (6,880)†	27,143 (22,232)†	1291	258,824	167,917
MTF at 55°C in Hours	6553	57,660	183,490 (144,015)†	3815	1,546,184	594,902

*MTF extrapolated

†Q calculated with 175°C data rejected

burned contacts observed. Metal migration between contacts 1 and 2 (see Figure 21), as seen for Al and Al+Cu samples, was common. The contacts identified by numbers 2 and 4 showed some pitting. Invariably at contact number 4, it appeared that metal film exploded at failure.

2. Test Structure HCSO3

All units used in electromigration testing were opened and examined with an optical microscope at magnifications ranging from 200X to 2000X. There were no surprises. The electrical opens were distributed at random along the length of the test stripe and Figure 22 shows the failures for the set of 20 Al film stripes tested at 195°C. Some of the failed units were further examined with the scanning electron microscope and typical failures for Al, Al+Cu and Al+Cu+Si film stripes are shown in Figure 23.

C. EFFECTS OF HIGH-TEMPERATURE STORAGE

1. Metallurgical Stability of Al-Alloy Films

Since the resistivity data for Al, Al+Cu and Al+Cu+Si films presented in Table 1 clearly show that resistivities decrease subsequent to a 450°C, 15-minute anneal, it is of considerable interest to examine the metallurgical stability of Al-Alloy film interconnections at device operating temperature. For this purpose, the HCSO3 test structure was selected to monitor the room-temperature resistance of the test stripe stored at 150°C for a cumulative total of 1000 hours. A sample size of 20 was chosen for each metallization and the average room-temperature resistance for each group determined at time t=0. The samples were stored at 150°C. Room-temperature resistance values of

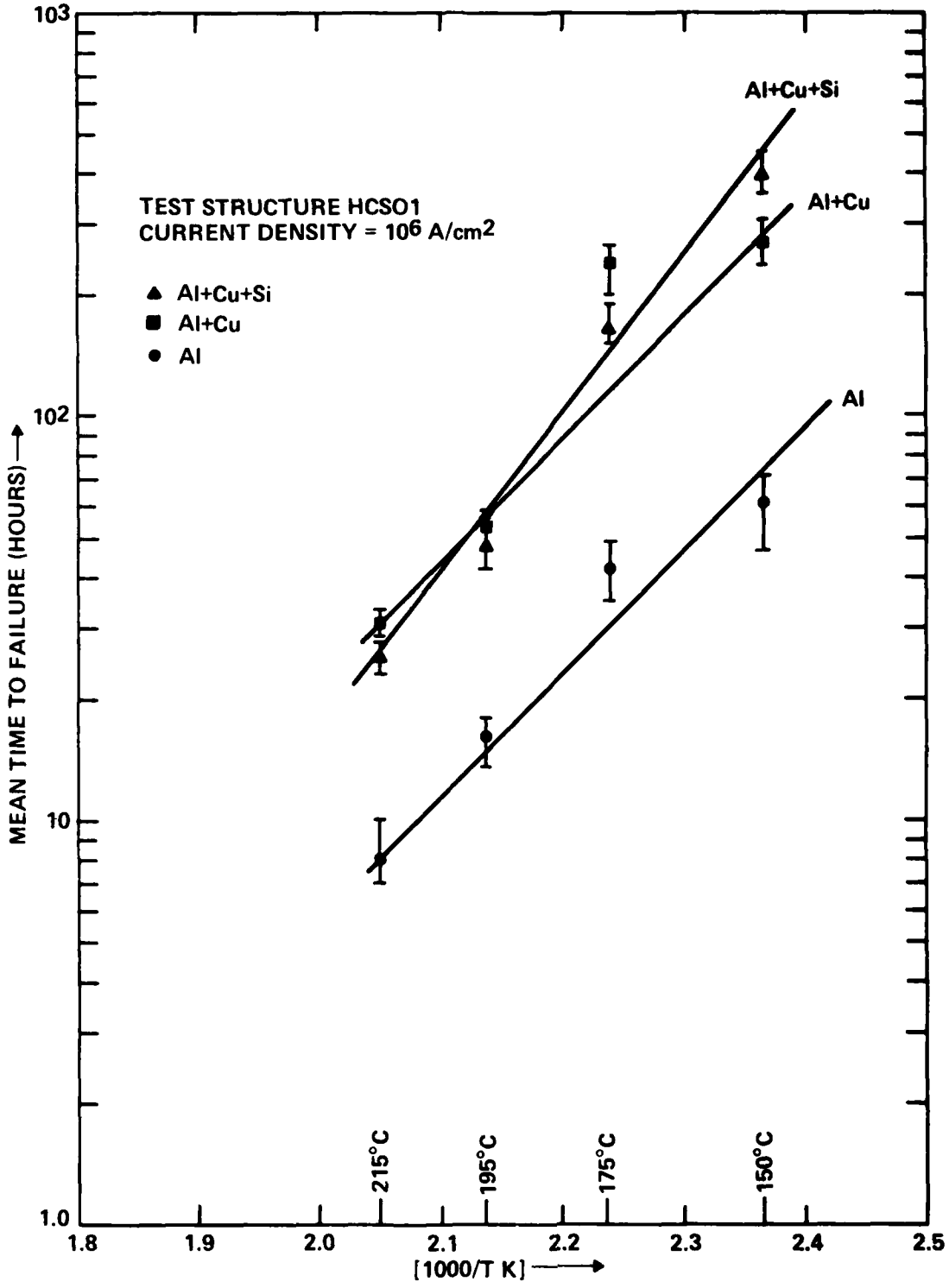

Figure 18. Arrhenius Plots of MTFs vs (1000/T K) for the Activation Energy Determinations at a Current Density of 1×10^6 A/cm^2 for Al, Al+Cu and Al+Cu+Si Metallized Si/Al-Alloy contacts (HCSO1 Test Structure)

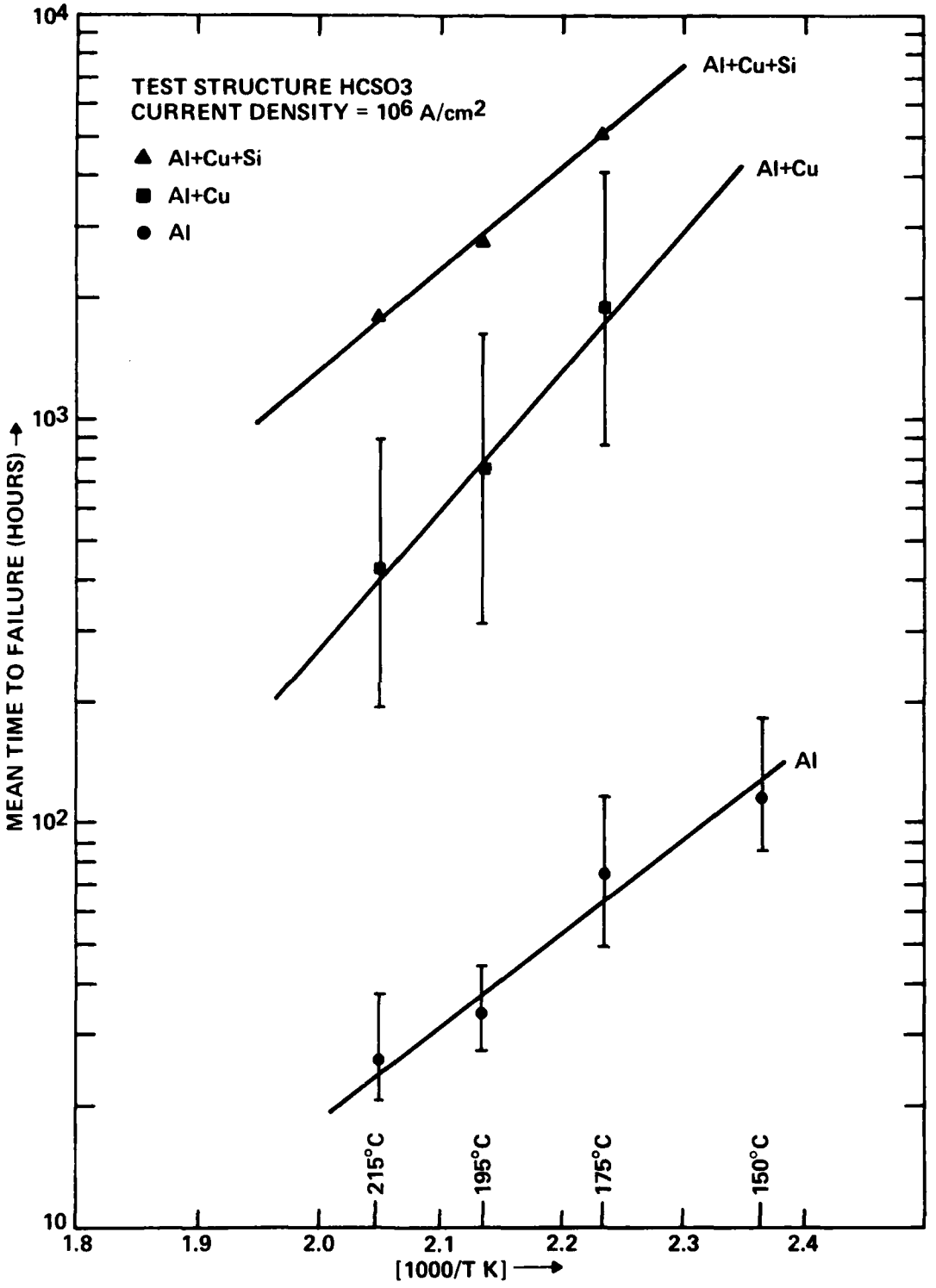

Figure 19. Arrhenius Plots of MTFs vs (1000/T K) for the Activation Energy Determinations at a Current Density of 1×10^6 A/cm^2 for Al, Al+Cu and Al+Cu+Si Film Conductors (HCSO3 Test Structure)

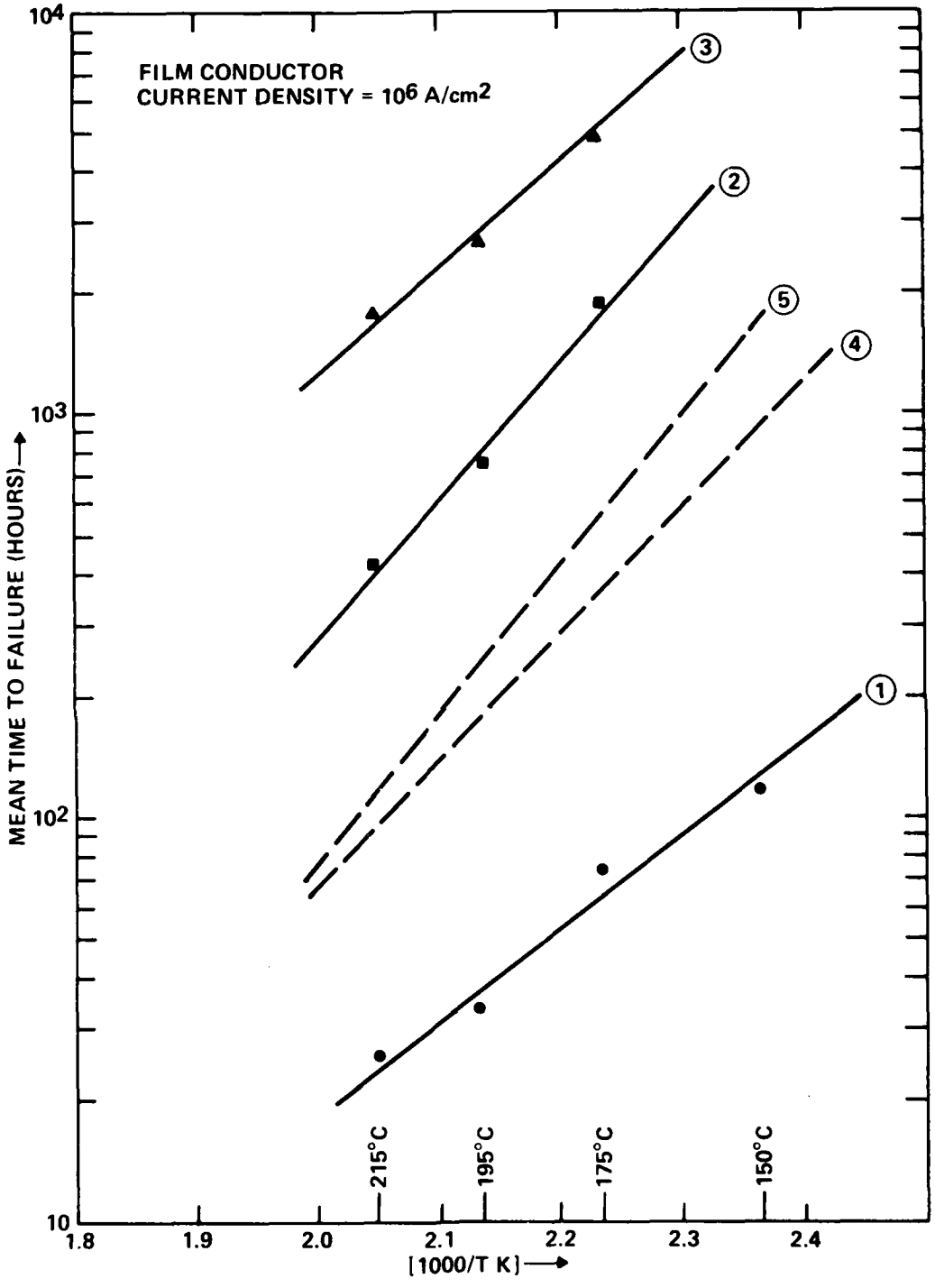

Figure 20. Arrhenius Plots of MTFs vs (1000/T K) for 6 μm Wide (1) M-S Al, (2) M-S Al+Cu and (3) M-S Al+Cu+Si Film Conductors (HCSO1 Test Structures) Tested at 1×10^6 A/cm^2 Along with Earlier Data on 9-μm Wide (4) Ti:W/Al and (5) Ti:W/Al+Cu (IN-S) Film Conductors also Tested at 1×10^6 A/cm^2.

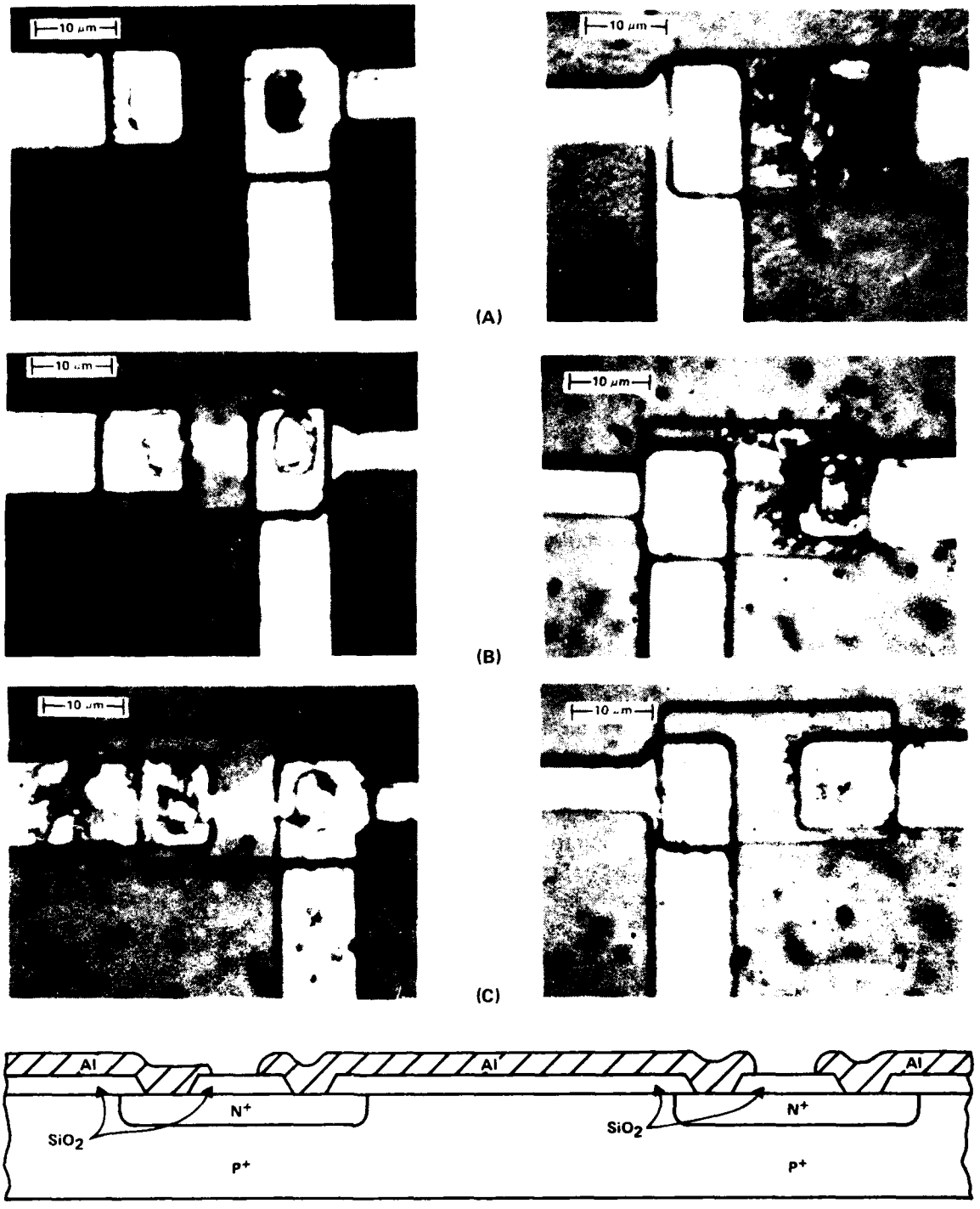

Figure 21. Contacts of HCSO1 Test Structures with (A) Al, (B) Al+Cu and (C) Al+Cu+Si Films Tested at 195°C Under a Current Stress of 1×10^6 A/cm^2.

Figure 22. Random Distribution of Open Failures Observed for a Set of 20 Al Film Conductors Tested at 1×10^6 A/cm^2 and 195°C Ambience

these samples were determined after 150, 500, 750 and 1000 hours of storage. Data are summarized in the Table 9. These data show that the average resistance values decrease approximately 4% in the first 500 hours of storage and these films are stable after that time. Also these data show that most of the resistance annealing has taken place in the previous 450°C, 15-minute anneal step (see process flow). Some further decrease in the resistance values of Al+Cu and Al+Cu+Si films may be anticipated due to further precipitation of Cu and Si. However, for all practical purposes, the resistance values of Al+Cu and Al+Cu+Si films past 1000 hours at 150°C are well within 5% of the values observed for pure Al films.

2. Contact Resistance of Si/Al-Alloy Interfaces

The primary objective of this experiment is to determine the contact resistance of Si/Al-Alloy interfaces and also the stability of these contacts. Test structures CRLT4 and CRLT7, especially designed for this experiment, have been used to monitor the contact resistance of Si/Al-Alloy contacts as a function of storage time at 150°C. The test structure CRLT4 (see Figures 1 and 4) consists of a chain of 200 silicon/metal contacts, each with an area (0.5×0.25 mil^2) 24.2×10^{-8} cm^2 in series with 100 n^+ diffused resistors of 1 square each. Thus a measured resistance value of CRLT4 test structure is given by

$$R_{CRLT4} = R_{metal\ leads} + 200\ R_c + 100\ R_s$$

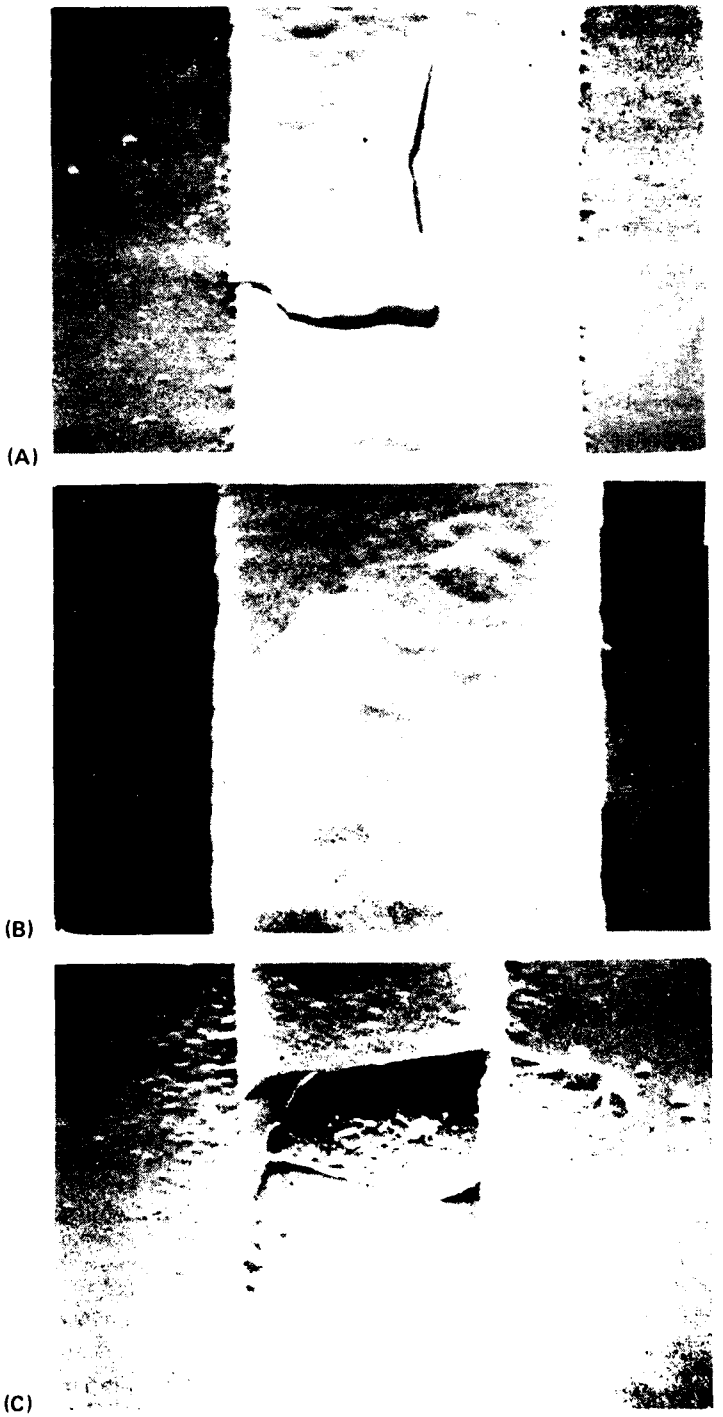

Figure 23. Typical Failures Observed with (A) Al, (B) Al+Cu and (C) Al+Cu+Si Film Conductors (HCSO3 Test Structures) Tested at 175°C and 1×10^6 A/cm^2

where R_c and R_s represent the contact resistance of each contact and the sheet resistance of the n^+ diffused regions respectively. Also, this test structure permits a resistance measurement of each string of 50 contacts and 25 squares of n^+ diffused regions. The resistance values of 1, 3 and 4 strings with 50, 150 and 200 contacts respectively were measured.

The sheet resistance measurement is accomplished with the aid of test structure HCSO5. The average value of the sheet resistance (R_s) has been determined from 30 measurements, with 10 measurements taken on each type of metallized slice.

$$R_s = 22.6 \pm 0.2\ \Omega$$

Hence, the contact resistance of 200 contacts (200 R_c) obtained by subtracting 100 R_s (2260 Ω) from a measured resistance value of CRLT4 (4 strings) is possibly in error by 20 Ω. Since the resistance of the metal leads connecting the contacts is on the order of 20 Ω, resistance of metal leads is neglected.

Similarly, test structure CRLT7 can be used for the contact resistance determination of Si/Al-Alloy interface by noting that the resistance of 200 contacts and 100 diffused resistors is 200 R_c + 115 R_s.

For this experiment, a sample size of 20 units from each type of metallization (Al, Al+Cu and Al+Cu+Si films) is chosen. The room-temperature resistance values of 1, 3 and 4 strings contacts of *test structure* CRLT4 for each unit are measured. All samples within each group were treated statistically equivalent and no attempt was made to maintain the identity of any sample. All the samples were stored in a 150°C ambience for a cumulative total of 1000 hours and the room-temperature resistance values were measured by interrupting the test at 150, 500, 750 and 1000 hours. Similar data was collected with the CRLT7 test structure for all three metallizations. The contact resistance values of 1, 3 and 4 strings corresponding to 50, 150 and 200 contacts in the CRLT4 and CRLT7 test structures for Al, Al+Cu, and Al+Cu+Si films were calculated and the normalized values of the resistances R(t)/R(0) as a function of storage time are presented in Table 9 and the data for 200 contacts with test structures CRLT4 and CRLT7 are presented in Figures 24 and 25 respectively.

Under simplifying assumptions (where current crowding, perimeter effects and others are neglected), the specific contact resistance ρ_c expressed in units of Ω-cm², a characteristic of the interface, is determined by the formula $\rho_c = R_c \times$ area of the contact window.

A quick glance at the data in the second column of Table 9 suggests that the average contact resistance value varies anywhere from 1.5 to 6 Ω for Si/Al-Alloy interface of (0.15 × 0.25 mil²) 24.2 × 10^{-8} cm². This corresponds to a specific contact resistance of 0.36 to 1.45 × 10^{-6} Ω-cm². This value is in general agreement with our earlier measurements on similar Si/Al interfaces.[13,14,29]

Table 9. Lead Resistance and Contact Resistance Data for Test Structures Stored at 150°C for 1000 Hours

Test Structure		Storage Time (hrs) →	Normalized Data $\frac{R(t)}{R(t=0)}$ 0	150	500	750	1000
HCSO3		Lead Resistance Ω R(t=0)					
Al		2.96 · 0.24	1.00	1.08	0.96	0.96	0.96
Al+Cu		3.04 · 0.26	1.00	1.05	0.96	0.94	0.96
Al+Cu+Si		2.84 · 0.19	1.00	1.07	0.96	0.96	0.96
CRLT4		Contact Resistance					
Al	1	207 · 87	1.00	0.35	0.26	0.24	0.27
	3	390 · 179	1.00	0.54	0.32	0.32	0.25
	4	481 · 222	1.00	0.76	0.46	0.46	0.44
Al+Cu	1	468 · 118	1.00	0.49	0.35	0.33	0.25
	3	988 · 312	1.00	0.77	0.52	0.47	0.36
	4	1250 · 407	1.00	0.91	0.67	0.61	0.50
Al+Cu+Si	1	287 · 83.4	1.00	0.86	0.62	0.59	0.67
	3	860 · 242	1.00	0.85	0.63	0.60	0.68
	4	1144 · 316	1.00	0.85	0.64	0.57	0.63
CRLT7							
Al	1	183 · 79	1.00	0.20	0.17	0.21	0.61
	3	248 · 142	1.00	0.40	0.15	0.16	0.43
	4	300 · 204	1.00	0.90	0.26	0.26	0.39
Al+Cu	1	496 · 127	1.00	0.43	0.32	0.34	0.71
	3	1025 · 385	1.00	0.68	0.53	0.47	0.66
	4	1272 · 506	1.00	0.88	0.67	0.62	0.66
Al+Cu+Si	1	292 · 81	1.00	1.01	0.85	0.78	0.79
	3	888 · 238	1.00	1.00	0.85	0.74	0.79
	4	1209 · 345	1.00	1.00	0.82	0.71	0.73

*Sample numbers 1, 3 and 4 correspond to 50 R_c, 150 R_c, 200 R_c

It should be pointed out that the average contact resistance values shown in Table 9 were obtained by rejecting the negative values obtained by subtracting 100 R_s from the measured CRLT4 resistance (and 115 R_s from the measured CRLT7 resistance) values. *A negative value is interpreted as a shorted device and hence a failure.* The number of failed units, as determined by the negative contact resistance criteria, are presented in Table 10.

The test structures CRLT4 and CRLT7 were automatically subjected to four different temperature storage tests during electromigration testing of HCSO1 and HCSO3 test structures. Once the visual inspection of the electromigration tested samples was completed, 20 samples from each metallization, 10 from HCSO1 and 10 from HCSO3, corresponding to each test temperature, were selected at random and the CRLT4 and CRLT7 test structures were electrically probed to collect contact resistance data. These data were analyzed and the number of failed units are summarized in Table 11. *In all cases, Al+Cu+Si metallization show zero failures.*

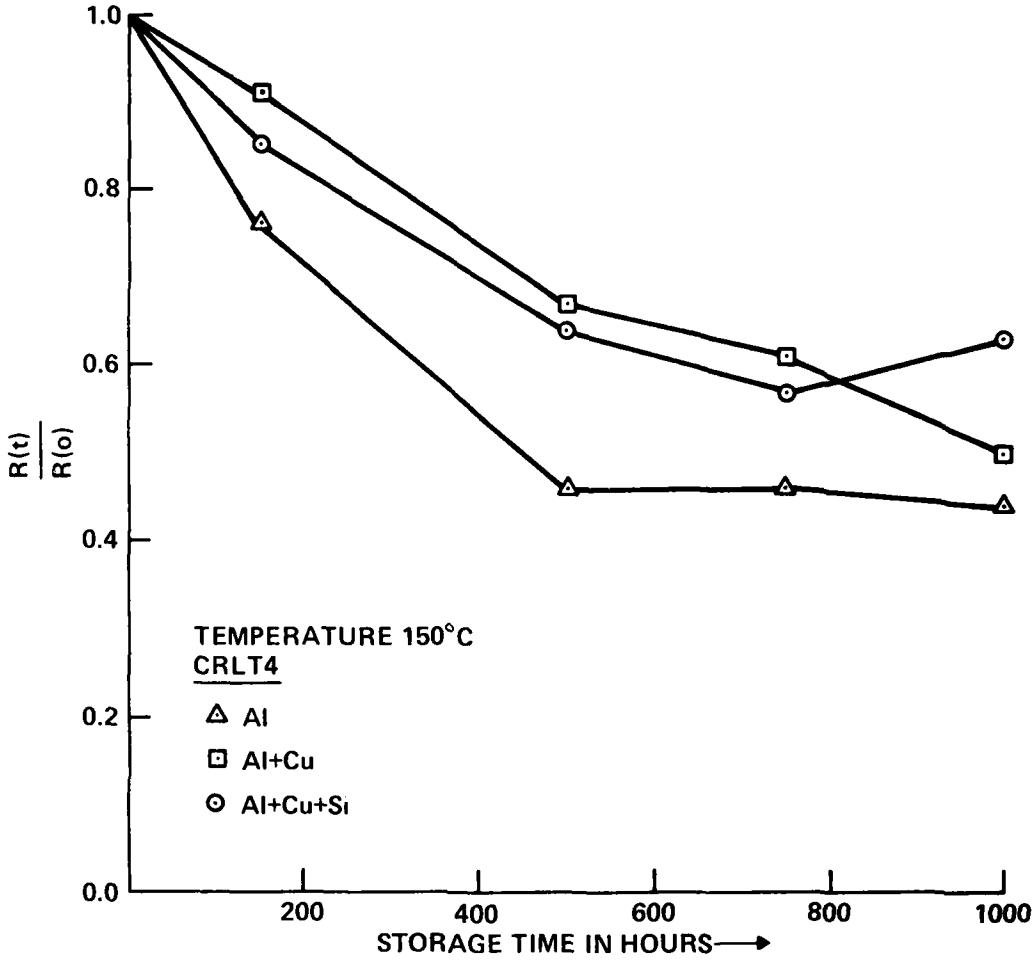

Figure 24. Normalized Contact Resistance of 200 Contacts as a Function of Storage Time at 150°C

Table 10. Failure Data on CRLT4 and CRLT7 Test Structures Stored at 150°C for 1000 Hours

Metal System		Storage Time in Hours				
		0	150	500	750	1000
Al	CRLT4	4/20	5/19*	9/20	9/20	10/20
	CRLT7	4/20	7/20	10/20	10/20	9/20
Al+Cu	CRLT4	1/20	1/17	2/17	1/17	2/15
	CRLT7	2/20	2/18	3/17	2/17	0/15
Al+Cu+Si	CRLT4	0/20	0/15	0/19	0/19	0/15
	CRLT7	0/20	0/19	0/19	0/19	0/20

* In this table, 5/19 implies 5 failures out of 19 units tested and the 20th sample was not included in the measurement.

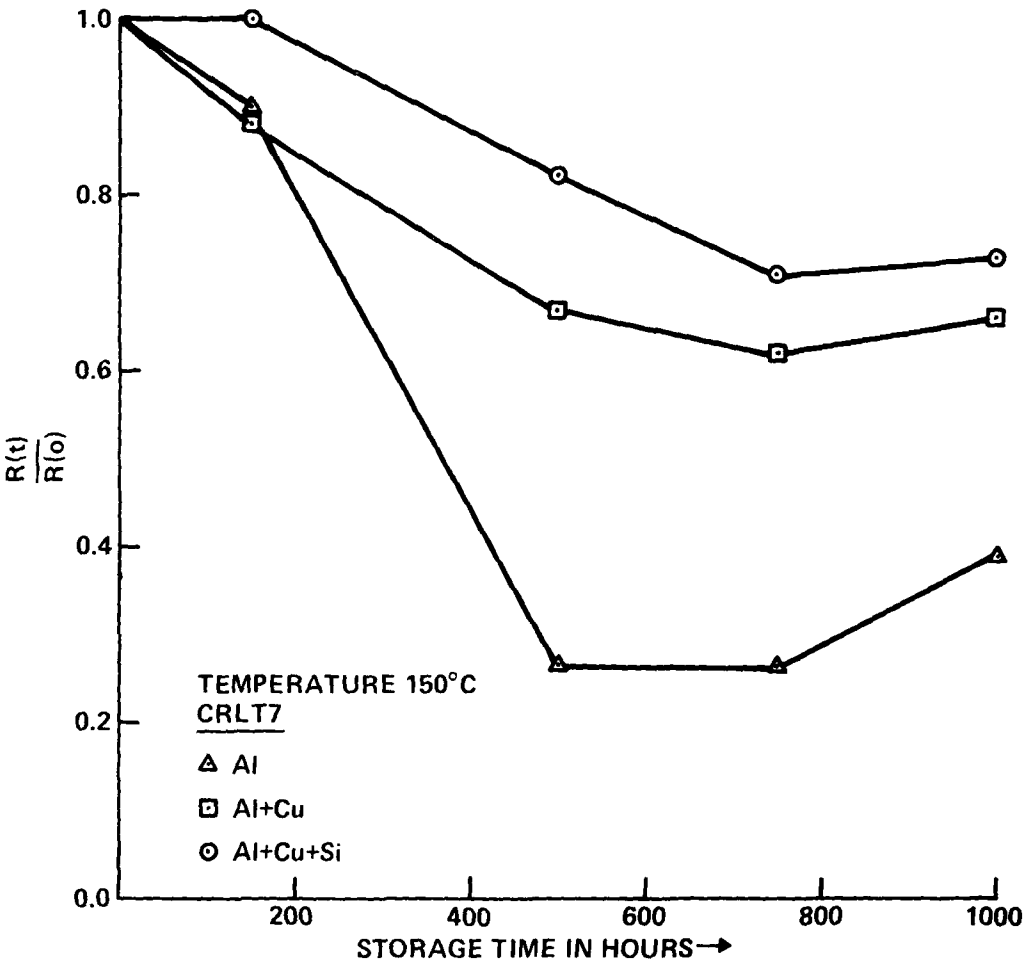

Figure 25. Normalized Contact Resistance of 200 Contacts as a Function of Storage Time at 150°C

Table 11. Failure Data on CRLT4 and CRLT7 Test Structures from a Group of Electromigration Tested Samples

Metal		Storage Temperature (°C)/Time(Hrs)			
		150/1840	175/1840	195/1650	215/256
Al	CRLT4	6/20	10(11)/20	11/20	14/20
	CRLT7	10/20	15(17)/20	16/20	16/20
Al+Cu	CRLT4	1/20	0/20	6/20	4/20
	CRLT7	2/20	0/20	8(10)/20	7(5)/20
Al+Cu+Si	CRLT4	0/20	0/20	0/20	0/20
	CRLT7	0/20	0/20	0/20	0/20

3. Leakage Current

In a companion experiment, the CRLT4 and CRLT7 test structures have been used to determine the leakage currents of 100 n^+/p^+ diodes as a function of 150°C storage time. Typical reverse breakdown voltage of this diode is 30 volts. For this experiment, three quadrants of electrically probed slices with Al, Al+Cu and Al+Cu+Si films were chosen. Backside contact was established and the substrate biased at −10 volts and the total leakage current of the 100 n^+/p^+ diodes of the CRLT4 structure determined at time t=0. Similar measurements repeated on nine more test bars on the same slice gave a sample size of 10 for each set of measurements. Leakage current data was collected with CRLT7. Once the leakage current data at t=0 was collected for all three slices, these slices were stored in 150°C ambience. Room-temperature leakage current data were collected at 200, 400, 750 and 1000 hours of storage at 150°C. These data are summarized in Table 12. In this table, the range of I_L for 10 measurements rather than the average value is shown. Data show that leakage currents of test structures fabricated with Al+Cu+Si films is on the order of 10^{-6} amps whereas leakage currents for Al metallized test structures are on the order of 10^{-3} amps. Because each CRLT4 test structure consists of 100 n^+/p^+ diodes, the average leakage current per diode (with an approximate junction area of 5×10^{-6} cm^2) is on the order of 10^{-8} amps when Al+Cu+Si metallization is employed.

Table 12. Leakage Current as a Function of 150°C Storage Time

Film	Test Structure	Leakage Current Units (Amps)	Ten Units Under Storage Test					Ten Random Units After 1000 Hr
			0 (hr)	200 (hr)	400 (hr)	750 (hr)	1000 (hr)	
Al	CRLT4	10^{-4}	1.4-2.0	1.2-2.1	1.3-2.0	1.2-1.8	1.3-2.9	1.4-2.0
	CRLT7	10^{-3}	1.2-2.0	1.2-2.0	1.3-2.3	1.1-1.7	1.3-2.1	1.4-2.1
Al+Cu	CRLT4	10^{-4}	0.6-1.4	1.0-1.8	0.9-1.8	0.9-1.8	0.9-1.8	0.9-5.8
	CRLT7	10^{-4}	0.3-1.6	0.6-1.5	0.6-1.7	0.6-1.7	0.6-1.6	0.4-1.8
Al+Cu+Si	CRLT4	10^{-6}	0.2-21	0.2-21	0.2-21	0.2-340	0.2-320	0.2-1.7
	CRLT7	10^{-6}	0.8-17	0.8-170	0.8-170	0.5-13	0.5-12	0.2-87

4. SEM Examination of the Si/Al-Alloy Contacts

Scanning electron microscopy was used to examine the physcial nature of Si/Al-Alloy contacts in the packaged units prior to 150°C storage test and after the 150°C 1000-hour storage test had been completed. SEM examination had been carried out on cross-sectioned samples and the micrographs for packaged samples prior to 150°C storage tests are presented in Figure 26. Note that considerable pitting was observed in Al metallized samples whereas erosion of Si from the contacts is not observable for Al+Cu+Si metallized samples.

An attempt was made to examine the contacts by removing the Al, Al+Cu and Al+Cu+Si films from contact areas in the packaged units prior to the 150°C storage test. Similar examination was carried out for samples stored at 150°C for 1000 hours. For all practical purposes, the two sets of micrographs look alike. Shown in Figure 27 are the micrographs for samples stored at 150°C for 1000 hours. The Al, Al+Cu and Al+Cu+Si films from the respective contact areas of the samples

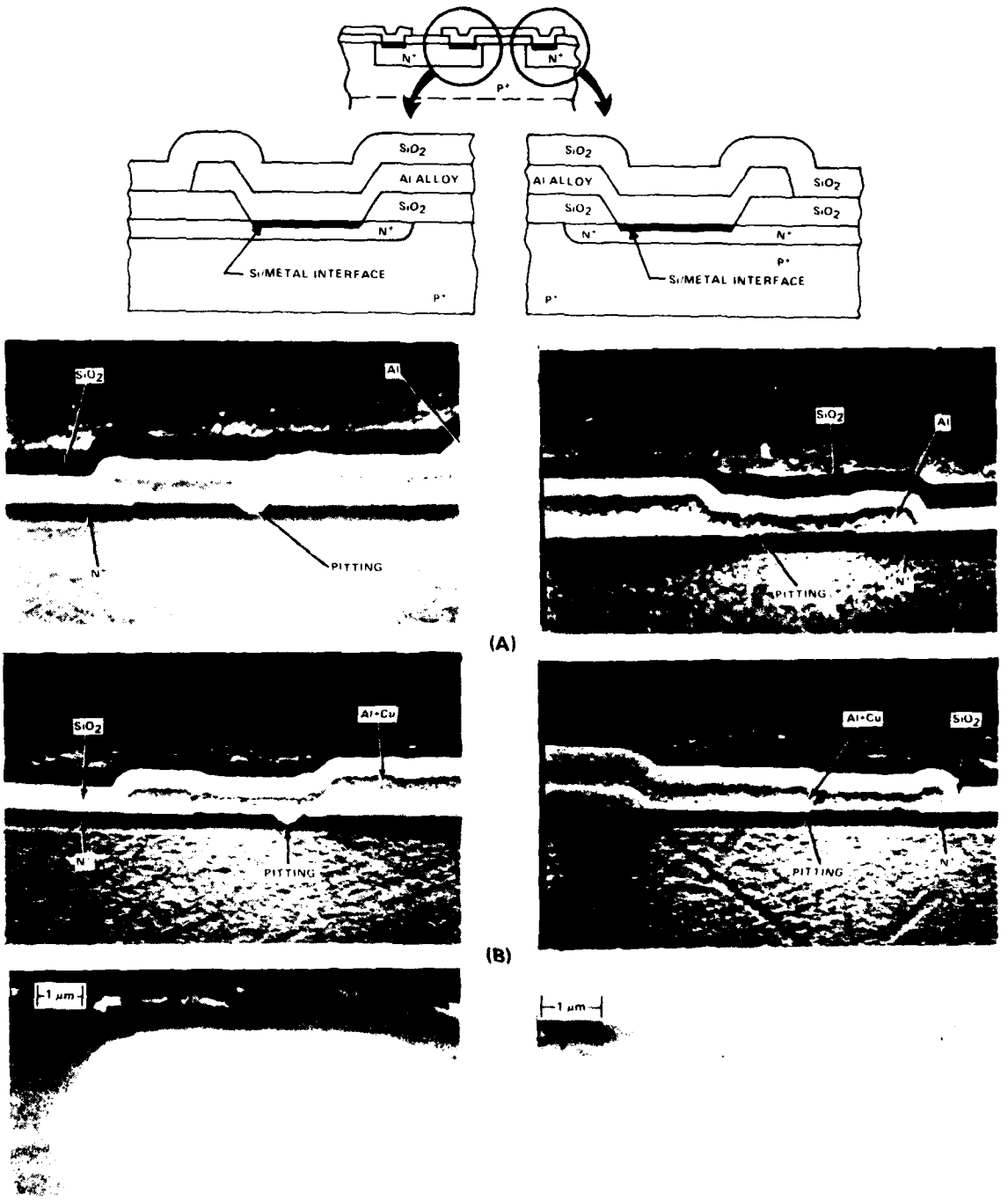

Figure 26. Cross Sections of CRLT4 Test Structures with (A) Al, (B) Al+Cu and (C) Al+Cu+Si Metallizations

(A) Al – METAL REMOVED FROM CONTACT AREA

(A) Al – METAL AND OXIDE REMOVED FROM CONTACT AREA

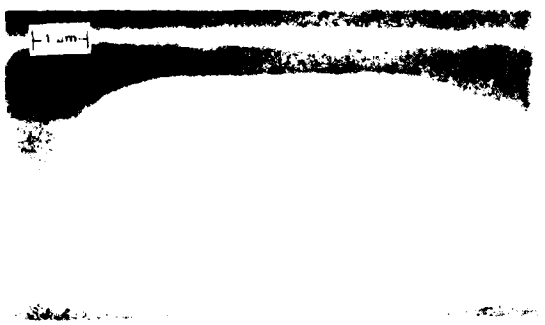

(B) Al +Cu – METAL REMOVED FROM CONTACT AREA

(B) Al+Cu – METAL AND OXIDE REMOVED FROM CONTACT AREA

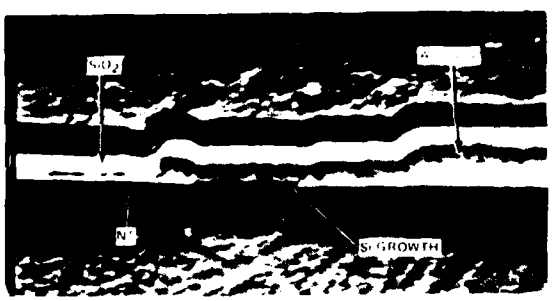

(C) Al+Cu+Si – METAL REMOVED FROM CONTACT AREA

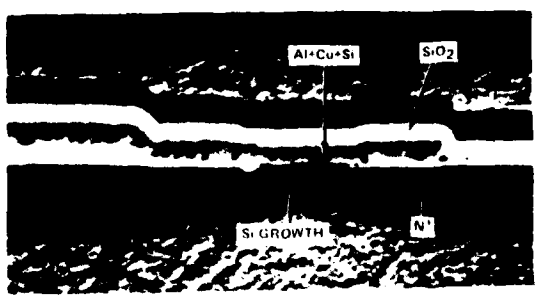

(C) Al+Cu+Si – METAL AND OXIDE REMOVED FROM CONTACT AREA

Figure 27. Si/Al-Alloy Contacts After 1000-Hour Storage at 150°C

were removed for examination. Erosion of Si from contacts, precipitation and regrowth of Si in contacts are readily seen for samples metallized with Al and Al+Cu films whereas only Si precipitates in the contacts are observable for samples metallized with Al+Cu+Si films.

5. Bond Strengths

Experiments were carried out to determine the effects of 150°C, 1000-hour storage on bond strength of ultrasonically bonded 25 μm (1-mil) Al (1% Si) wire to Al-Alloy film bond pad. A sample size of 10 each from Al, Al+Cu and Al+Cu+Si metallization was chosen from the samples stored at 150°C for 1000 hours. The glass sealed packages were carefully opened and four bonds per package were pull-tested to determine the bond strength. The average value of 40 bond pull tests on 10 samples of each metallization was treated as a characteristic bond strength for that metallization. Bond strength data on Al, Al+Cu and Al+Cu+Si metallization are given in Table 12. Initial values of the bond strengths similarly determined prior to any testing of the packaged units are also given in the same Table 12. These data show that average bond strengths are the same for all three metallizations before and after 150°C storage for 1000 hours.

D. TEMPERATURE CYCLING

Experiments were carried out to determine the effects of −65°C to +150°C temperature cycling on the bond strengths of ultrasonic 25 μm (1-mil) Al (1% Si) wire bonds to Al, Al+Cu and Al+Cu+Si bond pads and the contact resistances of Si/Al-Alloy interface packaged units with test structures CRLT4 and CRLT7 were used for this experiment.

A sample size of 20 units each of Al, Al+Cu and Al+Cu+Si film was chosen. The room temperature resistances of CRLT4 and CRLT7 test structures were determined prior to temperature cycling. Ten samples from each group were subjected to 50 temperature cycles of −65°C to +150°C with a dwell time of 12 minutes at each extreme temperature. After temperature cycling, room-temperature resistance measurements were repeated. The 10 units subjected to temperature cycling along with the other 10 units held as standard were used for bond strength tests. The glass sealed packages were carefully opened and four bonds per package were tested to determine the bond strength in grams. The average values of bond strengths determined from the 40 bond pull tests for each group of samples are shown in Table 13. These data suggest that no degradation of the bond strengths was observed after 50 temperature cycles for all three metallization systems.

Resistance values of CRLT4 and CRLT7 before and after temperature cycling have been analyzed to determine the contact resistance values for 50, 150 and 200 contacts corresponding to 1, 3 and 4 strings respectively. These data are summarized in Table 14.

Table 13. Bond Strengths in Grams for Test Samples Subjected to 150°C 1000 Hours Storage and 50 Temperature Cycles from 65°C to 150°C

Metal	Average Bond Strength in Grams		
	Before Temp Storage/ Temp Cycling	After 150°C – 1000 Hour Storage	After 50 Temp Cycles* from –65°C to 150°C
Al	2.73 · 0.86	2.55 · 1.23	2.54 · 0.65
Al +Cu	2.65 · 0.66	2.65 · 0.78	2.43 · 0.71
Al+Cu+Si	2.72 · 0.83	2.27 · 0.62	2.72 · 0.63

*These samples were not subjected to 150°C storage test.

Table 14. Contact Resistance Data for CRLT4 and CRLT7 Test Before and After 50 Temperature Cycles from 65°C to 150°C

Test Structure Sample			Resistance Values in Ohms	
			Before Temp Cycle	After Temp Cycle
CRLT4				
	Al	1	241 · 55	120 · 51
		3	432 · 171	314 · 175
		4	555 · 225	547 · 221
	Al+Cu	1	484 · 54	259 · 88
		3	1162 · 224	774 · 336
		4	1472 · 327	1200 · 434
	Al+Cu+Si	1	219 · 63	265 · 108
		3	651 · 199	787 · 314
		4	865 · 267	1060 · 404
CRLT7				
	Al	1	238 · 47	101 · 45
		3	432 · 156	312 · 142
		4	461 · 227	507 · 168
	Al+Cu	1	551 · 71	280 · 86
		3	1286 · 220	715 · 346
		4	1613 · 304	1328 · 310
	Al+Cu+Si	1	250 · 94	278 · 91
		3	678 · 243	824 · 276
		4	893 · 327	1104 · 371

*Sample numbers 1, 3 and 4 correspond to 50, 150 and 200 R_C respectively.

SECTION VI
DISCUSSION

The main objective of this work has been to carry out an in-depth study of Al, Al+Cu and Al+Cu+Si film interconnections and Si/Al-Alloy film contacts as they impact reliability of integrated circuits. Electromigration-inducted failures in Al-Alloy film interconnections and potential failures in shallow junction devices due to Si erosion from contacts leading to high leakage currents and/or junction shorting are the primary subjects of this study.

A. ELECTROMIGRATION – A BRIEF REVIEW

Mass transport under the influence of an impressed dc electric field is referred to as electromigration. Following Huntington and Grone,[30] the net atomic flux J_A in a lattice due to current density j can be expressed as

$$J_A = (ND/kT)\, Z^* e\, \rho j \qquad (1)$$

where

N = the density of ions

D = Do exp(-Q/kT) = the diffusion coefficient

Z*e = the effective charge on the migration ion

k = Boltzmann's constant

ρ = the resistivity of the conductor

T = the absolute temperature

In electromigration studies on single crystals at temperatures fairly close to the melting point, the diffusion coefficient D and the activation energy Q are well defined, and Z*e is a physical parameter describing the momentum exchange between the electrons and diffusing ions. In the case of electromigration studies on vacuum deposited metal film conductors, the problem is more complex because these film conductors are tested at moderately low temperatures $0.3\ T_m < T < 0.5\ T_m$ where T_m is the melting point of the material, and the mass transport is mainly controlled by grain boundary diffusion. In a film, all grain boundaries are not alike. For a film with an ideally textured grain structure, expression for the atomic flux given in Eq. (1) has been modified by replacing the lattice diffusion coefficient by a suitably averaged grain boundary diffusion coefficient and by a multiplicative factor, the ratio of the effective width of the boundary δ and the average grain size of the film. The effective charge Z*e still serves as a suitable physical parameter describing the momentum exchange between the electrons and the diffusing ion in a grain boundary.[9]

Electromigration alone cannot induce failures in film conductors unless there is a nonvanishing divergence of atomic flux. Two factors, inhomogeneities in the microstructure and the temperature gradients, are responsible for flux divergences. The first factor is far more influential than the others. Two well known inhomogeneities are those due to localized change in grain size, and those found at the junction of three grains, the so-called triple points illustrated in Figure 28. A flux divergence leads to mass depletion and hence to void formation. As these voids grow in size and coalesce to form larger voids, a crack develops which eventually leads to a discontinuity in the conductor path. Crack formation in large and small grain size film test stripes of the same width is also shown in Figure 28. A uniform textured grain size distribution [Figure 28(a)] is desirable to reduce the electromigration damage.[9] However, an average grain size comparable to the width of the conductor [Figure 28(c)] is less desirable than a small grain size film [Figure 28(d)], because this configuration enhances the chances for voids formed at triple points to coalesce into a continuous crack across the width of the conductor.

A preponderance of failures near the cathode end suggests that thermal gradients are causing flux divergences similar to the ones in bulk samples; however, a large number of observations on film stripes subjected to electromigration testing show randomly distributed failures along the stripe lengths and suggest that microstructural inhomogeneities in films are primarily responsible for atomic flux divergences which in turn lead to void formation and open failures.

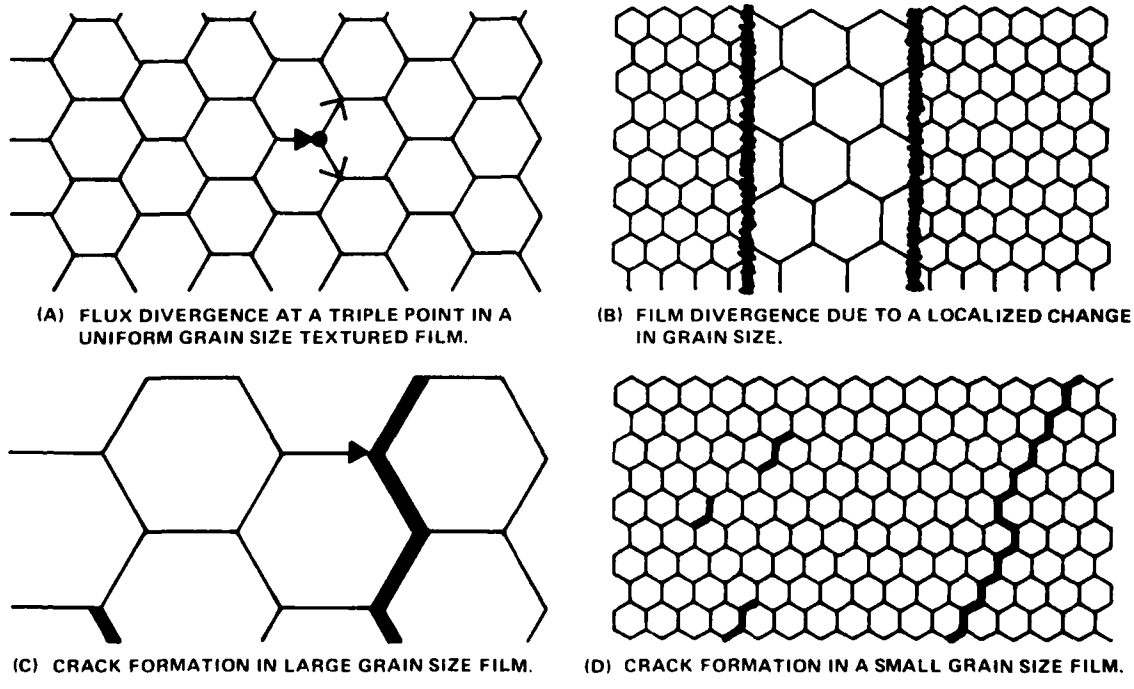

Figure 28. Schematic Representation of Microstructural Inhomogeneities in the Films and Electromigration Induced Damage

Attardo and co-workers[22] have proposed a metallurgical model of the random structural defects which cause electromigration failures in Al film conductors. This model takes into account flux divergences due to triple points, differences in grain sizes, distribution of tilt-type boundaries for a ⟨111⟩ oriented film and atomic mobilities in these grain boundaries. They have used experimentally determined grain size distribution to examine the MTF and standard deviation dependence on width, length, average grain diameter, and standard deviation of grain size. Conclusions of their study are as follows:

1) MTF decreases with increasing conductor length
2) Standard deviation of the failure distribution decreases with increasing length
3) MTF increases linearly with increasing width in the range of 0.2 to 1 mm
4) MTF increases with median grain size if the variance of the grain size is kept constant
5) MTF decreases with increasing variance of the grain size distribution if the main grain size is kept constant
6) Time to failure data closely approximates the log-normal distribution

Effects of grain size variation and temperature gradient on flux divergences have been considered to determine the time to failure of a film conductor.[9,31-33] Expressions have been developed to relate the mean time to failure (MTF) of film conductors to current density and temperature, and a general expression for MTF is as follows.

$$MTF = A\, j^{-n} \exp(Q/kT)$$

where

A = parameter depending on sample geometry and physical characteristics of film and substrate

j = current density (A/cm^2)

n = exponent ($1 < n < 3$).

A large number of life tests on Al film conductors have been carried out to determine the activation energy. Here a set of identical test resistors are subjected to a fixed current density, e.g., 10^6 A/cm^2, at a chosen ambient temperature and the MTF for this temperature is determined. Time to failure data are observed to obey log-normal distribution. The experiment is repeated at several temperatures and an Arrhenius plot of MTF vs (1/T) is constructed and the activation energy is determined. From the basic point of view, this activation energy cannot be directly related to the temperature variation of $\delta D_b Z^*_b$, a key parameter in the electromigration of thin films.[9] However, from the *reliability point of view*, this activation energy is a quantitative measure of the cumulative effects of microstructural inhomogeneities, average grain boundary diffusion, temperature gradients, underlying substrate, protective coatings, and electromigration in films. Though reported activation energies for Al vary over a wide range of 0.3 to 1.0 eV, this is to be anticipated because of the wide differences in film deposition procedures and grain sizes, and test conditions which have not been fully reported. However, most values of Q for Al films lie in the range of 0.6 ± 0.2 eV and support the point of view the electromigration-induced failures are grain boundary diffusion controlled.

Since d'Heurle and co-workers at IBM [34-36] reported an improvement in MTF by a factor of 70 by Cu doping Al films, there has been considerable interest in electromigration in Aluminum-Alloy films. It has been reported that MTF does increase with Cu content and peaks out around 8 wt % Cu in Al films and that activation energy varies with Cu content.[12] There is some difference of opinion as to the magnitude of increase in MTF due to Cu addition. Several studies have amply emphasized that life times of film conductors are strongly influenced by the average grain size and grain size distribution besides copper concentration. Agarwala and co-workers have concluded that below 0.6 wt % Cu, lifetime is influenced by both grain structure and Cu content, while above 0.6 wt % Cu, lifetime is primarily affected by the grain size distribution of the film.[37,38]

Erosion of Si from contact windows during the contact sintering step has been a common observation for ICs fabricated with Al metallization; however, this has not been a major yield limiting factor in fabrication of ICs with emitter junction depths > 1 μm. Increasing demand for high-performance (speed), high-density large-scale integrated (LSI) circuits has led to process techniques and device designs having junction depths approximately 250 to 500 nm. Interdiffusion of Si/Al during contact sintering can result in lowered life, junction leakage or even shorting in such devices. This can be avoided either by using Al+Si films or by interposing a barrier layer between the Si/metal contacts and interconnection metallization. Electromigration life test data on Al+Si film conductors, though limited, suggest that Si addition to Al increases MTF in the temperature range (150-220°C) but the activation energy for Al+Si is 0.3 eV, compared to 0.5 to 0.6 eV for pure Al films.[9,39]

With advances in film deposition technology, ternary alloy films of Al+Cu+Si are being explored to minimize the erosion of Si contacts in shallow junction devices and to realize the beneficial effects of Cu to enhance electromigration resistance. Anticipated improvements in MTF under electromigration testing have been observed for Al+Cu+Si films deposited by flash evaporation.[12,40] Activation energies varied from 0.43 to 0.77 eV for varying copper content and the activation energy was observed to peak for 8 wt % copper. Since these tests have been conducted in the temperature range of 200°C to 275°C, and the microstructure of Al+Cu+Si films can be expected to change, extrapolated MTF values at the operating temperatures of 55°C to 80°C need to be considered with caution. Furthermore, flash evaporation techniques for depositing Al+Cu+Si film do not seem to be receiving the enthusiastic attention enjoyed by IN-Source and magnetron sputter deposition techniques. Life test data on Al+Cu+Si film conductors in series with Si/Al-Alloy contacts are not available.

B. Al-ALLOY FILMS FOR IC INTERCONNECTIONS

1. Selection of Al-Alloy Film Compositions

A brief survey of electromigration life test data on Al film conductors show a strong microstructure dependence. Also a review of life test data on Al+Cu film conductors suggests that MTFs and activation energy are strongly influenced not only by the copper content but also by the microstructure homogeneity (uniform grain size distribution) of the films.[37,38] Data on Al+Si films are somewhat limited. Since electromigration behavior of metal film conductors is known to depend on microstructure and film composition, fully characterized Al, Al+Cu and Al+Cu+Si films as

functions of film deposition parameters and subsequent process parameters have been used for electromigrat on testing. Choice of Cu and Si concentrations for the Al+Cu and Al+Cu+Si films is dictated by several factors such as:

1) Cost-effective film deposition methods with reasonable process control
2) Resistivity and microstructure
3) Patternability
4) Contact annealing to form Si/Al-Alloy contacts
5) Metal coverage on oxide steps
6) Bondability
7) Electromigration resistance
8) Surface smoothness for multilevel interconnections and/or protective coating.

We have chosen 2 wt % copper content for Al+Cu because:

1) High Cu content in Al films is known to produce highly reflective films[16] which are less desirable for lead patterning
2) Resistivity of Al+Cu films will not be greater than 20% of that of pure Al films and that increased metal thickness to achieve same sheet resistance films is not compatible with patterning narrow lead widths with minimum spacings
3) Higher Cu concentration is likely to produce large Cu precipitates which may increase corrosion susceptibility of the leads
4) MTFs of Al+Cu films are considered to be a strong function of microstructure for copper content greater than 0.6%[37,38]
5) Electromigration life test data on 9-μm wide and 1140-μm long conductors of fully characterized Al+Cu films are available for comparison.[41]

Once the copper content of Al+Cu films has been selected, 1% silicon concentration for the films is chosen because:

1) It is adequate to satisfy the solid solubility of Si in Al at 525°C – a probable maximum temperature for contact annealing and/or packaging
2) Higher Si content increases size of Si precipitates and surface roughness
3) Higher Si content adversely affects bondability[16]
4) Higher Si content increases the possibility of growing large precipitates and/or epitaxial silicon in contact windows and it may adversely affect contact resistance.

Also, no data exist for fully characterized Al+Cu+Si films with 2% Cu and 1% Si in films. Among the several methods available for Al-Alloy film depositions, IN-Source and dc-magnetron sputter deposition techniques have been employed because both techniques are potentially capable of producing Al-Alloy films of desired compositions.

2. Resistivity

The first part of this study has been devoted to depo: ing Al, Al+Cu and Al+Cu+Si films by IN-Source (room temperature and heated substrates) and dc magnetron sputtering. These films have been fully characterized in terms of resistivity. Microstructure, film composition and resistivity are presented in Tables 1 and 2.

The room-temperature resistivity of aluminum ρ_{Al} is close to 2.71 $\mu\Omega$-cm.[13] In general, resistivity of vacuum deposited Al films lie in the range of 2.7 to 3.0 $\mu\Omega$-cm depending on the vacuum ambience and substrate temperature. Pure films with grain sizes of 1 μm and above show a resistivity very close to bulk resistivity. The resistivity contributions of Cu and Si impurities in and out of solution in Al are as follows:[42]

Impurity Content	Resistivity Contributions in $\mu\Omega$-cm	
	In Solution	Out of Solution
1 wt % Cu	0.34	0.030
1 wt % Si	1.02	0.0088

Hence ρ_{Al+Cu} for films with 2 wt % will lie in the range of 2.8 to 3.7 $\mu\Omega$-cm depending on whether Cu is out of solution. Similarly, $\rho_{Al+Cu+Si}$ for 2 wt % Cu and 1 wt % Si film can be expected to lie in the range of 2.9 to 4.7 $\mu\Omega$-cm. Data presented in Tables 1 and 4 are consistent with this prediction. As the films are annealed, Cu and Si impurities precipitate and resistivities are expected to decrease. *Our data show that resistivities of annealed Al+Cu and Al+Cu+Si films are within 20% of the resistivity of pure Al films.*

3. Microstructure

In general, vacuum deposited metal films are polycrystalline and microstructure (grain size distribution) of the films depends on several parameters such as substrate temperature and film deposition. Earlier studies on Al films have shown that average grain size of the films increases with the substrate temperature and that these films display a preferred [111] orientation when deposited on hot substrates ($T > 150°C$) and that Al films with randomly oriented grains develop some (111) texture after a 450°C, 15-minute anneal.[13] Also, it is known that as-desposited small grain size films do not attain the same characteristics of as-deposited large grain size films even after a 450°C anneal for 30 minutes followed by a 150°C anneal for 1000 hours.

In the present series of experiments, scanning and transmission electron microscopy has been employed to examine the microstructure of Al, Al+Cu and Al+Cu+Si films deposited by IN-Source and dc magnetron sputtering, before and after a 450°C, 15-minute anneal in N_2. Analysis of the microstructure data on these films can be summarized as follows:

1. Average grain size of Al films increases with substrate temperature for IN-Source deposited films.
2. Microstructure of dc magnetron sputter deposited Al films on unheated substrates look very similar to that of Al films deposited from an IN-Source on hot substrates (150°C to 200°C range). Grain size is larger because sputtered Al ions arriving at the substrate are highly energetic and more mobile as compared to atoms arriving from a molten source.
3. Grain size distributions tend to obey the anticipated log-normal distribution.
4. Addition of Cu and Si to Al reduces the average grain size of the film when compared to that of pure Al films.

5. Cu precipitates (possibly $CuAl_2$), appearing as black dots and striations in the films, are uniformly distributed in the Al+Cu and Al+Cu+Si films with approximately 2 wt % Cu in the films.
6. The grain size distributions of Al films before and after a 450°C, 15-minute anneal are, in general, broader as compared to those of Al+Cu and Al+Cu+Si films.
7. The average grain size of Al+Cu+Si films in the as-deposited condition is very small on the order of 120 nm and that of annealed films is on the order of 250-300 nm. Since the grain size of Al+Cu+Si films is small, TEMs printed at 100,000X have been analyzed. Most of the grains fall in a narrow range of 200-300 nm in size.
8. Area diffraction patterns indicate that IN-Source deposited films on unheated substrates are randomly oriented and that after anneal these films develop some degree of ⟨111⟩ texture. Also, films deposited on hot substrates (> 150°C) produce textured films. In the case of dc magnetron sputter deposition, as-deposited Al+Cu and Al+Cu+Si films are randomly oriented, and a ⟨111⟩ texture is observed for as-deposited Al, annealed Al, Al+Cu, and Al+Cu+Si films. The degree of texturing decreases from Al to Al+Cu to Al+Cu+Si, irrespective of the film deposition method.
9. For all practical purposes, the microstructure of IN-Source and dc magnetron sputter deposited films under controlled conditions appear to be equivalent.

4. Film Composition

We have employed primarily three methods for composition analysis of Al-Alloy films: Chemical Analysis, X-Ray Fluorescence and Electron Microprobe.

The Chemical Analysis (wet chemistry) technique requires a large size sample (e.g., a typical film on a three-inch diameter substrate) for reproducible results. For the determination of Cu and Si concentrations in Al-Alloy films, films deposited on oxidized Si substrates and on sapphire substrates respectively have been employed. In general, these experimental values are good to ±10%.

The X-Ray Fluorescence technique requires a film sample on 1 cm × 1 cm substrate (equipment design limitation and not the limitation of the technique) and provides an answer for the Cu content per unit area with no depth resolution. Here, x-rays penetrate the entire thickness of the samples. Experience in our laboratory has shown that the X-Ray Fluorescence technique consistently yields reproducible results. The Cu concentrations shown in the tables are computed from film thickness measurements and the copper content per unit area determined by X-Ray Fluorescence techniques. These values are good to within ±10%.

The Electron Microprobe technique is well suited for composition analysis of Al-Alloy films on integrated circuits. Bond pad or any suitable spot on the interconnection (≅3 to 4 μm wide) can be chosen. However, preliminary calibration of the equipment is needed. If there are precipitates in an alloy film, it is desirable to select the energy of electrons to excite the entire depth of the film for a composition analysis. It is also desirable to scan a larger area of the film to obtain a reproducible composition. Analysis data presented in Table 2 highlight the possible composition variations observed in this type of an analysis.

Finally, we have used the Ion Microprobe technique combined with depth profiling techniques to examine the Cu and Si concentration profiles in a limited number of Al-Alloy films. These profiles suggest that there is *some accumulation* of Si and Cu near the SiO_2/Al-Alloy film interface. One cannot rule out the possibility that these accumulations are somewhat magnified due to the artifacts of sputter yields as an interface is approached. Auger depth profile studies have reported similar results of Si accumulation near the interface. Scanning electron micorgraphs of substrates subsequent to Al removal from areas previously covered with Al+Cu+Si films indeed show Si precipitates and support the Ion Microprobe results. However, the Cu concentration appears to be fairly uniform in annealed films.

In summary, composition analysis of Al+Cu and Al+Cu+Si films by the three different methods are internally consistent and depth profiles developed by Ion Microprobe suggest some degree of accumulation of Si and Cu near the substrate/film interface.

C. ELECTROMIGRATION TESTING

Our primary interest is to determine mean time failure and failure rates of Al-Alloy film interconnections and Si/Al contacts under high current stress that limit the reliability of microelectronic devices, especially large-scale integrated circuits. We have tested Al, Al+Cu and Al+Cu+Si film conductors and also Si/Al-Alloy contacts by using the test structures HCSO3 and HCSO1 respectively to evaluate electromigration resistance by measuring the mean time to failure or t_{50}, which is the time to reach a failure of 50% of test samples. In the HCSO3 test structure, a film conductor stripe (sometimes referred to as a test stripe) 0.8 μm thick, 6 μm wide, and 380 μm long is subjected to a current density of 1×10^6 A/cm^2 at four temperatures in the range of 150°C to 215°C. Current is fed to the test stripe from 25 μm (1-mil) Al wire at the Al (or Al+Cu or Al+Cu+Si) film pad. In the case of HCSO1 test structure, a test stripe identical to that of HCSO3 in physical dimensions, is located between two n^+ Si diffused resistors, each with an approximate resistance of 22 Ω, and current is fed to the stripe at the Si/Al-Alloy interface. For a chosen test temperature, 20 test samples each of test structures HCSO1 and HCSO3 and metallized with Al, Al+Cu and Al+Cu+Si films [a total of 120 (120 × 2 × 3)] have been subjected to a current stress of 48 mA, equivalent to 1×10^6 A/cm^2, and time to failure data have been collected. These data have been analyzed further by using log-normal probability plots to determine the respective MTF values. Arrhenius plots of MTF vs (1/T K) (reciprocal temperature K) have been developed for each type of metal film to determine the respective activation energies and these data have been summarized in Table 8. These results will be examined in light of the current state of our understanding of electromigration in thin film conductors.

1. HCSO3 Test Structure

a. Al Film Conductors

MTF data presented in Figure 19 for M-S Al, Al+Cu and Al+Cu+Si film conductors, of identical physical dimensions, and subjected to equivalent current stress of 1×10^6 A/cm^2 in the same ambience clearly show that pure Al films display the least electromigration resistance in comparison with Al+Cu and Al+Cu+Si film conductors. This result is anticipated. Also the failures (similar to

the ones shown in Figure 22) are distributed at random along the length of the test stripes. In Figure 20 the present MTF data on pure Al films (0.8 μm thick, 6 μm wide, 380 μm long) is compared with the earlier data on Al film conductors (Ti:W/Al, there is an underlying barrier layer of Ti:W between Al and SiO_2) conductors (8 μm thick, 9.6 μm wide, and 1.14 μm long), and subjected to an equivalent current stress of 1×10^6 A/cm^2. We observe *a factor of 4* degradation in MTF as the width of the conductor decreases from 9.6 μm to 6 μm. The activation energy of 0.45 eV, determined from the present MTF data, is lower than the value of 0.61 eV reported earlier. It should be pointed out that earlier MTF data on pure Al films and Ti:W/Al films differ only by 30 to 50%

$$[\text{MTF(Ti:W/Al)/MTF(Al)}] = 1.3 \text{ to } 1.5$$

and activation energy appears to be unaffected by the underlying Ti:W layer.

These experimental results are consistent with the statistical model[22] which predicts random failure distribution along the stripe length and also a decrease in MTF by approximately 30% in arbitrary units as the width decreases from 10 μm to 6 μm (see ref. 22, Figure 7, which illustrates computer-simulated width dependence of MTF of a 250-μm long conductor). Hence the ratio

$$\frac{\text{MTF (Al 9.6 } \mu\text{m wide)}}{\text{MTF (Al 6.0 } \mu\text{m wide)}} = 4\,\frac{\text{(hours)}}{\text{(hours)}}$$

$$= 1.3 \text{ (arbitrary units from the model)}$$

This analysis suggests multiplying the ratios derived from arbitrary units (of Figure 7 of Ref. 22) by a factor of 3 to estimate real ratios of MTFs in hours.

b. Al+Cu Film Conductors

Present MTF data on M-S Al+Cu film conductors, shown in Figure 19, are consistent with an activation energy of 0.7 eV. This value is in excellent agreement with that reported earlier for IN-S Al+Cu (Ti:W/Al+Cu) with 1.6 wt % Cu.[41] Also note that M-S Al+Cu films display a longer MTF than IN-S Al+Cu under equivalent current stress by a factor of 3.

$$\frac{\text{MTF(M-S Al+Cu, 2 wt \% Cu, 6 } \mu\text{m wide)}}{\text{MTF(IN-S Al+Cu, 1-6 wt \% Cu, 9.6 } \mu\text{m wide)}} \cong 3$$

The MTF data for M-S Al+Cu show a broader distribution than that for IN-S Al+Cu.

$$\frac{\sigma \text{ (M-S Al+Cu)}}{\sigma \text{ (IN-S Al+Cu)}} \cong \frac{0.8}{0.3 \text{ to } 0.6} \cong 2$$

Where σ is the standard deviation of the log-normal distribution of the time to failure data. Also note the length of M-S Al+Cu film conductor is 380 μm as compared to the 1140 μm length of IN-S Al+Cu film conductor. Furthermore, the Cu content of M-S Al+Cu films is nearly 2 wt % (see Table 4) and that of IN-S Al+Cu is 1.6 wt %. The film composition data are good to within ±10%,

hence the Cu content in MS Al+Cu films is greater (0.4 ± 0.2) than that in IN-S Al+Cu films. Since *the Cu content in both films is greater than 0.6 wt %*, distribution of Cu and grain size distribution (i.e., microstructure) will strongly influence the MTF data.

The present MTF data are consistent with the anticipated improvement in electromigration resistance due to Cu addition.[34-36] The observed random failures along the stripe length are consistent with the statistical model for electromigration-induced failures.[22] The observed increase in MTF for M-S Al+Cu as compared to that of IN-S Al+Cu is possibly due to: (1) a decrease in length, 380 μm vs 1140 μm, (2) a slight increase in Cu content, and (3) somewhat stronger (111) texture (possibly due to high substrate temperature during film deposition resulting from energetic sputter atoms). No decrease in MTF due to decrease in width (6 μm vs 9.6 μm) is noted because the average grain size for both films is small, 0.7 to 1.0 μm, as compared to the width of the conductor.

For all practical purposes, both sets of MTF data need to be considered equivalent because of the experimental constraints of incorporating 2 wt % Cu in vacuum deposited films, the statistical nature of grain size distributions and the cross-sectional variations in a set of test samples. *The important thing is that under high current stress M-S Al+Cu films with 2 wt % Cu are equivalent to or better than In-S Al+Cu films with equivalent Cu content and microstructure.*

e. Al+Cu+Si Film Conductors

The present series of experiments were designed to fabricate Al, Al+Cu and Al+Cu+Si film conductors of identical physical dimensions and to subject them to equivalent current stress under similar temperature ambience. Since IN-S Al+Cu+Si and M-S Al+Cu+Si films displayed identical microstructure, a uniform distribution of small grain size on the order of 0.25 μm-0.3 μm, M-S Al+Cu+Si films of 2 wt % Cu and 1 wt % Si were selected for electromigration testing along with Al+Cu films with 2 wt % Cu.

It is encouraging to note that M-S Al+Cu+Si film conductors out-performed the M-S Al+Cu films by at least a factor of 3 (or maybe 4) under equivalent current stress. Because of the limited number of failed samples, MTF values had to be extrapolated and these values are listed in Table 8. Since only one failure was observed after 1600 hours in a 1840-hour life test at 150°C, at ambient temperature, no extrapolated MTF value at 150°C is shown in Table 8. Though some degree of bias cannot be ruled out in extrapolation of MTF values, it is worth pointing out that these extrapolated MTF values are conservative estimates.

Because of the uncertainty in MTF values, the activation energy for Al+Cu+Si films is estimated to be 0.50 eV though it is more likely to be in the range of 0.6 to 0.7 eV.

The superior performance of Al+Cu+Si films is attributed to (1) very uniform grain size distribution with an average grain size of 0.25 μm, (2) uniform Cu distribution throughout the films, and (3) no degradation effects due to either Cu or Si precipitates.

2. HCSO1 Test Structure

a. Al Film Conductors

The primary purpose of this experiment has been to determine the failure mode of a film conductor in series with a Si/Al contact under a high current stress. These experiments have been designed to evaluate the merits of using Al+Cu or Al+Cu+Si films on similar test structures. The shallow junction depths ($\approx$ 350 nm) of the n^+ diffused resistors were chosen to simulate the shallow junction devices being developed for LSI and VLSI.[27,28] The contact areas are 3.80 X 6.35 μm^2 (0.15 X 0.25 mil^2) are typical in today's LSI circuits. The resistance of each n^+ diffused resistor (1 square) is on the order of 22 Ω. Thus a 48-mA current ($\equiv 1 \times 10^6$ A/cm^2) to be fed to the film stripe (6 μm wide and 380 μm long), has to pass through four Si/Al contacts. The total resistance of this test structure is greater than that of HCSO3 by $2R_s + 4R_c$ where R_s = 22 Ω and R_c varies anywhere from 1.5 Ω to 6 Ω (see Table 9 for data on CRLT4 and CRLT7 test structures). Since a decision was made to use the same current density (1×10^6 A/cm^2) for both HCSO3 and HCSO1 test structures, HCSO1 test structures were dissipating more heat, and the average temperature of these samples was 16°C to 17°C higher than that of HCSO3 test samples. (This is estimated by considering the difference in resistance values of the central stripes of HCSO1 and HCSO3 test samples tested at the same temperature and by using an average temperature coefficient of resistance of 4000 ppm/°C.) At elevated temperatures and under high current stress, electromigration of silicon in Al is anticipated to result in depletion of Si from the contacts and in turn Al will fill in the depleted volume in silicon contact.[43] This will eventually lead to junction shorting. In the course of testing, an observation of a vanishingly small ($\approx$ 0) voltage drop would indicate that both junctions on either side of the test stripe are shorted to the substrate and that a low resistance current path via substrate has been established. Thus, time to failure data correspond to the time required to short two junctions. Since both junctions are identical and current paths are symmetrical, time to failure data (with some statistical variation) represent the time required to short one junction. Optical examination of the contacts clearly shows that primary failure mode is contact pitting and junction shorting. Opens in the conductor stripes are not observed. The failed units also show the migration of Al from one contact to the other along the surface (see Figure 21).

The Si/Al contacts have been examined with the SEM (see Figure 26) and the micrographs indicate that contact sintering is very nonuniform. Hence, the MTF data collected in this experiment cannot be used to estimate the uniform erosion rate of Si up to the junction depth in a contact of known area but it provides a quantitative estimate of the life time of a Si/Al contact commonly encountered in ICs.

The MTFs of HCSO1 test structures are smaller than those of HCSO3 (Table 3). The activation energy determined from these experiments is 0.58 eV. Since the failure of the HCSO1 test structure depends on erosion of Si from the contact window, it seems reasonable to attribute this value to the activation energy for diffusion of Si in Al.

$$Q_{Si+Al}\ (\text{Film}) = 0.58\ \text{eV}$$

If one takes into account the statistical nature of these failed contacts and that ambient temperatures have been used in the Arrhenius plot of MTF vs 1/T K, this value is considered to be in qualitative agreement with the 0.79 eV value reported by McCaldin and Sankur for diffusion of silicon in aluminum.[44]

b. Al+Cu Film Conductors

Data presented in Table 8 strongly suggest a definite improvement in MTF, almost by a factor of 3 to 4, with the addition of Cu to Al. The activation energy for failure is almost equal to that observed for Al films. The SEM examination of Si/Al+Cu contacts, after metal removal, shows almost identical characteristics of Si/Al contacts, i.e., erosion of Si from isolated areas in the contact. *These observations suggest that addition of Cu impurity to Al suppresses the Si dissolution and possibly migration rates.*

c. Al+Cu+Si Film Conductors

These test samples out-performed Al and Al+Cu films as anticipated. The activation energy of 0.76 eV determined from the MTF data is in very good agreement with the reported value of 0.79 eV for diffusion of Si in Al but it differs from the activation energy of 0.89 eV determined by Black[43] from the failures due to electromigration of Si in Al. It differs from the activation energy of 0.89 eV reported by van Gurp who studied precipitation of Si from a supersaturated Al/Si solid solution.[39] Since atom transport in thin films is greatly affected by microstructure of the films, it was concluded that the difference in activation energy of 0.12 eV noted here is possibly due to the differences in microstructure of the films. It may be concluded from these measurements that activation energy for diffusion of Si in Al lies in the range of 0.79 to 0.9 eV.

D. CONTACT RESISTANCE OF SILICON ALUMINUM-ALLOY CONTACTS

Data collected with CRLT4 and CRLT7 test structures and presented in Tables 7, 9 and 13 show that for all practical purposes contact resistances of Si/Al, Si/Al+Cu and Si/Al+Cu+Si contacts are equal to each other (within a factor of 4) and the resistance of a 3.80 X 6.35 μm^2 contact varies in the range of 1.5 Ω to 6 Ω. SEM examination of Si/Al and Si/Al+Cu contacts (after metal removal) clearly shows that erosion of Si from contacts is nonuniform, and highlights the common observation of nonuniform sintering (Si/Al interaction) in Si contacts. This variation in interfacial area that provides electrical contact is considered to be the primary cause for resistance variation of Si/Al-Alloy contacts. It was also noted that Si dissolved in Al and Al+Cu during high-temperature (annealing operation) precipitated out on cooling, possibly along the grain boundaries of Al on Al+Cu film. The micrographs of Si/Al+Cu+Si contacts display the anticipated result, *"no erosion of silicon in contacts."*

Si growth in contact windows is a function of the Si/Al (and Si/Al+Cu+Si) system and not a function of film deposition technique. Similar growth of Si precipitates has been observed for IN-Source deposited Al+Si and Al+Cu+Si films on shallow junction devices (approximately same junction depth) fabricated on (111) substrates. Also, the growth pattern of Si precipitates was random as is observed in this series of experiments.

Analysis of the 150°C, 1000-hour storage data shows that the contact resistance decreases first and then reaches an asymptotic value (approximately 0.5X or 0.6X of the original value. However, the failure data presented in Tables 10 and 11 along with the leakage data presented in Table 12 suggest that erosion of Si from the Si/Al and Si/Al+Cu contact continues and Al migrates into the depleted regions and this process eventually leads to junction shorting. These data also show *zero failures for Si/Al+Cu+Si contacts* and no erosion of Si from the contacts.

Contact resistance values of 200 contacts presented in Figures 24 and 25 indicate that contact resistance of Si/Al+Cu+Si contacts tends to increase by a few percent after 750-hour storage at 150°C. Increase in contact resistance is considered to be related to the growth of Si precipitate or an epitaxial layer of Si in the contact windows. We have examined the contact resistance of test samples stored at 150°C for 1840 hours. (These are the samples used for electromigration testing at 150°C ambience for 1840 hours and it was found that the average contact resistance values for Si/Al+Cu+Si samples are slightly higher than those observed after 1000-hour storage.) We note that our data are limited and do not permit a realistic estimate of the rate of increase in contact resistance as a function of temperature and time (i.e., as a function of growth of Si precipitate).

E. TEMPERATURE CYCLING AND BOND STRENGTHS

Bond strength of 25 μm (1 mil) Al wire (with 1 wt % of Si) attached to Al, Al+Cu and Al+Cu+Si film pads was examined before and after 50 temperature cycles from −65°C to +150°C. Data in Table 12 show that the bond strength is on the order of 2.7 gms regardless of the underlying Al-Alloy films and that 50 temperature cycles did not degrade the bond strength.

Contact resistance data presented in Table 14 show that temperature cycling has enhanced the Si-Al intermixing at the interface, possibly by rupturing a contact inhibiting barrier layer due to mechanical stress. Similar improvements in contact resistance of Al/Al interface in the via contacts of Al/SiO_2/Al two-level test structures have been reported.[13]

SECTION VII
CONCLUSIONS

1. IN-Source and dc magnetron sputter deposition techniques are equally capable of producing Al, Al+Cu (2 wt % Cu) and Al+Cu+Si (2 wt % Cu + 1 wt % Si) films of comparable compositions, resistivity and microstructure.

2. Availability of automated dc magnetron sputter deposition equipment in the market place has been a primary factor in the selection of magnetron sputter deposited Al, Al+Cu and Al+Cu+Si films for electromigration testing.

It is recognized that composition of the source material needs careful process control to realize reproducible Al-Alloy films. In the case of IN-Source deposition, process control needs to be exercised at each deposition run, whereas in dc magnetron sputter deposition composition of the target needs to be controlled which assures uniform film composition through the useful life of the target, provided the target has a homogeneous composition.

3. Al-Alloy film compositions can be determined by any one of the three techniques used: (1) Chemical Analysis, (2) X-Ray Fluorescence, and (3) Electron Microprobe. The first two methods provide an average composition over a large area of the film sample, whereas Electron Microprobe is inherently capable of providing a spatial resolution on the order of couple of μm^2. Since the composition values determined by any one of these methods are good to within ±10%, it is recommended that composition values be cross-checked. Limited Ion Microprobe data on depth profiles of Al+Cu and Al+Cu+Si films suggest that Cu and Si tend to precipitate near the film substrate interface.

4. Microstructure of Al films is strongly influenced by the addition of Cu and Si impurities. For the Cu and Si compositions (2 wt % Cu and 1 wt % Si) chosen here, Al+Cu+Si films have the smallest grain size on the order of 0.2 to 0.3 μm and it is uniformly distributed – the average grain size of Al+Cu is larger than that of Al+Cu+Si films. Grain sizes of annealed Al films vary over a wide range from 0.2 to 2 μm.

Micrographs suggest that more microstructural inhomogeneities (abrupt changes in grain sizes) are present in Al as compared to Al+Cu and Al+Cu+Si films. Also, the copper precipitates in Al+Cu films are uniformly distributed.

5. Electromigration life tests on Al, Al+Cu and Al+Cu+Si film conductors (0.8 μm thick, 6 μm wide, and 380 μm long) at 1×10^6 A/cm^2 in the 150°C to 215°C temperature range show that:

   a. Failures are distributed at random along the stripe length and hence microstructure inhomogeneities appear to be responsible for atomic flux divergences leading to open failures.

b. Mean time to failure (MTF):
$(MTF)_{Al+Cu+Si} > (MTF)_{Al+Cu} > (MTF)_{Al}$

c. Activation energy (Q):
$Q_{Al+Cu+Si} = 0.5$ eV; $Q_{Al+Cu} = 0.7$ eV, $Q_{Al} = 0.44$ eV

d. Activation energy of 0.7 eV determined for M-S Al+Cu films (2 wt % Cu) is equal to that of IN-Source Al+Cu films (1.6 wt % Cu).

e. Activation energy Q_{Al} determined from the present series of experiments is on the low side of the range of values 0.6 ± 0.2 eV reported by several workers.

f. Present data on Al film conductors indicate that MTF degrades approximately by a factor of 4 with the decrease in width from 9.6 μm to 6 μm. These results are consistent with predictions of the statistical model on electromigration-induced failures proposed by Attardo and co-workers.

With the ever increasing trend toward shrinking interconnection widths for VLSI, the present data suggest that for 3.6-μm wide conductors (0.6 × 6 μm), present MTF data need to be derated approximately by a factor of 4.

Recently it has been reported that MTFs of e-beam evaporated Al+0.5 wt % Cu film conductors will decrease as the width decreases from 8 to 2 μm and suddenly turn around and start increasing below a width of 2 μm. The authors have rationalized their data on the basis of a "bamboo"-type grown structure of narrow lines in contrast to the much more homogeneous structure of the wider conductors.[45,46] Electron-beam evaporation is not well suited for controlling 0.5 wt % Cu in the film and also the resulting microstructure. More data are needed to verify their observations and conclusions.

6. Electromigration life tests on *Si/Al, Si/Al+Cu and Si/Al+Cu+Si contacts* in series with respective film conductors indicate that the open failures at the contacts are primarily due to Si diffusion in Al.

a. Mean time to failure (MTF): $(MTF)_{Al+Cu+Si} > (MTF)_{Al+Cu} > (MTF)_{Al}$

b. Activation energy (Q): $Q_{Al+Cu+Si} = 0.76$ eV; $Q_{Al+Cu} = 0.64$ eV; $Q_{Al} = 0.58$ eV

7. Contact resistance of Si/Al, Si/Al+Cu and Si/Al+Cu+Si contacts are equal to each other within a factor of 4. For the surface concentrations of Si chosen for our experiments, a contact resistance on the order of 1.5 to 6 μm for 3.80 × 6.35 μm^2 contact area corresponds to 0.36 to 1.45×10^{-6} Ω-cm^2 specific contact resistance. SEM examination shows nonuniform Si/Al interaction in the contacts and it is reflected in the contact resistance value.

8. For shallow junction devices, with junction depths on the order of 0.35 μm, Al+Cu+Si films are superior to Al+Cu and Al in terms of leakage currents and stability at 150°C temperature storage. Growth of Si precipitates in contact areas is observed.

9. Bond strengths of ultrasonically conded 25 μm (1 mil) Al (1 wt % Si) wire to Al, Al+Cu and Al+Cu+Si are equal to each other (≈ 2.7 gms), (1) before and after 50 temperature cycles from −65°C to +150°C, and (2) 1000-hour storage at 150°C.

10. Al+Cu+Si films with 2 wt % Cu and 1 wt % Si show a superior electromigration resistance as compared to Al+Cu (2 wt % Cu) films and can be used for establishing contacts to shallow junction devices with junction depths on the order of 0.35 μm. Though Si precipitates are observed in contact areas, present data are not sufficient to estimate the adverse effects, if any, on the contact resistance of these contacts.

SECTION VIII
PROPOSED ELECTROMIGRATION TEST PROCEDURES FOR Al-ALLOY FILM CONTROL

With ever increasing complexity of ICS, MSI, LSI, and now VLSI, contacts and metallization requirements are changing rapidly. Metallization is one of the last critical steps in integrated circuits fabrication and the selection of a metallization process is influenced by several factors such as: device designs and layout rules, device structures with shallow junction depths, silicon/metal contacts (ohmic & Schottky), low resistance for interconnections, bilayers (barrier layer-conductor), metal coverage on oxide steps, patternability of film interconnections, electromigration resistance, protective coating, bonding (ultrasonic, flip chip, beam leads, etc.), and Si/metal interactions during device packaging. Since Al film interconnection reliability is known to be limited by electromigration-induced failures, efforts will continue to improve electromigration resistance of these interconnections by replacing Al with some suitable Al-Alloy films. Literature survey indicates that Al-Alloys with a number of dopants of varying amounts have been tried. Reported life test data vary over a wide range. No unique Al-Alloy film composition can claim to be superior over another and life test data for same film composition may differ because of the mode of film deposition. Since the reliability of film interconnections impact the effective reliability of LSI circuits, it becomes abundantly clear that fully characterized metallization processes and a well-defined test procedure are needed to compare data from two different tests. The following test procedure is suggested:

1. The test structure stripe shall have the minimum interconnection width used for that set of IC family. For example, if the design rules of circuit layout call out a minimum conductor width of 5 μm, then the test stripe must have a 5 μm width.

2. The length of the stripe shall be greater than 250 μm (10 mils) since the failure rate is known to reach an asymptotic value. Any stripe longer than 250 μm should be considered acceptable.

3. Current to this test stripe needs to be fed by a wider lead (no larger than five times and smaller than twice the width) and leads longer than 125 μm on either side must be used to reach the bond pads. Large bond pads adjacent to the 250-μm long test stripe should be avoided since this structure does not truly represent IC interconnections.

4. The test stripe fabrication process should simulate the practiced interconnection process for that IC family. For example the test stripe should:

    a) Have the same film deposition parameters and film thickness
    b) Receive an identical protective coating
    c) Be subjected to *all* temperature excursions, contact sintering step, H_2 anneal step, or some magic bake to improve h_{fe}, and so on
    d) Be packaged in a standard IC package very similar, if not identical, to that used for IC family.

5. Film thickness data (after film deposition and/or lead patterning) coupled with the width of the conductor stripe should be used to calculate the current density. If a multilayer metal system is used, e.g., a barrier layer/conductor metal, cross section of the primary conductor metal system should be used for current density calculation.

6. A current density of 1×10^6 A/cm^2 is recommended.

7. Ambient temperature for tests should not exceed 215°C because microstructure properties of films change and will lead to erroneous results. It is recommended that tests be conducted in the temperature range of 125°C to 215°C.

8. Test temperature should be reported. If the resistance of the leads and the temperature coefficient of resistance are accurately determined, stripe temperature may be reported as test temperature.

9. A set of samples between 15 and 20 should be used for electromigration testing at a chosen test temperature.

10. Log-normal probability plots are recommended for the determination of mean time to failure (MTF) and standard deviation σ.

11. Arrhenius plot of MTF vs (1/T K) with a minimum of three (four are recommended) data points should be used for activation evergy determination; otherwise use $Q_{Al} = 0.45$ eV, $Q_{Al+Cu} = 0.6$ eV, or $Q_{Al+Cu+Si} = 0.5$ eV.

12. MTF data are represented by

$$MTF = A\, J^{-n} \exp(Q/kT)$$

where

A = parameter

J = current density A/cm^2

Q = activation energy meV

k = Boltzmann's Constant = 8.617×10^{-5} eV/K

T = absolute temperature

n = exponent

Because electromigration-induced failures are caused by divergences of atomic fluxes and the atomic flux is directly proportional to the current density, use of n=1 for the exponent in the above equation is recommended.

Use of n=2 leads to optimistic estimates of MTF at operating temperatures and current densities less than 1×10^6 A/cm^2.

The acceleration factor is given by

$$F = \left(\frac{J_1}{J_0}\right) \frac{\exp(Q/kT_0)}{\exp(Q/kT_1)}$$

where

J_1 and T_1 = current density and temperature at current stress

J_0 and T_0 = current density and temperature at operating condition.

13. Use the average MTF from all measurements to develop time to failure distributions. Failure times are assumed to obey log-normal distribution.

$$f(t) = \frac{1}{(2\pi)^{1/2}} \frac{1}{\sigma} \frac{1}{t} \exp\left[0.5 \left(\frac{\ln t - \ln t_{50}}{\sigma} \right)^2 \right]$$

The instantaneous failure rate f(t) by definition corresponds to the decrease in the number of surviving samples at time t and is given by

$$\lambda(t) = \frac{f(t)}{1 - F(t)}$$

Where the cumulative failure density function

$$F(t) = \int_0^t f(t)\, dt$$

corresponds to the probability of failure in the total time t.

Note that the failure rate increases with time and reflects the true wear-out mechanism of the interconnection due to electromigration-induced damage.

14. If the conductor crosses an oxide step, a thinning factor for film thickness should be determined and minimum cross section of the conductor at the oxide side should be used to calculate the maximum current density.

15. If a pulsed current is used for testing, peak current and not the average current in a lead should be used for current density calculation. MTF is equal to the cumulative time the interconnection is subjected to this peak current.

16. Since reliability of the film interconnections is determined by microstructure and alloy composition, detailed test procedures should be established to characterize as-deposited and annealed films (annealing to simulate device fabrication). Routine process control procedures should be followed to verify that film properties are reproduced.

17. MIL Standard M-38510D specifies current density design guidelines. These seem to be appropriate for 0.8-μm-thick, 6-μm-wide leads. However, if the lead width is further reduced, MTF data recommended by the above mentioned procedure should be developed and failure data along with film characterization data should be made available.

18. It is recommended that the present maximum current density design guideline of 5×10^5 A/cm^2 for Al-Alloy film interconnections be revised downwards to 2×10^5 A/cm^2 for lead widths approaching 2 μm.

SECTION IX
REFERENCES

1. I. A. Blech and H. Sello, Tech. Report TR-66-31 (Dec. 1965), Rome Air Development Center, Griffiss Air Force Base, New York; *Phys. Failure Electronics* **5**, 496 (1967), 374045.

2. W. R. Mutter, *J. Electrochem. Soc.* **113**, 59C (1967), Abstract No. 62.

3. P. B. Ghate, *J. Appl. Phys. Letters* **11**, 14 (1967).

4. J. K. Howard and R. F. Ross, *ibid.* **11**, 85 (1967).

5. I. A. Blech and E. S. Meieran, *ibid.* **11**, 263 (1967).

6. J. R. Black, *IEEE Trans. Electron Devices*, **ED-16**, 338 (1969).

7. L. Braun, *Microelectronics and Reliability* **13**, 215 (1974).

8. F. M. d'Heurle and R. Rosenberg, "Electromigration in Thin Films," *Physics of Thin Films*, Vol. 7, 257 (edited by Haas, Francombe and Hoffman), Academic Press, New York (1973).

9. F. M. d'Heurle and P. S. Ho, "Electromigration in Thin Films," *Thin Films:Interdiffusion and Reactions*, 243-304 (edited by J. M. Poate, K. N. Tu and J. W. Mayer), John Wiley, New York (1978).

10. I. Ames, F. M. d'Heurle and R. Horstmann, *IBM J. Res. Develop.* **14**, 461 (1970).

11. P. A. Totta and R. P. Sopher, *IBM J. Res. Develop.* **14**, 461 (1970).

12. A. L. Learn, *J. Electron. Mat* **5**, 531 (1976).

13. P. B. Ghate, *Failure Mechanism Studies in Multilevel Metallization Systems*, Final Tech. Report, RADC TR-71-186, Rome Air Development Center, Air Force Systems Command, Griffiss Air Force Base, New York, September 1971.

14. P. B. Ghate, J. C. Blair and C. Fuller, *Thin Solid Films*, **45**, 69 (1977).

15. F. H. Blevis, Technical Report 10, issued in 1976 by Applied Materials Inc., 3050 Bowers Avenue, Santa Clara, California 95051, 731796.

16. L. D. Hartsough and D. R. Denison, Tech. Rep. 79.01 and 79.02, Perkin-Elmer, Ultek Division, Palo Alto, California, 1979, and other reports available from Perkin-Elmer.

17. Materials Research Corporation, Orangeburg, New York 10762.

18. Varian-Specialty Metals Division, 3515 Grove City Road, Grove City, Ohio 43123.

19. C. R. Fuller and P. B. Ghate, *Thin Solid Films* **64**, 25-37 (1979).

20. C. S. Smith and L. Gutman, *Trans. Am. Soc. of Metals* **44**, 81 (1952).

21. P. Fletham, *Acta Met.* **5**, 97 (1957).

22. M. J. Attardo, R. Rutledge and R. C. Jack, *J. Appl. Phys.* **42**, 4343 (1971).

23. Joseph A. Keenan, *Am. Lab.* **7**, 23 (1975).

24. Wilhad Reuter, *Surface Sci.* **25**, 80-119 (1971).

25. Hemut Liebl, *J. Appl. Phys.* **38**, 5277-83 (1967).

26. A. J. Socha, *Surface Sci.* **25**, 147-170 (1920).

27. S. A. Evans, S. A. Morris, J. Englade, C. Fuller, and L. A. Arledge, *IEDM Digest*, 196 (1979).

28. P. L. Shah, K. S. Rao, G. Pollack, J. Bartelt and G. L. Varnell, The Electrochemical Society, Inc., Spring Meeting, May 11-16, 1980, St. Louis, Missouri. Abstract No.252.

29. J. C. Blair and P. B. Ghate, *J. Vac. Sci. Technol.* **14**, 79 (1977).

30. H. B. Huntington and A. R. Grone, *J. Phys. Chem. Solids* **20**, 76 (1961).

31. D. S. Chhabra and N. C. Ainslie, Electrochemical Society Meeting, Dallas, Texas, May 1967.

32. J. D. Venables and R. G. Lye, *Proc. 10th Ann. Reliab. Phys. Symp., IEEE*, 159 (1972).

33. R. A. Sigsbee, *J. Appl. Phys.* **42**, 880 (1971).

34. F. M. d'Heurle, "The Effect of Copper Additions on Electromigration in Aluminum Thin Films," *Met. Trans.*, Vol 2, 681-689 (1971).

35. F. M. d'Heurle, *Proc. IEEE* **59**, 1409 (1971).

36. F. M. d'Heurle, N. G. Ainslie, A. Gangulee and M. C. Shino, *J. Vac. Sci. Technol.* **9**, 298 (1972).

37. B. N. Agarwala, B. Patnaik and R. Schnitzel, *J. Appl. Phys.* **43**, 1487 (1972).

38. B. N. Agarwala, L. Berenbaun and M. Peressini, *J. Electron. Materials*, **3**, 137 (1976).

39. G. J. van Gurp, *Appl. Phys. Letters* **19**, 476 (1971).

40. A. J. Learn, *Thin Solid Films* **20**, 261 (1974).

41. P. B. Ghate and J. C. Blair, *Thin Solid Films* **55**, 113 (1978).

42. K. R. Van Horn (ed.), "Aluminum," *Am. Soc. of Metals*, Vol. I, 174 (1967).

43. J. R. Black, *16th Annual Proc. of Reliab. Phys.* (IEEE Cat. No. 78CH1294-8PHY), 233 (1978).

44. J. O. McCaldin and H. Sankur, *Appl. Phys. Letters* **19**, 524 (1971); **20**, 171 (1972).

45. S. Vaidya, T. T. Sheng and A. K. Sinha, *Appl. Phys. Letters* **36**, 464 (1980).

46. E. Kinsborn, *Appl. Phys. Letters* **36**, 968 (1980).


DAT
FILM